DIGITAL TWINS WITH UNCERTAIN AND IMPERFECT DATA

By

Eric VanDerHorn

Dissertation

Submitted to the Faculty of the

Graduate School of Vanderbilt University

in partial fulfillment of the requirements

for the degree of

DOCTOR OF PHILOSOPHY

in

Civil Engineering

August 31, 2022

Nashville, Tennessee

Approved:

Sankaran Mahadevan, Ph.D.

Douglas Adams, Ph.D.

Hiba Baroud, Ph.D.

Mitchell Wilkes, Ph.D.

Xiaozhi Wang, Ph.D.

To my Parents and Teachers

ACKNOWLEDGEMENTS

First and foremost, I would like to express my deepest gratitude to my advisor Prof. Sankaran Mahadevan without whom this dissertation would not have been possible. His advice and guidance throughout this process has been beyond invaluable and I would not have gotten here today without his ongoing patience and understanding. I am greatly indebted to him for all that I have learned and accomplished.

I would also like to acknowledge the help and support I received from my committee members Prof. Doug Adams, Prof. Hiba Baroud, Prof. Mitch Wilkes, and Dr. Xiaozhi Wang, who provided useful comments and suggestions during this research.

I express my sincere thanks to the American Bureau of Shipping who sponsored my research and specifically to Chris Wiernicki who encouraged me to begin this journey. I'd also like to thank Dr. Don Liu, whose guidance was invaluable. And I am also grateful to all my leaders and co-workers who enabled me to balance working full-time with completing this work.

I would like to thank all the students and faculty members of the Reliability and Risk Engineering doctoral program at Vanderbilt University with whom I engaged in many technical discussions that helped this dissertation and my professional development. In particular, I would like to thank Saideep Nannapaneni, Chenzhao Li, Xiaoge Zhang, Zhen Hu, Paromita Nath, and Kyle Neal. I also acknowledge the wonderful company, co-operation, and encouragement of my colleagues and friends during my stay at Vanderbilt.

This dissertation would not have been possible without the support of my family. I thank my parents David and Donna VanDerHorn for their constant encouragement and support during my graduate education.

TABLE OF CONTENTS

LIST OF TABLES

LIST OF FIGURES

CHAPTER 1

INTRODUCTION

1.1 Motivation

Digital Twin is one of the promising digital technologies being developed to support digital transformation and decision making in multiple industries. While the concept itself is over 20 years old, Digital Twins have gained considerable attention in both industry and academia in recent years. This can likely be attributed to a combination of hype as well as a desire to progress digital transformation efforts in a wide variety of industries. Digital Twins are comprised of three primary components: (1) a physical reality, (2) a virtual representation of that physical reality, and (3) interconnections that exchange information between the physical reality and virtual representation. The physical reality represents the system of interest for the given use case, and the virtual representation is comprised of the data models and computational models used to describe the physical reality of interest. Finally, the interconnection between the physical reality and the virtual representation allows for both the data models and computational models to be updated to be in alignment with the physical reality. Further, when this update process for the data models and computational models incorporates uncertainty, the Digital Twin can be said to be a probabilistic Digital Twin.

As the Digital Twin continues to evolve as it expands to new industries and use cases, this has resulted in a continually increasing variety of definitions that threatens to dilute the concept and lead to ineffective implementations of the technology. There is a need for a consolidated and generalized definition, with clearly established characteristics to distinguish what constitutes a Digital Twin and what does not. Furthermore, a comprehensive framework for the implementation of a Digital Twin considering the generalized characterization of its key components is essential to facilitate its effective use.

In addition to a framework for the implementation of Digital Twins, the consideration of uncertainty quantification during the Digital Twin model updating process is also of interest. Digital Twins are being used to represent engineering systems that are increasingly complex, often with imperfect input data being the only basis for the update of these models. As such, Digital Twin implementations must also consider the integration of uncertainty quantification during the model updating process. When considering data of unknown or questionable quality, it is important to ensure that the Digital Twin does not draw the wrong inference from the data. To accomplish this, the update process must extract the maximum information from the provided data during inference while mitigating the possible negative impact when the data is of questionable credibility.

This dissertation starts by establishing a clear and concise definition and characterization of a Digital Twin, generalized so that it can be applied in all possible use cases. Given this generalized definition and characterization, a framework for a Digital Twin implementation is developed and demonstrated. Additionally, this work considers the fusion of heterogeneous data sources for the purposes of reducing the epistemic uncertainty associated with imperfect data. Several computational methods are proposed to overcome different challenges with imperfect data sources. A Bayesian approach is pursued for the treatment of the incorporation of this uncertainty. The rest of this Chapter develops the objectives of this dissertation. Section 1.2 briefly discusses the various aspects of imperfect data and the considerations for Bayesian updating. Section 1.3 provides the research objectives of this dissertation and Section 1.4 highlights the significant contributions of this research. Section 1.5 describes the organization of this dissertation.

1.2 Imperfect Data

Research in the area of reasoning with different forms of imperfect data has produced a wide variety of techniques and approaches that vary in both fundamental philosophy and mathematical implementation. One of the major challenges introduced during the consideration of these various approaches occurs when decisions need to be made based on the information that has been acquired about the state of the system.

The first form of imperfect data that is addressed in this study relates to the loss of information resulting from summarized data. This occurs when raw data has been reduced to a simplified representation of portions or the entirety of the raw dataset. Representation of summarized data as the outcome of a statistics function is accomplished through the inclusion of a functional node in the Bayesian network as described in Section 4.2. A challenge arises when considering inference in a Bayesian network, since observations of the outcomes of functional nodes cannot be directly incorporated. This is resolved by applying a methodology to transform the Bayesian network to a form that can be used to incorporate observations of the statistics function and thereby enable the updating of the model parameters. An additional related challenge addressed in this research includes the incorporation of the epistemic uncertainty related to unknown sample sizes for an observed summarized data. Identification of methodologies for obtaining the required sampling distribution for the statistic function is also considered.

The second type of imperfect data considered in this research occurs when observations of the system result in uncertain and/or ambiguous interpretations. In deterministic inference, evidence about the system is interpreted as data regarding the state of the system which is accepted with certainty. Uncertain data in this research is defined as evidence which cannot be interpreted in certain terms with respect to the possible states of the system as defined by the formal model. Consider the case of classification, where the categorical outcome of a set of input parameters cannot be assigned with absolute certainty but instead can only be stated along with some measure of confidence in

the assignment. Current probabilistic approaches for this type of uncertain data consider some form of combination of the possible representative states through either a weighted likelihood or weighted posterior which are presented in Section 5.2. This type of imperfect data can often occur when considering the outputs of machine learning models, which often provide measures of confidence in their predictions along with the prediction itself. A methodology is proposed which incorporates the model prediction, along with its associated confidence measure, as part of the Bayesian inference process.

Once the knowledge regarding the uncertainty in the Digital Twin has been updated, this information is then propagated to determine the uncertainty in the forecasted outputs of the Digital Twin which can then be utilized to support future decision making.

1.3 Research Objectives

The overall goal of this dissertation is to propose a generalized approach for the implementation of Digital Twins and address some of the challenges that arise in this implementation due to imperfect and uncertain data. The various objectives are grouped into two headings: Digital Twin Implementation and Integration of Imperfect and Uncertain Data.

1.3.1 Digital Twin Implementation

The first major objective is the development of a framework for the implementation of a Digital Twin. This first includes the development of a generalized definition, taking into consideration past definitions in the literature, the specific components of these definitions, and an overview of the most common lexicon. Once a generalized definition is proposed, the concept of the Digital Twin is further characterized by establishing descriptions of each of its primary components. Finally, a generalized framework for implementation is developed which describes the establishment of each of the Digital Twin components. This proposed implementation is demonstrated through a case study of a Digital Twin applied to track the fatigue life of a containership. The various objectives related to Digital Twin implementation are addressed under the following topics:

1. Digital Twin generalized definition and characterization
2. Digital Twin implementation
3. Case Study – Digital Twin for monitoring fatigue life accumulation of a containership

1.3.2 Integration of Uncertain and Imperfect Data

The second major objective focuses on the implementation of Digital Twins with abstracted and/or uncertain data. Consider a Digital Twin of a critical structural connection subjected to a fatigue crack. Applying fracture

mechanics modeling within this Digital Twin to represent the crack growth requires model parameters associated with the material properties of the material of the connection, such as material yield strength. In many instances, the exact material properties of the connection are unknown and must be represented by material property distribution determined from material tests performed by the manufacturer of the material. In some instances, these material results are performed in batches where the resulting properties are only be available in the form of summary statistics, an abstracted form of the raw test data.

A Bayesian network approach is developed to update the model parameters using abstracted data forms. Common forms of abstracted data include summary statistics, such as the mean and variance for continuous variables and observed frequencies for discrete variables. The concept of arc reversal is exploited to transform the Bayesian network to a form that can be used to incorporate the statistics function and thereby enable the updating of the model parameters.

Another form of uncertain data arises when considering the use of categorical data provided by machining learning models, such as in classification-based diagnosis of the system. This type of uncertain input data is often the result of inspections, where the responsibility of the classification of the inspection result is shifting from human-based inspectors to classification models developed by machine learning. Similar to human-based inspection results, the inspection results of these classification models may need to be incorporated into Digital Twin models. An example of this type of Digital Twin is in the management of corrosion. Visual inspections of the structural components are used to identify and grade the breakdowns in the protective coatings applied to prevent corrosion from occurring. Using machine-learning trained tools to grade images of the structure results in classification model categorical data to be incorporated into the Digital Twin. When considering the categorical data resulting from the classification model, in addition to the assigned class, a measure of the confidence in that assigned class may also be provided. This confidence measure is incorporated into the likelihood function as an error term which down-weights data observations with lower levels of confidence. The various objectives related to the integration of abstracted and uncertain data are addressed under the following topics:

1. Integration of abstracted data in Bayesian inference
2. Integration of categorical data confidence in Bayesian inference

1.4 Highlights of the Dissertation: What's New?

1. A generalized definition and characterization for Digital Twin is proposed based on analysis of a number of existing definitions in the literature (Section 2.2). The distinction between a Digital Twin and similar concepts is also provided.

2. A framework for Digital Twin implementation is developed outlining the approach for addressing each of the key components of the Digital Twin outlined in its characterization (Section 2.3).
3. An end-to-end development, integration, and automation of a Digital Twin framework for monitoring vessel-specific fatigue damage is developed (Section 3.2). This methodology addresses the lack of available on-board sensor data through the incorporation of publicly available data sources for vessel routes and ocean condition data. Several vessel-specific fatigue accumulation methodology options are compared as part of the Digital Twin framework (Section 3.3).
4. A methodology is developed to incorporate "observations" of abstracted data through a Bayesian network representation to enable the Bayesian inference process in the presence of abstracted data (Section 4.3). The proposed approach is based on a Bayesian network representation, which can be easily extended beyond the simple inference of distribution parameters of random variables (based on observations of that random variable) to the calibration of model parameters in Digital Twins.
5. A methodology is developed to incorporate "observations" in the form of classification model results to enable the Bayesian inference process in the presence of uncertainty in the classification model results (Section 5.2). A confidence measure is assigned for each individual classification model result, which is then incorporated in the Bayesian inference procedure.

1.5 Organization of the Dissertation

The remainder of this dissertation is organized into several chapters that address the research objectives described in Section 1.4.

Chapter II provides the foundation for the research by proposing a generalized and comprehensive definition for a Digital Twin based on a review of 46 existing definitions found in the literature. A consolidated definition is required because as the Digital Twin concept has evolved and expanded to new industries and use cases over the past 20 years, the increased variety of definitions has threatened to dilute the concept and could lead to ineffective implementations of the technology. This chapter also provides a detailed characterization of the various key components of a Digital Twin which include criteria to distinguish the Digital Twin from other similar digital technologies. Finally, the process and considerations for the implementation of Digital Twins are presented along with Digital Twin future needs and opportunities. A detailed engineering implementation of the Digital Twin concept is then provided in Chapter III.

In Chapter III, the concepts for the implementation of a Digital Twin are applied for the monitoring and prognosis of vessel-specific fatigue damage. During design, fatigue damage estimates are based on conservative assumptions regarding operational conditions and structural response. However, variability in the vessel-specific operations from

those assumed during design needs to be considered when supporting engineering-based decisions for maintenance deferrals and service life extensions. The use of Digital Twins is proposed to provide this necessary vessel-specific decision support. Digital Twins typically rely on sensor-based data to update their models, however structural health sensors for fatigue monitoring can be prohibitively expensive to install and maintain in ship structures, so the proposed method addresses this by instead combining publicly available vessel-specific operational data (global vessel position data coupled with ocean weather data) with computational models to monitor the environmental exposure and track the vessel fatigue accumulation over time. This approach is demonstrated through a case study of a containership that has been in operation for seven years.

The updating process of a Digital Twin model requires the relevant input data from the physical model of interest. This data may often be incomplete, imperfect, uncertain or abstracted in some way that limits is ability to be directly incorporated in the Digital Twin model updating. Several of these challenges are addressed in Chapter IV and Chapter V. Chapter IV considers the case of model updating with input data that has been abstracted, where the original raw data have been reduced to a summarized representation. Common forms of abstracted data include summary statistics, such as the mean and variance for continuous variables and observed frequencies for discrete variables. Another common form of available information is summarized reliability data for various mechanical components (e.g., failure rates or failure probabilities) instead of detailed actual test data. Chapter IV presents a methodology for updating the model parameters using these abstracted data forms through a Bayesian network. First, the concept of a statistics function is developed and linked to the abstracted data forms. The concept of arc reversal is then exploited to transform the Bayesian network to a form that can be used to incorporate the statistics function and thereby enable the updating of the model parameters. Several numerical examples are used to demonstrate the applicability and generality of the proposed method for several different forms of abstracted data.

In Chapter V, the use of categorical data resulting from classification models in the updating process of Digital Twins using the Bayesian inference process are considered, specifically, the uncertainty in classification-based diagnosis. Machine learning-based classification models are becoming more prevalent in mechanical system damage diagnosis, such as cracking or corrosion. In some applications, the results of these classification models may also be further incorporated into downstream Bayesian analysis, such as model calibration. In addition to the classification model result itself which can be treated as the observation, the classification model also commonly includes a probability measure describing the level of confidence in the classification result. Incorporation of this confidence measure in the subsequent Bayesian analysis can be used to correct errors resulting from poor classification model performance. Chapter V proposes a methodology for incorporating the classification model confidence measure in conjunction with the classification model result in subsequent Bayesian analysis. Numerical

examples are used to demonstrate the applicability and generality of the proposed method for binary and multi-class data.

Finally, Chapter VI summarizes the findings of this study and suggests directions for future work.

Each of the above chapters review the relevant literature and discuss the current state of art prior to the discussion of the proposed methods. Each individual chapter introduces and describes the notations and symbols used. The chapters also include numerical examples to illustrate the proposed methods using both simple illustrative examples as well as more complex engineering applications.

CHAPTER 2

DIGITAL TWIN DEFINITION, CHARACTERIZATION, AND IMPLEMENTATION

2.1 Introduction

Digital twin technology is part of the rise of new digital technologies that support digital transformation by providing capabilities to enable new business models and decision support systems. Many organizations have already incorporated or are in the process of incorporating data, information, and analytics capabilities as part of their service offerings [1]. Similar to other digitalization concepts, such as the internet of things (IoT), cloud computing, machine learning/artificial intelligence, and augmented reality, the Digital Twin concept has seen increasing interest in recent years in both academia and industry as indicated by the growth of publications, articles, and commercial marketing. The existing literature highlights many of the potential and perceived benefits of the Digital Twin concept, including reducing costs [2–4] and risk [5]; improving efficiency [6], improving service offerings [7,8], security [9], reliability [10,11] and resilience [12]; and supporting decision-making [13–15]. However, the literature is lacking a consistent presentation of what the Digital Twin is and how it can be applied to support an organization's operations. In fact, the varied use cases to which the Digital Twin has been associated with have resulted in a wide variety of definitions and frameworks across the industry causing confusion that risks weakening the concept and limits its ability to achieve the stated benefits. To reduce the confusion and unreasonable expectation surrounding this technology, there is a need for a generalized and consolidated definition of a Digital Twin as well as a characterization of elements of the concept to provide a clear classification of what constitutes a Digital Twin, distinguishing it from other similar digital technologies.

It is also noted that most of the current Digital Twin literature focuses primarily on technical approaches, analysis methodologies, and the challenges associated with data collection and integration into the Digital Twin. There is a need for examples of practical implementations of Digital Twins that consider the implementation strategies and decision support to achieve targeted outcomes with measurable benefits. A strategy for implementing Digital Twins must also consider the current technical and cultural challenges that prevent Digital Twins from realizing their desired benefits. Finally, Digital Twins require the incorporation of a variety of different enabling technologies, whose technical maturity and development must also be considered.

This Chapter evaluates the status of Digital Twins as part of a family of digitalization efforts intended to enhance existing processes and support new services. The contributions of the Chapter are as follows. First, existing Digital Twin definitions are reviewed and a consolidated definition and description of the key characteristics of the Digital Twin is provided (Section 2.2). Next, the approach and considerations for the implementation of Digital Twins for practical applications are discussed (Section 2.3). The implementation approach and related considerations are then demonstrated

through an industry case study (Section 2.4). Finally, current Digital Twin implementation challenges and future needs and opportunities for further development are discussed (Section 2.5). Section 2.6 provides concluding remarks.

2.2 Digital Twin Definition and Characterization

The concept of a Digital Twin originates from Michael Grieves' 2003 presentation on product life-cycle management based on his work with John Vickers [4]. Grieves and Vicker's motivation for developing the concept was to shift from the predominantly paper-based and manual product data to a digital model of the product which would become foundational for life-cycle management. Similar concepts such as Cyber Physical Systems (CPS) [16] and Internet of Things (IOT) [17] all focus on the idea of connecting a physical system to data collection, computational and/or communication systems, but approaching it from differing perspectives: CPS concept from the system engineering and control perspective, IOT from a networking and IT perspective, and Digital Twin from a computational modeling (machine learning/artificial intelligence) perspective.

Grieves provided the first characterization of the Digital Twin concept by stating that it consisted of three components, a physical product in Real space, a virtual representation of that product in the Virtual space, and the connections of data and information that tie the virtual and real products together [4]. Over the past two decades, the interest in Digital Twins has grown across many industries and this has led to a wide variety of definitions and characterizations that has diluted Grieves' original description, to which this Chapter seeks to return and generalize.

2.2.1 Digital Twin Definitions in the Literature

An overview of some of the varied lexicon found in the literature is presented in Table 2.1, based on 46 different definitions found in the literature. Due to space limitations, these various definitions are not listed here, but are provided in GitHub via the link (https://github.com/evanderhorn/DSS_DT_Public). In addition to providing a concise statement of what a Digital Twin is, most of the available definitions also include descriptions of selected specific attributes of the Digital Twin, including: representation fidelity, data collection/exchange, synchronization frequency, and model/simulation capabilities. These definitions also occasionally include references to the specific use case being considered and the lifecycle phases that apply. After reviewing the breadth of definitions in the literature, a consolidated and generalized definition for a Digital Twin is proposed here as "*a virtual representation of a physical system (and its associated environment and processes) that is updated through the exchange of information between the physical and virtual systems*." This definition is general enough to encompass the 46 reviewed definitions provided in https://github.com/evanderhorn/DSS_DT_Public, yet it restricts itself to only the essential elements while avoiding use case-specific Digital Twin characteristics or terminology.

The terminology choices for this proposed definition for a Digital Twin can then be reviewed in relation to the terminology used in the other definitions found in the literature. This comparison is focused on the three key components of the proposed definition: *virtual representation*, *physical system* and *updated through the exchange of information*.

As mentioned earlier, many of the definitions in the literature combine a definition with specific characterizations about Digital Twins that are unique to the use case(s) that they are describing. Much of the confusion surrounding the Digital Twin concept appears to be in the qualifiers on certain characterizations which are used to designate what constitutes a Digital Twin and what does not. The following sub-sections provide a generalized overview of these characterizations which covers the breadth and variety of descriptions and use cases provided in the literature.

Table 2.1: Proposed Lexicon vs Alternate Lexicons

Proposed definition lexicon	Alternate lexicons used in the literature
virtual	digital, cyber, computerized, computational, living, system
representation	model, simulation, counterpart, copy, mirror, part product, instance, substitute, information, clone, description, replication
physical	physical, real/real-world
system	system, product, object, artifact, production lines, item, world, counterpart, device, parts, twin, entities, element, process state, vehicle, aircraft, structure, asset, component, instance
updated	update, integrate, incorporate, include, synchronization, adapts, reflects, mirror, reflect
exchange	connections, communication, collecting
information	data, sensor updates, fleet history, physical knowledge, flight histories, fatigue damage, data space, performance, maintenance, health status

2.2.2 Digital Twin Characteristics

Using the generalized definition proposed above, the Digital Twin can be characterized by three primary components: (1) A physical reality, (2) a virtual representation, and (3) interconnections that exchange information between the physical reality and virtual representation shown in Figure 2.1.

The following sub-sections discuss these three components in further detail.

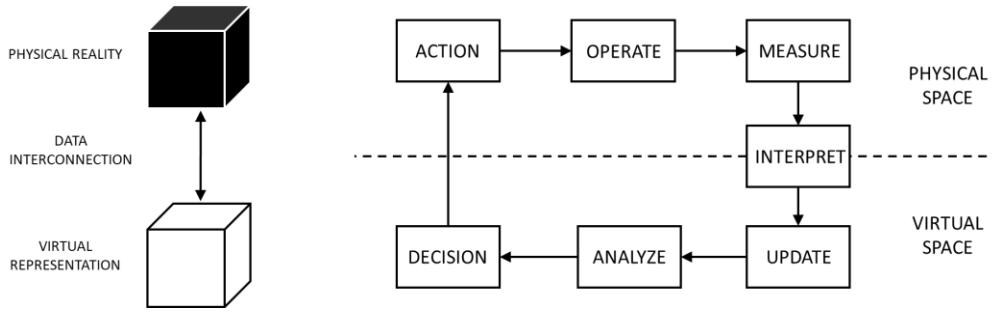

Figure 2.1: Digital twin components and high-level processes

2.2.3 Physical Reality

In the Digital Twin literature, a wide variety of terminology has been used to describe the physical reality of interest and the selected terminology is often domain specific. The term *physical reality* is proposed here as it is the most general form to represent what may be attempted to be modeled, since physical reality encompasses the entirety of the system, both known and unknown. The physical reality can be decomposed into the physical system, the physical environment, and physical processes.

2.2.3.1 Physical System

The physical system consists of the group of interacting and interrelated entities that form a unified whole [18]. This group of entities is often described by its structure or purpose and delineated from other systems by boundaries in space and time. The selection of the boundary often takes advantage of natural segregations associated with the more typical meaning of the word *system*. For example, the physical system of interest can range from a single machinery part, sub-component or component, to a complete piece of machinery, to a machinery system, to all of the interconnected systems of a single asset. It can be seen that generally, the physical system of interest is man-made, but as the concept of Digital Twin expands to other domains, such as healthcare [19] and agriculture [20], the physical system of interest may be some aspect of the natural environment or the human body.

2.2.3.2 Physical Environment

The physical environment is where the physical system of interest resides. The physical system is surrounded and influenced by its physical environment and interacts with the environment through physical processes. The delineation between the physical system and physical environment is often determined based on each specific Digital Twin application. In some applications, this delineation may be simple, but in others it may be complicated. An example of a simple delineation case is the Digital Twin of a manufacturing process such as additive manufacturing. In this case, the physical system of interest is the 3D printer, and the physical environment includes relevant external influences on the process such as room temperature, air flow, ambient vibration, etc. In an example of a more complicated delineation case,

the physical system of interest may be a single room in a large building, and the physical environment may include other parts of the building, such as adjacent rooms, ventilation systems, etc. as well as other external factors that impact the building as a whole, such as weather, etc. In many applications, both the physical system and the physical environment will be represented in the virtual space. This means that data for the relevant environmental parameters will be collected from the physical environment and stored in the virtual representation similar to that of the physical system. This allows the physical environment to be reconstructed in the virtual space to allow for simulations, forecasts, and/or decisions to be made which will impact the physical system of interest.

2.2.3.3 Physical Processes

Physical processes are how the system expresses itself in the physical environment and is the mechanism by which the entities of the system undergo changes in state. For example, in the case of manufacturing, some of the physical processes of interest may include casting, forging, welding, etc. For asset lifecycle management, the processes of interest may be loading processes based on the system's operation in the environment or degradation processes which can result in the physical system states changing over time. Similar to the physical system and physical environment, the physical processes may also be represented in the virtual space to support simulations, optimization, and forecasting.

2.2.4 Virtual Representation

As presented in Table 2.1, the Digital Twin definitions in the literature use a variety of terminology to discuss the virtual representation. This Chapter proposes using the term *virtual representation* as this captures the idea that the entity in the virtual space is merely a representation of an idealized form of the physical reality.

2.2.4.1 Idealized Representation of Physical Reality

It is recognized that any attempt to model the physical reality requires the idealization of that reality based on some level of abstraction. These idealizations often take the form of data models (data structures) and/or behavior models (mathematical or computational models). A data model here refers to a data structure that retains all the variables describing the reality at the level of abstraction chosen. Behavior models refer to the computational models that describe the how the variables of interest relate to each other. In engineering applications, behavior models are often based on the laws of physics; however, the exact physics that describe the relationships between variables may not always be known and use of data-driven models to describe the relationships between different variables is becoming more prevalent. Reality is then represented in this idealized form by assigning values to the model variables based on the interpretation of the data collected from the physical reality.

The decision on the level of abstraction must be consistent with the intended use case(s) as it will impact data collection processes as well as introduce uncertainty. Due to the abstraction of reality, the evidence collected about that reality must

be transformed into data consistent with the virtual representation of the idealized reality. The process by which the data consistent with the idealized representation gives evidence about reality is called the interpretation process and is shown in Figure 2.2.

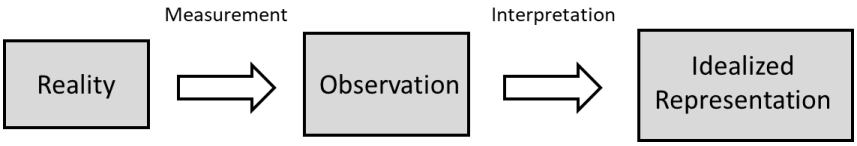

Figure 2.2. Data abstraction process

2.2.4.2 System States and Parameters

When describing the types of data and information that are to be managed by the virtual representation, a wide range of terms may be considered, including *properties*, *parameters*, *states*, *attributes*, *characteristics*, *features*, *variables*, and *dimensions.* As noted earlier, the meaning and use of these terms is often dependent on the technical domain in which they are being referred. A primary motivation for the use of a Digital Twin in many applications is the monitoring of the system as it changes over time. Tracking and modelling these changes within the virtual representation as a function of inputs to the system enables the representation and estimation of past, present, and future behavior to guide decision-making. These objectives align closely with the concept of state space modelling in system identification and as discussed below, state estimation is a common methodology used in the exchange of information between the physical reality and the virtual representation. Therefore, in this Chapter, we propose adopting the terminology used for state space modelling which uses the terms *states* and *parameters* to describe the information managed by the virtual representation [21].

In state space modelling terminology, *states* refer to the aspects of the system that evolve through time based on their previous values and inputs to the system (often externally imposed by the system's interaction with the environment). Monitoring the states of the system therefore provides the history of how the system is behaving over time. The term *parameters* in state space modelling is used to refer to the aspects of the system *model* that describe how inputs to the system affect the states and how the different states relate to each other over time. In many cases, system parameters remain fixed or are slowly varying over time. Defining the states and parameters for a specific Digital Twin representation is determined by the level of abstraction selected for the idealized representation. This information includes information about the system itself, in addition to its environment and associated processes.

Note that while the system states and parameters retained in the virtual representation provide an idealized representation of the physical reality, not all this information is readily exchanged between the physical reality and the virtual representation. This is because not all system states can be directly measurable with available inspection methods, due to limitations of either technology or economics. For example, the state of fatigue damage accumulation may be of

interest, but crack initiation is not feasible to monitor, especially in large structures. In such cases, the values for these states are assumed based on data not directly associated with the current physical reality of interest (e.g. historical data, design data, etc.) or inferred from the observed data using state estimation. In the example of representing fatigue damage accumulation, measured states, such as structural motion and strain using sensors, can be used in combination with computational models to infer the fatigue damage state. Some of the unobservable system information may also include the system parameters which must be inferred through parameter estimation. This process of determining which states to directly monitor and which states to infer is an important part of the Digital Twin scoping and implementation process.

2.2.4.3 Virtual System

The primary component of the virtual representation is the virtual system. The virtual system contains the data and models of the entities of interest from the physical system at a chosen level of abstraction. It is important to note that the virtual system may contain multiple models of the physical system at different levels of abstraction and these models may or may not interact with each other. An example of interaction is aeroelasticity analysis of an airfoil, where the results of the aerodynamics model may be used as input to the structure model and vice versa (two-way coupling).

2.2.4.4 Virtual Environment

Like the virtual system, the virtual environment is the virtual representation of the physical environment. Similar to above, the virtual representation of the physical environment is at a chosen level of abstraction.

2.2.4.5 Virtual Processes

Virtual processes describe how the virtual system expresses itself at the level of abstraction chosen for the virtual representation. The most common form this takes is a computational model of the corresponding physical processes. These computational models to represent how the physical system undergoes state changes to help generate the insights required to support decision-making.

The computational models used to accomplish this are built based on the relationships established between the inputs and outputs of a given process that changes the system states (e.g. load application and system dynamics, degradation mechanisms, etc.). The relationships between the inputs and outputs of these processes are determined based on known physics or generated via data-driven models using input and output data, or a hybrid of both. Machine learning (ML) and artificial intelligence (AI) techniques can be used to establish simulation models for processes based on the collected data without knowing the specific model form (i.e. a “black-box” model).

Virtual processes play a valuable role in the Digital Twin, as many of the use cases rely on simulated future states rather than the present system state. These include diagnostics and prognostics [10,12,14,22–24], design verification [25], simulation and optimization [2,4,13,22,26–29], and “what-if” scenario and sensitivity analyses [26]. The application of

virtual processes on the virtual system alters the virtual system states in a manner similar to how the physical processes alter the states in a physical system. This allows the user of the Digital Twin to hypothesize how the physical system would perform under similar physical processes, thus helping to decide what actions to undertake based on whether the simulated outcomes are aligned with the desired outcomes.

2.2.5 Interconnection between Physical and Virtual

The final component of the Digital Twin definition is the interconnection between the physical reality and the virtual representation where data/information is exchanged in two directions: physical-to-virtual and virtual-to-physical [30].

2.2.5.1 Physical-to-Virtual Connection

The physical-to-virtual connection enables the process by which data collected from the physical reality is used to update the states maintained in the virtual representation. In general, the physical-to-virtual connection requires three steps: the process of collecting the relevant information including the direct measuring of the physical reality, interpreting the collected data to a form that is consistent with the level of abstraction and the updating process that uses the data to update the states of the virtual representation.

In the first step, when discussing data collection for the Digital Twin, the Internet of Things (IoT) and sensor technology are commonly referenced [20,31–33]. While not strictly required for a Digital Twin, these technologies are often credited with supporting the increased interest in Digital Twins since they allow for a larger amount and frequency of measurements. It is important to note that offline and manual data collection means are also relevant in this context, such as visual inspection, non-destructive evaluation, repair logs, etc.

The second step of the process, interpretation of the collected data (Figure 2.2), may typically contain several steps depending on the data, including data processing, data curation and data conversion. An example of this is the conversion of voltage changes in a strain gauge to strain measurements, but a more abstract representation may need further interpretation, for example converting the strain measurements to load cycle counts.

The third step of the process is the use of data to update the states of the virtual representation. In the simplest cases, the measured data corresponds exactly to a state maintained in the virtual representation and the virtual representation is updated such that it reflects the observed physical system state. In many cases, updating of the unobserved system states of interest and the model parameters is achieved through the techniques of system identification, which may also involve information fusion, i.e., use of data from multiple sources.

2.2.5.2 Information Fusion

The concept of information fusion is focused on combining the multiple available sets of information to create a derived set of information which reduces redundancy and uncertainty. Information fusion techniques can be classified into three categories: (i) data association, (ii) state estimation, and (iii) decision fusion [34]. For the virtual representation update process, the state estimation techniques are of greatest interest, but data association may also be applied where it is necessary to reduce the dimensionality of a large volume of data. Data association and state estimation are part of the physical-to-virtual connection process. Decision fusion may be applied during the virtual-to-physical connection process, where a consensus must be made from the outcomes of various analyses as to the actions that will be undertaken to affect the states of the physical system of interest.

2.2.5.3 Virtual-to-Physical Connection

The virtual-to-physical connection is the process that results in the transfer of information from the virtual representation back to the physical reality. This connection closes the loop in the Digital Twin, by allowing the insights and decisions generated through the virtual representation to be realized in the physical system; either through actions that result in a change in the physical system states or actions that collect additional information from the physical system to further update the virtual representation. It can also be noted that the decision resulting from the Digital Twin insights may be simply to take no action at all at the present time and simply continue updating and monitoring the physical system.

This information flow is realized in the physical reality by undertaking specific actions which impact the physical process(es) that result in a change of the states of the physical system. As with the physical-to-virtual connection, this process occurs in two steps: (1) the virtual representation is used to determine whether and what change in the physical state is required, and what action is required to achieve the targeted state; (2) then the required actions that impact the necessary physical process(es) are performed to achieve the targeted physical state.

Table 2.2 summarizes the above descriptions of various elements of a digital twin.

Table 2.2. Summary Description of Digital Twin Components

Component	Description
Physical Reality	
Physical System	The portion of the physical reality chosen for modelling which includes all relevant interacting and interrelated entities that form a unified whole
Physical Environment	The aspects of everything outside the selected physical system which affect that system
Physical Processes	The functions being performed by the physical system that result in the system undergoing changes in state
Virtual Representation	
Virtual System	The data and computational models of the physical system of interest at a chosen level of abstraction
Virtual Environment	The virtual representation of the physical environment for the physical system of interest
Virtual Processes	The virtual representations of the corresponding physical processes, used to simulate how physical processes will affect the physical system; these are the primary means to generate insights to meet target outcomes
Information Interconnection	
Physical-to-Virtual Connection	The means by which information from the physical system is collected, interpreted, communicated and used to update the virtual representation states and parameters
Virtual-to-Physical Connection	The means by which an action is decided and undertaken based on the virtual representation to affect physical processes that result in change of the physical system's states and parameters

2.2.6 Digital Twin Qualifiers

In the review of definitions provided in the literature, it was observed that several definitions included specific qualifiers for certain Digital Twin characteristics to designate what constitutes a Digital Twin and what does not. This section will review the qualifiers mentioned in the literature and then propose a clear set of qualifiers that distinguish Digital Twin from similar technologies while not being overly restrictive.

2.2.6.1 Digital Twin vs Digital Model

Descriptions of Digital Twins and their usage in the literature often sound similar to more traditional digital modeling approaches, such as computer-aided design (CAD), computer aided engineering (CAE), and product lifecycle management (PLM) tools, which lead to confusion amongst practitioners as to what distinguishes a Digital Twin from these existing approaches. As these tools are also incorporated and used with Digital Twins, it can be challenging to determine when the use of these tools/models fits the definition of a Digital Twin and when it does not. The two key

requirements for a Digital Twin that make it unique from traditional digital modelling approaches are that a Digital Twin represents a *single instance* of the system of interest (i.e. its corresponding physical twin) not a class or fleet of systems and that the Digital Twin updates its description of that system as it changes over time.

2.2.6.2 Digital Twin vs Simulation Model

Simulation modeling is the process of using a digital prototype of a physical system to predict how the system will perform in reality [35]. Simulation models are often used during the design phase to understand how the system of interest will perform based on assumed operation, loads, degradation mechanisms, etc. This replication of physical system behavior in a virtual environment can sometimes lead to simulation models being mistaken as Digital Twins. The major difference between a simulation model and a Digital Twin is that the simulation model is predicting future states of a physical system based on a set of initial assumptions, rather than tracking current and past states of a single instance of the physical system. A Digital Twin would then track the actual experienced states as that specific instance of the system is used in operation.

A reason that simulation models may be confused with Digital Twins is that while a simulation model is not by itself a Digital Twin, the use of simulation modeling combined with Digital Twins is common. Often the computational models which are used to infer the current state of the Digital Twin are the same models which can be used in simulation to predict future states. This can be even more advantageous when the parameters of these computational/simulation models are updated to reflect the behavior of the specific instance the Digital Twin is representing. These simulation models can then be used to provide additional insights to guide decision-making for optimizing future operations, forecasting degradation mechanisms, and predicting future failures and remaining useful life.

2.2.6.3 Digital Twin vs Surrogate Model

Surrogate modeling is an engineering method that uses approximate models that are computationally cheaper, such as response surfaces, kriging, support vector machines, neural networks, etc. [36] to mimic the behavior of more computationally expensive physics models. It is likely that the confusion between surrogate models and Digital Twins arises from the similarity in how they both use data to update the knowledge about their form. Surrogate models are constructed using data-driven approaches that use a set of training data (inputs and outputs) from the original simulation model to construct a model that mimics the behavior of the original computational model; this approach is similar to ML/AI models.

Thus surrogate/ML/AI models are similar in concept to the way a Digital Twin uses data from the physical system to update its virtual representation. However, despite this similarity, a surrogate model alone is not a Digital Twin as it does not maintain a virtual representation of the states of an instance of a physical system but rather to create a mimicry of a computational model. While a surrogate model is not a Digital Twin, it could be used within a Digital Twin to improve

its functionality when the original computational model is too time-consuming to provide insights within a required decision interval.

2.2.6.4 Digital Twin Data Interconnection

Descriptions of Digital Twins in the literature often put further qualifiers on the data interconnection component. More specifically, to be considered a Digital Twin it is sometimes required that this data interconnection be online and bi-directional [37–40].

The requirement that the virtual-to-physical connection must result in a change in the physical system states is restrictive. While the insights generated from the Digital Twin should provide feedback that serves a targeted outcome, this outcome may not result in a physical state change. An example of such a use case is using a Digital Twin to prioritize and optimize inspection campaigns of large structures. Identifying the highest risk areas for targeted inspections based on the specific operation of this system increases the probability of detecting anomalous conditions and reducing overall risk without resulting in a change of state of the physical system.

The second added requirement is that this data interconnection be *online* [37]. It is implied that *online* means that the data is exchanged automatically between the physical system and the virtual representation and vice-versa. The reason for placing such a requirement on the classification of Digital Twins is likely based on specific use cases. However, such a requirement is overly restrictive and does not account for the many different *offline* human-in-the-loop (HITL) interactions with the physical system, including data collection methods, such as physical inspection, NDE, maintenance logs, etc., and system repair/maintenance actions that could be used to update the virtual representation of system states. Additionally, there are use cases where the immediate exchange of information is not required for the decision-making process [14]. It is proposed that the requirement for a Digital Twin be that information be exchanged between the physical system and the virtual representation to update the virtual system states and parameters. The bi-directional connection from virtual to physical may not always result in change in the physical state (e.g. the action could be additional inspection/data collection). Any additional requirements on how (or how often) this data is collected and exchanged should be determined based on the specific use case and implementation.

2.2.6.5 Digital Twin Fidelity

Another common Digital Twin qualifier found in the literature is with respect to the fidelity of the Digital Twin virtual representation [10,11,37,41–45]. Many of these definitions argue for the Digital Twin to have the highest level of model fidelity feasible. As discussed earlier, the level of model fidelity directly relates to the level of abstraction of reality that is chosen for the virtual representation. While it is typically assumed that a higher fidelity model ensures that the physical system and virtual representation are more closely aligned, this assumption may not be the case if the data that can be collected from the system is not appropriate for the level of model fidelity. Observation and modelling uncertainties

resulting from insufficient data may negate the benefits of the higher fidelity model. Even if the required data could be collected, additional challenges of a high-fidelity approach may also include data storage management, data transfer limitations, computational processing power, and turnaround time for decision support.

In addition to the practical limitations of applying a high-fidelity approach, using such a requirement to classify a Digital Twin is challenging as there is no accepted definition as to what would constitute a high-fidelity representation. From the reviewed literature it is found that the choice of Digital Twin modelling fidelity is primarily driven by the use case; and there are no papers in literature yet to present a Digital Twin implementation which could be considered high-fidelity. This further supports the argument that the level of model fidelity should not be used to define what is classified as a Digital Twin. The only requirement is that the model be a virtual representation of a specific physical system; the fidelity of that model will be dependent on the use case.

2.2.6.6 Data Update Frequency

The final commonly mentioned Digital Twin qualifier is the rate at which data is exchanged between the physical system and the virtual representation. As mentioned in the previous sections, information is exchanged bi-directionally between the physical and virtual spaces. An important component of this interconnection is the frequency at which information is exchanged between the physical space and virtual space. In the literature, this update is commonly described as being real-time [37,38] where changes in the physical state are updated in the virtual representation nearly instantly. While such a qualifier represents an ideal Digital Twin, allowing the physical system and virtual system to act nearly synchronous with each other, placing such a requirement on all Digital Twins is not practical with current technology and is not required for many of the use cases.

As different data streams may be available at different frequencies, the update process may occur as the different datasets become available or may be selected to occur at set intervals based on the use case and the frequency in which a decision will need to be made. For example, in [14], a Digital Twin for fatigue crack growth on an aircraft wing collected data during each mission, and state estimation was performed to update the virtual representation after each mission. This frequency was consistent with the decision-making interval for this use case where mission planning was desired on a flight-by-flight basis.

While real-time update of all the system states of interest is ideal, it is often not practical to define a Digital Twin by this requirement given varying frequencies of different data collection systems and HITL data collection efforts. The proposed approach is to instead implement a model updating process appropriate for the specific use case, which utilizes all the available system information at the time of the update to provide the inference of the current system states.

2.2.6.7 Summary of Qualifiers

Distinguishing a Digital Twin from other digital modeling and simulation approaches is based on the following qualifiers:

1. The virtual representation represents a *single instance* of a physical system; and
2. Data/information from the physical system is used to update the states of the virtual representation over time.

Any additional requirements placed on specific characteristics of the Digital Twin, such as the examples provided in this section, should not be included in the definition; rather, they should be based on the specific use case being considered and established during the Digital Twin implementation.

2.3 Digital Twin Implementation

Digital transformation is viewed as an enabler of more innovative, optimized, and effective products and processes and is a key component of Industry 4.0 [46]. The practical implementation of Digital Twins aligns with the concept of digital transformation, where a principal objective is the innovation of business models to reflect the value that can derived from data. Similar to the definition and characteristics of a Digital Twin, there is also a breadth and variety of technical elements that comprise a Digital Twin implementation that we seek to generalize. The key aspects of a Digital Twin implementation include specifying intended outcomes, scoping the solution (both defining the physical system of interest and levels of abstraction), creation of the virtual representation, and establishing required data interconnections.

A brief review of current industry implementations of Digital Twins can be generally grouped into three categories: Digital Twin component solutions, commercial off-the-shelf solutions, or custom hybrid combinations. A large number of the marketed Digital Twin product offerings are component solutions, provided by companies that provide platform services, such as Microsoft [47], or by digital model/digital simulation companies, such as Ansys [48]. These providers typically market Digital Twin approaches that utilize components from their product offerings that can be combined together to create a customer-specific Digital Twin implementation but how the Digital Twin is constructed is left to the end user. This category of solutions has also led to collaborations between companies to enable easier integrations between their capabilities as customers seek functionality that may not be wholly available within a single solution providers product portfolio. The next most common category is off-the-shelf Digital Twin solutions. These are typically provided by the original equipment manufacturer (OEM), such as GE [49], for common industry uses cases. The final group are completely custom hybrid approaches, where the end-user constructs their own solution, usually from a combination of commercial and custom products. The extent of the industrial application of a hybrid approach is challenging to estimate since it is for an organization's internal use, however this case may be the most effective at achieving specific outcomes,

since the capabilities can be wholly customized to a specific use case and the features can be implemented incrementally based on evaluated cost and business value.

2.3.1 Digital Twin Outcome Identification

Colin Parris, Vice President of Software Research at the GE Global Research Center, described a Digital Twin as "*a living model that drives a business outcome*" [32]. Identifying the intended outcomes enables the scope of the Digital Twin to be realistically bounded to achieve these outcomes. The targeted outcomes should be measurable and quantifiable, which allows for the value proposition for a Digital Twin to be defined by its ability to result in a positive change toward the targeted outcomes. These outcomes can be wide-ranging and industry-specific; some common outcomes associated with Digital Twins include including reducing costs [2–4] and risk [5], improving efficiency [6], improving service offerings [7,8], security [9], reliability [10,11], resilience [12], and supporting decision-making [13–15].

2.3.2 Digital Twin Scope

When designing the Digital Twin, the principle of parsimony should be observed to ensure that the determined scope can meet the intended outcomes without adding additional complexity or cost that might compromise its feasibility. While Digital Twins may theoretically be used to represent the chosen system to an atomistic level of resolution, the intended application and desired outcomes determine the rationale by which to select the appropriate scope and abstraction level of the Digital Twin.

The first aspect of setting the scope for the Digital Twin is determining the portion of the physical reality that will be modeled, which sets the boundary between the physical system of interest and its surrounding physical environment, as described in the previous section. This boundary should be selected to ensure the appropriate level of detail to achieve the targeted outcomes while minimizing the resulting model complexity.

The second aspect of setting the Digital Twin scope is determining the required level of abstraction. The level of abstraction determines the collection of physical system states that are to be modelled and maintained. The selected level of abstraction also determines the fidelity of the computational models that are to be used. Considering the principle of parsimony, the level of abstraction/model fidelity should be only as detailed as required to achieve the targeted outcomes. Refer to Section 2.2.6.5 for further discussion.

When scoping the Digital Twin implementation, consideration could be given to supporting models at varying levels of abstraction, allowing the users to switch between the levels as needed to achieve the targeted outcomes. Consideration should also be given to the varying time constants for the different physical processes being modeled. For example, vibration is typically measured on the order of milliseconds and corrosion is often measured on the order of years. For

this to be managed, the Digital Twin must often support models of different levels of abstraction, while ensuring that the shared system states between models of different levels of abstraction remain consistent.

2.3.3 Digital Twin Virtual Representation

The first element of the virtual representation is creation of the data models. The states of interest, both current and historical, are retained in the data models. In the literature, when discussing data management, cloud computing environments are mentioned [3,41,44]. A cloud-based data management system provides advantages in accessibility, scalable data storage and processing power, and efficient data transfer. Local data storage systems may also be used and may be required in cases where security of the data is a concern. Practical implementations may consider combinations of local and remote data management approaches (edge, mainframe, fog and cloud). Further, data visualization may often be used in conjunction with data models to provide additional insight into the data. The purpose of these visualizations is to represent the raw data in a format that supports more efficient decision-making and may include simple statistics, summary data, and data tagged to visual representations of the system of interest.

The second element of the virtual representation is the implementation of the relevant computational models. The use of models in Digital Twins is generally for two purposes: the inverse problem and the forward problem. The first is the data fusion and system identification process where states and parameters of the Digital Twin must be estimated using the observed information (i.e., inverse problem). The second purpose (i.e., forward problem) is to apply virtual processes to the virtual system to simulate how the system states will change based on forecasted changes in the physical environment or the application of physical processes (e.g., loading on a structure). The goal of these simulations is to result in action decisions which are transferred from the virtual space to the physical space to result in physical system state changes that support the outcomes. As discussed earlier, computational models can be categorized as either physics-based models or data-driven models, and the selection of the appropriate model is dependent on the available data/information collected from the physical system and the known relationships between the collected data and the states of interest that cannot be directly measured.

In addition to the data models and computational models, visualization is a critical aspect of the Digital Twin implementation, in order to provide the decision-maker with a clear interpretation of the data to provide confidence in the decision. Also, visualization tools serve to improve the overall acceptance of the Digital Twin and demonstrate its value to the organizational leadership and non-domain experts.

Since there are very few end-to-end Digital Twin solutions currently available in the market and given the breadth of Digital Twin applications and the variety of technologies a Digital Twin employs, it is likely that a hybrid approach that combines custom Digital Twin data management systems that can be easily connected to COTS tools will be applied. For

this approach to succeed, there will need to be an ongoing effort to facilitate more efficient and consistent data exchange, supported by future standards. This has been recognized in the industry and such efforts are currently ongoing [50].

2.3.4 Digital Twin Data Interconnections

The implementation of Digital Twin data interconnections requires decisions regarding how data is to be collected, the frequency at which the data is collected, and how the data is exchanged between the physical and virtual spaces.

After the Digital Twin creation, ongoing data collection for Digital Twins largely focuses on sensor technology. However, as previously mentioned, offline data collection is also relevant, including inspections and NDE. Further heterogenous data may also be available from logbooks, maintenance records, pictures/video, subject matter expert opinions, etc. The required technology and processes to collect, process and fuse these data sources should be considered during implementation.

The next aspect of the data interconnection is the frequency at which data is collected and exchanged, also known as the Digital Twin update frequency. This is often driven by the decision interval, which is defined as the time scale on which a decision needs to be undertaken. In cases of operational decision making, the decision interval may be on the order of seconds or minutes, however for asset integrity management cases, the decision interval may be on the order of months or years. It should also be noted that there also may be cases where sensor data is collected at a high frequency, but it is only exchanged with the virtual representation on a periodic basis in batch format due to data transfer limitations.

A final consideration is the technology and processes that need to be implemented to support the virtual-to-physical connection. As noted earlier, this exchange may be through the use of the Digital Twin to control actuators in the physical space that result in the states of the physical system changing. Similar to the physical-to-virtual interconnection, this requires establishing the required data exchange processes and control systems that allow for the Digital Twin to enact the specified actions. Another approach is the use of HITL to use information/insights from the Digital Twin to lead to physical actions which either result in a physical state change or in the collection of additional information from the physical system. In these cases, consideration must be given to existing processes. As the implemented Digital Twin should by design align with these processes, the information exchange and decision-making points in the process need to be identified. Once these points are identified, the mechanism by which the information is to be exchanged and the procedures for making decision based on this information should be codified.

2.4 Digital Twin Implementation Case Study

The proposed implementation process is demonstrated through a case study where a Digital Twin is developed to support the ongoing asset integrity management of a naval vessel.

2.4.1 Digital Twin Outcomes

It was observed that prescriptive scheduled inspections of the vessel's structure often resulted in finding unexpected structural issues that were leading to extended drydock stays resulting in higher costs and reduced mission availability [51]. Based on these observed challenges, the primary outcomes of the Digital Twin implementation are an increase in the operational availability and a reduction in the associated operational expenses over the life of the asset.

Additionally, secondary outcomes include the reduction of risks associated with emergency response situations where detailed engineering analysis, such as Finite Element Analysis (FEA), is required to answer stakeholder questions before any resumption of operations and the extension of the vessel's life beyond its original intended design life [51].

2.4.2 Digital Twin Scope

Based on the targeted outcomes, the physical system to be represented as a Digital Twin is selected to be the hull structure of the vessel. Based on this selection, the corresponding physical environment that is of interest is the local wave environment and local weather environment that the vessel operates in. The physical processes of interest include the loading processes (e.g. wave loads, thermal loads, and cargo loads) and degradation processes (e.g. coating breakdown, corrosion, and structural fatigue).

The fidelity of the Digital Twin was maintained at several different levels of abstraction within several data models and computational models based on their intended use. For example, a lower fidelity compartment-based model, shown in Figure 2.3, was used for recording the asset condition during visual inspections. The condition and the presence of any anomalies are tagged to the relevant compartment and the database supports the storage of accompanying supporting information, such as written reports and pictures. These results are then tagged directly to the relevant structural components in a higher fidelity data model maintained onshore. The higher fidelity model can then be used to generate computational models, such as finite element analysis (FEA) models at varying levels of fidelity based on the analysis requirements. In this use case, the term *model fidelity* refers to the level of detail at which the structural components are represented. For example, at the lowest level, only the boundaries of each of the structural compartments are represented. At the highest level, every structural component down to an individual bracket is modeled.

The vessel initially had very few sensors available for monitoring the hull structure, so this limited the fidelity of several of the computational models, particularly the loading models. Other data sources were used in combination with computational models to infer the vessel response to the experienced wave conditions and determine the resulting stresses at representative critical areas.

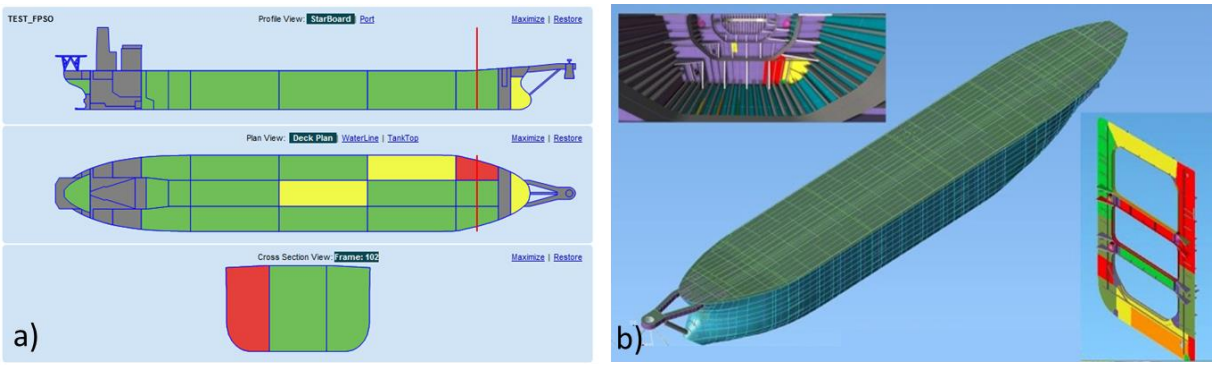

Figure 2.3. Example Digital Twin models: a) low-fidelity compartment model, b) high-fidelity structural component model

2.4.3 Digital Twin Virtual Representation

It was determined that no available solution could achieve the targeted outcomes, so a hybrid approach was adopted which required the integration of several different solutions for both the data models and computational models. It was also recognized that an incremental implementation approach should be adopted to reduce the upfront implementation costs and identify where incremental enhancements to the Digital Twin, both in terms of scope and fidelity, would be best applied to achieve the targeted outcomes. For this use case, a series of data models and computational models were implemented to represent both the system and its corresponding environment.

First, the data model for the virtual system representing the structural condition was selected as a CAD-based system that had been optimized for managing marine inspection data. This model also provided the necessary fidelity to support all the other planned data models and computational models. The advantage of the selected system is that it also included the lower fidelity compartment-based model for use in the field to collect inspection data. The advantage of using a lower-fidelity model for data entry in the field is the reduced computational requirements for loading and running the model, and the easier data entry, since information is tagged based on the compartment the inspector is in rather than having to tag it to the specific structural component. This aligns with existing inspection processes, and any findings during the inspection can be tagged to the specific structural components in the high-fidelity model by engineers in the office. These two models operate on a shared database, so that inspection results and anomalies tagged in one model are also represented in the other model at the appropriate fidelity which also ensures that the Digital Twin virtual representations remain in synch as a single representation instance.

In addition to the data models, two computational models were implemented as part of the virtual system. The first was a set of FEA models, including a full-ship model and several local models of critical connections. These models are linked to the high-fidelity condition data model, so that the relevant properties can be updated as the condition changes. The results of the computational models can also be fed back to the condition data model if an anomalous condition is

determined from the analysis. The other computational model is the hydrodynamics model, which is used to determine the vessel response to specific wave conditions.

As previously mentioned, there were limited sensors installed aboard the vessel so the vessel response to the environment could not be measured directly. As an alternative, use of location analytics (LA) integrated with non-location analytics (NLA), is employed enable spatial modeling of the vessel's environmental exposure [52]. A data model of the vessel's GPS position information is fused with wave exposure data from hindcast weather models. By creating a virtual representation of the corresponding environment, this data can be used with the computational models in the virtual representation to determine the resultant loading and impact on the structure.

The final models are the degradation process models, which provide virtual representations of the physical degradation processes, particularly coating breakdown, and corrosion. These models are data-driven models which use machine learning to update the computational model parameters based on the observed data. Developing vessel-specific degradation models is useful in providing forecasts of the future structural condition to be used in determining inspection and repair intervals.

2.4.4 Digital Twin Data Interconnections

The final component of the implementation is the set of data interconnections. The first interconnections are the ship-to-shore data exchanges for the limited sensor data and the inspection data collected in the low-fidelity data model. Ships often have limited bandwidth to exchange data, so it is often batched ashore during port visits. A database replication is performed during these batch data exchanges to ensure that the shore-based and ship-based databases are synchronized.

The second set of interconnections is the collection of data from third party sources for tracking the position and weather information. This data is collected daily and stored in a shore-based database.

The final data exchange is the digitizing and entry of HITL data. Some of this data is captured and digitized when it is input to the low fidelity data model. However, other sources, such as thickness measurements are collected by third-party contractors and must be digitized and entered manually in the data model. To reduce the level of manual effort, the data model can be used to generate a thickness measurement plan that is provided to the third-party contractor. After data is input to the provided plan, it can be automatically mapped back into the data model, significantly reducing the manual effort.

2.4.5 Initial Results and Next Steps

One challenge in evaluating Digital Twins is quantifying their value. This is often because they align with an existing process that may provide a majority of the business value and the advantage the Digital Twin provides is the digitalization of that process to provide further efficiency or automation. Also, part of the benefit provided by a Digital Twin is as a

type of insurance, reducing risks and costs during emergency scenarios which may only occur in rare instances. Finally, as a Digital Twin is intended for use during the entire life of the asset, the accumulated benefits may take time to observe and quantify.

In this case study, while the implementation has not been in use long enough to confirm that the primary outcomes are being achieved, the Digital Twin implementation has been successful in supporting the resolution of an observed structural design deficiency. The availability of the data and models enabled an efficient root cause analysis and supported redesign of the problem region.

2.5 Digital Twin Implementation Challenges and Opportunities

This section highlights the challenges associated with developing and incorporating Digital Twins in practical applications in additional to some possible paths forward. Many of the enabling technologies for Digital Twins are in various states of advancement, progressing as a function of both industry need and technology readiness/maturity. Digital Twin solutions, driven by specific desired outcomes, are being pieced together based on industry need, but there are still some significant challenges limiting the Digital Twin technology potential, as discussed below.

- **Terminology:** Consistent terminology needs to be defined to facilitate a common understanding and prevent miscommunication across multiple interacting technical domains and stakeholders.
- **Standardization:** A wide range of technologies ranging from data collection to insight generation to decision-making need to be standardized. However, the standards development process is often slow, resulting in slow wide-scale adoption of digital twins.
- **Organizational culture:** Cooperation and collaboration in the sharing of data and models is required among multiple stakeholders, with potentially competing business objectives. Fair value, data security and intellectual property rights need to be ensured among the stakeholders.
- **Technology Maturity:** Digital Twins are likely constructed from a patchwork of technologies and solutions from several different vendors. Technology development needs to prioritize technologies that offer the most meaningful increases in efficiency and effectiveness, considering the current technology maturity which impacts the timeline and cost for such development.
- **Verification and Validation:** The Digital Twin is typically comprised of a number of different models and processes which require both V&V individually and as a comprehensive system. However, since the Digital Twin by definition is unique to the specifically modeled physical system, it may not be possible to validate a single instance, full system model. Extrapolation from individual component model V&V to the full system is challenging.

- **Automation:** A prominent targeted outcome in many digital twin implementations is to reduce the manual effort through automation of data exchange and analysis. While development efforts are underway, there is still a strong reliance on human-in-the-loop as part of current solutions.

2.6 Summary

This Chapter has sought to generalize the characterization of the Digital Twin and provide a consolidated definition that can be used to clearly classify what is and is not a Digital Twin. After providing a definition and characterization, the process by which Digital Twins can be practically implemented was discussed, highlighting the key design decisions and implementation strategies. This approach was explored through a representative case study.

The design and implementation of a Digital Twin, including the details of its components, should be driven by desired outcome(s). This will help to set the requirements for the required data, models, and processes to update the models based on the data. Digital Twin implementations require the incorporation of a variety of different enabling technologies, and bringing these technologies together is still an ongoing challenge. Several approaches can be considered: build a Digital Twin using existing commercial tools, construct a Digital Twin from commercial components, or a hybrid approach.

Some of the challenges to Digital Twin implementation are technical in nature and can be resolved through continued research and development. Other challenges are cultural and will require disrupting current operating models and ways of thinking. The Digital Twin concept is clearly still evolving, as seen in the diversity of new industries and use cases that Digital Twins are being applied to. This continued concept evolution is also apparent in the lack of concrete examples demonstrating the clear benefits of Digital Twins in practice. Despite the concept's popularity, this has raised questions regarding the technology's ability to provide tangible improvements over existing processes. Answering these questions will require successful demonstrations of the technology's value.

CHAPTER 3

DIGITAL TWIN IMPLEMENTATION FOR VESSEL-SPECIFIC FATIGUE DAMAGE MONITORING AND PROGNOSIS

3.1 Introduction

Historical evidence has shown that fatigue damage is one of the dominant failure mechanisms in ocean-going vessels. Fatigue cracks in marine vessels reduce the overall reliability and can pose a threat of causing further significant damage when exposed to severe operating environments. Accurate fatigue assessment is critical for decision making regarding structural inspection and maintenance planning, future operations, and potential life extension. This assessment includes both the estimation of the vessel's current fatigue damage accumulation and the forecasting of future fatigue damage based on the vessel's historical operations in order to optimize planned maintenance and future operations to improve vessel reliability.

Multiple uncertainty sources affect vessel fatigue damage assessment, and the influence of these uncertainty sources has been investigated by several studies in the context of two commonly used fatigue analysis approaches: S-N curve-based [53–55] and fracture mechanics-based [56–59]. Most studies using these two approaches focused on S-N curve parameters uncertainty, model uncertainty (e.g. model uncertainty relevant to stress calculation), and random variables related to fracture mechanics (e.g. initial crack size, crack growth parameter, geometry factor, and stress distribution parameter). However, relatively limited research has been performed so far to investigate the influence of uncertain wave conditions on the vessel's fatigue damage assessment, which contributes significantly to the vessel fatigue damage accumulation. As a result of all these sources of uncertainty and the variability in vessel-specific operation, population-based design approaches must err on the side of conservatism. To support operational decision-making, the approach can be individualized, to continuously update based on the vessel-specific operation. Some work has been done for floating storage and offloading (FPSO) units [60–62], however this assessment did not require taking into account vessel movement (i.e. vessel routes, speed, and heading). Therefore, it is necessary to investigate the effect of vessel-specific wave conditions on the fatigue damage estimation and prediction, accounting for vessel routes. This provides the motivation for the development of a Digital Twin solution for ocean-going marine vessels.

Digital Twin is one of the promising digital technologies being developed at present to support digital transformation efforts in multiple industries. Defined as "*a virtual representation of a physical system (and its associated environment and processes) that is updated through the exchange of information between the physical and virtual systems"* [63], the Digital Twin provides the components necessary to acquire, manage, and analyze the required vessel-specific information to continuously update the knowledge regarding the current state of fatigue damage accumulation in a particular individual vessel. The data and engineering analysis models maintained in the vessel's Digital Twin can then be used to forecast future fatigue damage.

One of the key characteristics of a Digital Twin is the interconnection of information between the virtual representation and the physical reality. This is often achieved through the use of sensors which can directly measure the structural response and take into account many of the complex or unknown contributing factors. For monitoring fatigue, hull monitoring systems can be used to directly record the strain or motion measurements of the structural response as a function of the operating environment; then this data can be used to estimate the accumulated fatigue damage. However, the implementation of such monitoring systems is often cost prohibitive which limits their regular usage. As an alternative, this Chapter explores an approach which uses publicly available vessel operational data to incorporate the experienced wave conditions when estimating the structural response and the corresponding accumulated fatigue damage. Several studies have investigated the use of numerical models combined with observed wave to account for the uncertainty associated with the experienced wave environment when monitoring fatigue damage in marine vessels. In Magoga et al. [64], a fatigue monitoring system used strain gauge sensor data in a cumulative fatigue damage approach, but the study also mentioned how a wave spectral approach based on recorded encountered wave environment could be used as an alternative input. Thompson [65] performed a preliminary study for determining the resulting stress spectra based on metocean hindcast data without instrumentation and compared the results with data obtained from a single midship strain gauge, but this study did not include the determination of the resultant fatigue damage accumulation or forecast of the remaining useful life. Nielsen et al. [66] applied an alternative approach based on measured vessel response, also called "ship as a wave buoy," which used wave data and transfer functions as an alternative to direct hull strain monitoring. Hulkkonen et al. [67] proposed a similar methodology to the one applied in this study. This work extends the existing literature by demonstrating an end-to-end framework for a Digital Twin implementation of the proposed approach.

The objective of this Chapter is to investigate the novel use of a Digital Twin to incorporate the effect of vessel-specific wave conditions on the estimated accumulated fatigue damage and future fatigue damage prediction considering the uncertain future wave conditions. The Digital Twin for this solution is comprised of data models and computational models to infer and monitor the fatigue damage based on the Spectral-Based Fatigue Analysis (SFA) approach [68]. The resulting vessel-specific fatigue models are then used in a Monte Carlo simulation to forecast future fatigue damage and estimate the remaining fatigue life. Limitations in the vessel-specific input data related to the experienced sea states are also examined and the various approaches to managing these data gaps are compared. The future fatigue damage prediction using Monte Carlo simulation considers both historical routing and experienced waves and the wave conditions for unrestricted services. The integration of this entire end-to-end process in a Digital Twin provides a scalable solution to monitor vessel-specific fatigue damage across a fleet via automation. The application of this methodology is demonstrated through a case study.

Contributions of this Chapter include the end-to-end development, integration, and automation of a Digital Twin framework for monitoring vessel-specific fatigue damage. The damage estimate is updated based on publicly available

position and ocean condition data in the absence of on-board sensor data. This framework also proposes and compares several vessel-specific fatigue accumulation methodology options as part of the Digital Twin framework.

The proposed Digital Twin methodology for fatigue management is developed in Section 3.2. The results from a case study applying the methodology to a containership that has operated a trans-Pacific route for 6.5 years is presented in Section 3.3. Conclusions and future work are discussed in Section 3.4.

3.2 Methodology

First, based on the intended outcomes, the Digital Twin is developed, comprised of the necessary data and computational models. The Digital Twin is then used to update the ship fatigue damage accumulation based on performing fatigue assessments using publicly available vessel operational data. The Digital Twin updating methodology is comprised of two major processes; the collection, processing, and analysis of the operational data to obtain the vessel-specific wave conditions and the use of these wave conditions in the fatigue analysis. In this section, the basic elements of the Digital Twin are discussed first, followed by a description its implementation for the monitoring and prognosis of vessel-specific fatigue damage.

3.2.1 Digital Twin

Colin Parris, Vice President of Software Research at the GE Global Research Center, described a Digital Twin as "*a living model that drives a business outcome*" [32] which sets the scope for the design of the Digital Twin. This scope includes the selected physical reality to be modeled, a virtual representation of that selected physical reality, and the data connections between a physical reality and the virtual representation, as shown in Figure 3.1. As the physical system is operated, information is collected and interpreted to update the corresponding virtual representation. The updated representation can then be used to provide insights which guide decision-making to achieve the intended outcomes.

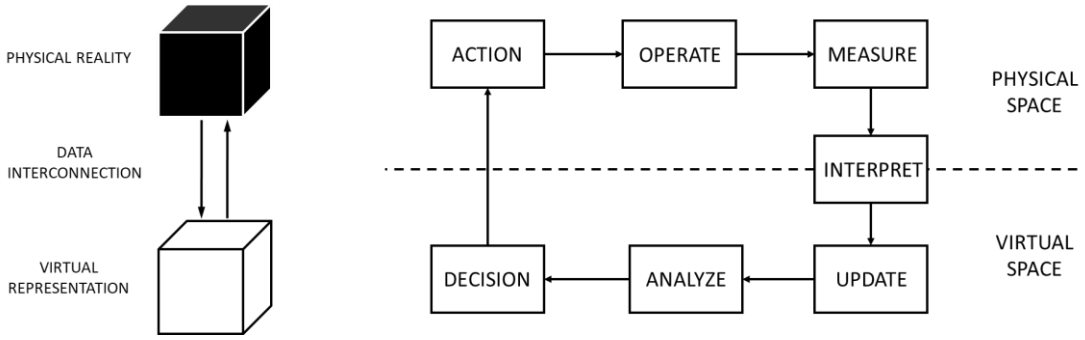

Figure 3.1. Digital twin components and high-level processes

In this Chapter, the outcome the Digital Twin is intended to deliver is the monitoring and prognosis of the fatigue damage accumulation in order to support maintenance and operational decisions. Fatigue damage accumulation can be challenging to directly observe in large structures, especially during the crack initiation stage. When fatigue damage cannot be directly observed, it can instead be inferred from the available data and the vessel-specific analysis models associated with the virtual representation.

The first component of the digital twin is the physical reality. This is comprised of the physical system, which is the portion of the physical reality chosen for modeling, and the physical environment which are the aspects of the physical reality outside of the selected physical system which affect the system. Based on these desired outcomes for this Digital Twin application, the physical system of interest is set to be the selected representative critical areas that are to be monitored for fatigue. However, while only these critical areas are of interest for the fatigue monitoring, the physical system must also include the entire hull system to account for the hydrodynamics and structural response that govern the fatigue damage accumulation for these critical areas. The aspects of the corresponding physical environment that are of interest are the wave conditions experienced by the vessel due to its operation. Finally, the physical processes considered include operational conditions, such as vessel loading, vessel speed, heading, etc.

The second component of the Digital Twin is the virtual representation. The virtual representation is the collection of data and computational models of the selected physical system and physical environment at a chosen level of abstraction. For this application, based on the selected physical system and environment, the Digital Twin virtual representation can be characterized as the combination of the resulting data models and computational models described below and shown in Figure 3.2. The term data model is used here to refer to the combination of both data collection, storage, and processing.

- Data Models:
    - Vessel position data model (e.g. AIS position data)
    - Experienced wave condition data model
    - Fatigue damage accumulation model (one for each representative critical area considered)
- Computational Models:
    - Hydrodynamic seakeeping model
    - Full-ship FEA model
    - Spectral fatigue analysis model
    - Monte Carlo fatigue prognosis model

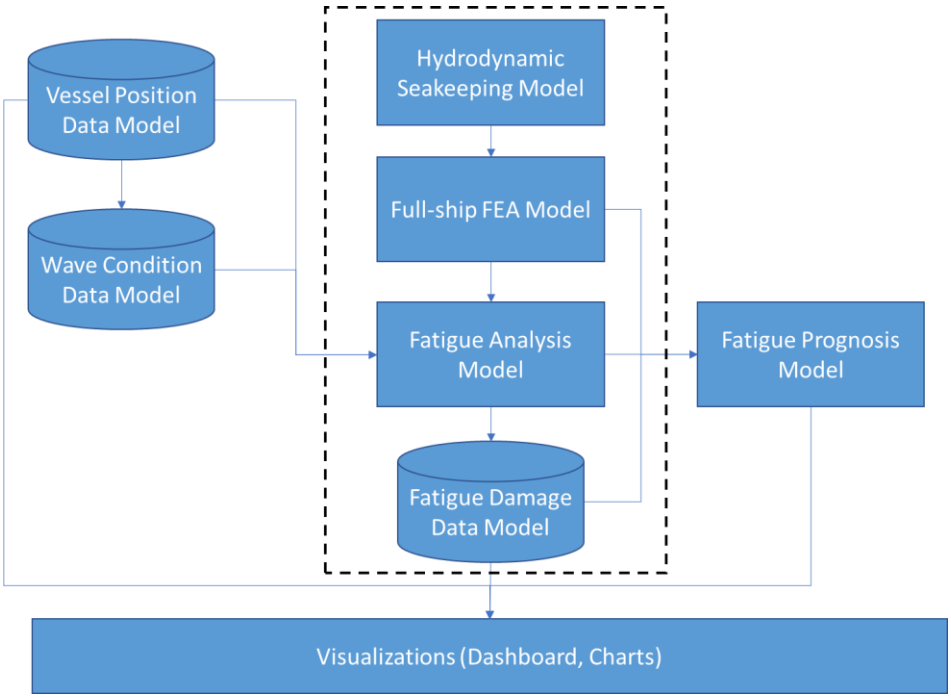

Figure 3.2. Digital Twin virtual representation setup

The final component of the Digital Twin definition is the interconnection between the physical reality and the virtual representation where data/information is exchanged in two directions: physical-to-virtual and virtual-to-physical [30]. For this use case, the data being exchanged from the physical reality to the virtual representation is the vessel position and wave condition data. The information exchange from the virtual representation to the physical reality is through informed decision-making; which could include changing vessel operations to minimize fatigue damage or planning for future inspections or maintenance.

The implementation of the above data models and computational models and the use of these models in the updating and prognosis processes to achieve the targeted outcomes is detailed in the following sub-sections.

3.2.2 Vessel Position Data Model

The Digital Twin vessel position data model is the data repository for importing, processing, and storing the vessel position data. For this application, the position data is stored and managed in cloud-based SQL databases.

3.2.2.1 AIS Position Data

Vessel position can be monitored using the ship's GPS or by publicly available Automatic Identification System (AIS) data. AIS data also provides the ship's operational history, including position, speed, heading, and draft. In this study, the vessel's AIS data is used to provide the vessel's position data. AIS is an automatic tracking system utilized in the maritime sector to supplement marine radar for the purposes of collision avoidance. AIS data includes information such as unique

vessel identification, position, course, and speed. Global AIS transceiver data is also collected via terrestrial antennas and satellite networks, aggregated and then made available online through a number of service providers. Figure 3.3 shows an example of AIS position data. AIS data is becoming a more common source of data in studies of vessel risk analysis as it can be easily combined with additional data sources to better understand and study and quantify potential risks to the vessel as a function of its operation [69–72].

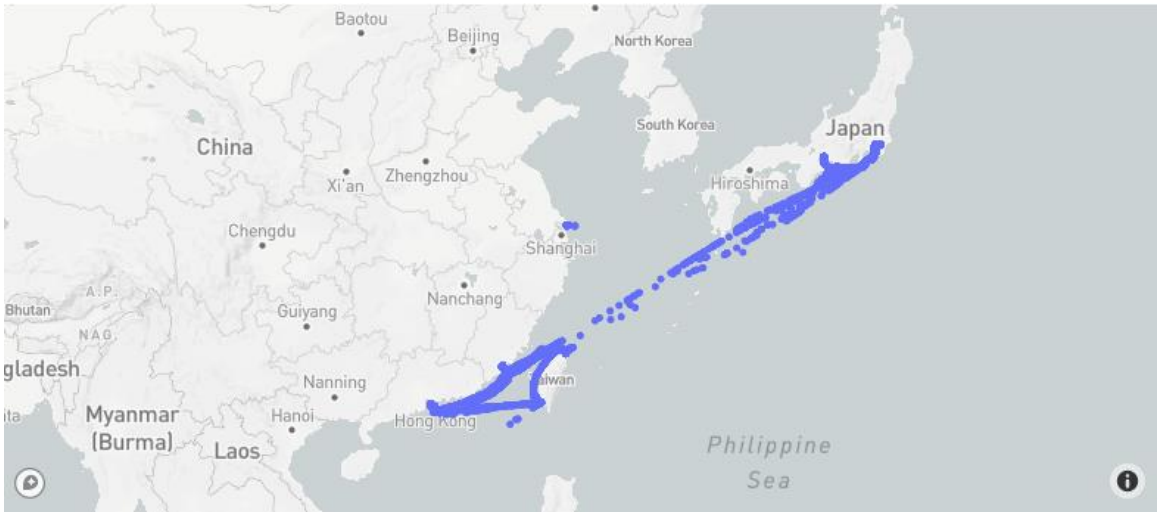

Figure 3.3. Example of AIS data (AIS data provided by Spire Global, Inc)

For this application, AIS data for the worldwide fleet is automatically retrieved from the service provider's API every five minutes and stored in the SQL database. AIS position messages containing the unique vessel identification, position, course, and speed are stored in one data table. AIS static and voyage data messages which contains information about the vessel's draft are retrieved with a separate API and stored in a different SQL table. Creation of the vessel specific position SQL table uses the unique vessel identifier to retrieve the corresponding position messages and static messages which are then merged to create a single vessel-specific position data model. This vessel-specific table is updated daily from the global fleet data to be used in the fatigue damage estimation.

While AIS position messages are transmitted every 2 to 10 seconds while the vessel is underway and every 3 minutes while the vessel is stationary (in port or at anchor), the data collected via the receiver networks rarely contains AIS data at the same fidelity as transmitted. It is quite common for specific vessels to have data gaps of multiple hours or sometimes even days when AIS data is unavailable as the message was not received by the global network [73]. Since these gaps limit the ability to interpolate the corresponding sea state experienced during the vessel's operation, it is necessary to develop an approach to account for the uncertainty introduced by these data gaps.

3.2.2.2 AIS Data Resampling and Rerouting

Since the AIS data is a sequence of observations strictly increasing in time but with non-constant spacing, it can be considered an irregularly-spaced time series. A method to process irregularly-spaced time series is to transform the data into equally-spaced observations using an interpolation method. This is the approach that is used in this Chapter. First the AIS data is upsampled (i.e., increased number of data points) to have an evenly-spaced time series with the spacing consistent with the smallest time difference between the original position data time stamps. The position latitude and longitude values are linearly interpolated for the upsampled time stamps. Since the smallest time difference is often less than a minute, this results in more data points than needed for determining the sea state exposure; therefore, the resultant position data is then downsampled to a 1-hour interval. In addition to providing complete coverage, this route interpolation approach also supports improved data management. When the vessel is in operation, AIS messages may be available at a high frequency (i.e. sub-minute) which can result in a large volume of position data. While beneficial for applications such as collision avoidance, this high volume of data does not provide any additional benefit for the fatigue calculation and simply increases the overall calculation effort. Initial testing of the proposed upsampling and downsampling approach increased temporal coverage by 30% while reducing data volume by 80%.

In most cases, the straight-line interpolation produced by the upsampling/downsampling approach produces tracks that do not overlap or avoid coming too close to a land mass. However, when the simple method does not produce acceptable results, the resulting interpolated vessel positions must be rerouted accordingly. This may occur when the vessel is navigating around a land mass but has position data gaps during this period. In these cases, the upsampling/downsampling approach may result in invalid vessel positions that fall on or near land and therefore cannot be used to obtain the corresponding metocean data. To resolve this, a simple rerouting approach is proposed here to ensure that all points fall outside of land masses allowing for the corresponding metocean conditions to be estimated. Ocean shapefiles from the North American Cartographic Information Society [74] are used to represent the landmasses in the region of transit as multi-polygons. To ensure that that updated points fall within the region where the metocean data can be interpolated, the bounding polygon is scaled outward by a factor of 1.05 and then smoothed. An example is shown for the island of Taiwan in Figure 4, where the blue line represents the original coastal multi-polygon boundary, the orange line represents the scaled bounding polygon, and the green line is the smoothed polygon. Each vessel position points are iteratively checked to determine if they fall within the resulting boundary curves of any landmass multi-polygons. Any point that is determined to fall within a boundary curve must be moved to an adjacent location outside of the landmass. To determine where these points should be moved, each position point identified as falling within the original land mass multi-polygon is projected onto the resultant multi-polygon. Finally, since the projection of these points results in a path that of a different length than the originally interpolated path, the projected position points are re-spaced to match the sampling time interval.

Each step of the process is shown in Figure 3.5. First the original position points (orange points) are upsampled and then downsampled to create the complete data set (red points) in Figure 3.5b. These points are then evaluated to determine if they fall within the scaled and smoothed boundary multi-polygon (green boundary in Figure 3.4 Those points determined to be within the boundary are then projected onto that boundary. This results in the update position points (green points) in Figure 3.5c. Finally, the adjusted position points are respaced to ensure that the original sampling time interval is maintained.

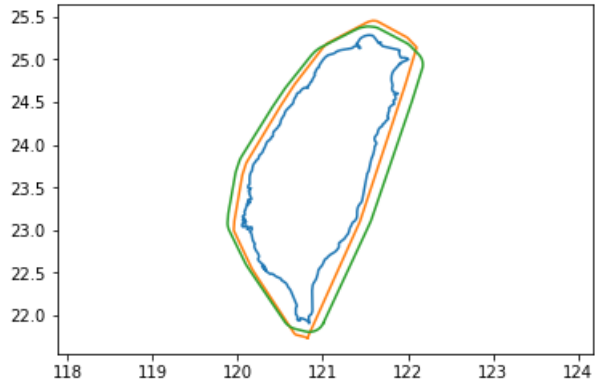

Figure 3.4. Landmass polygon creation

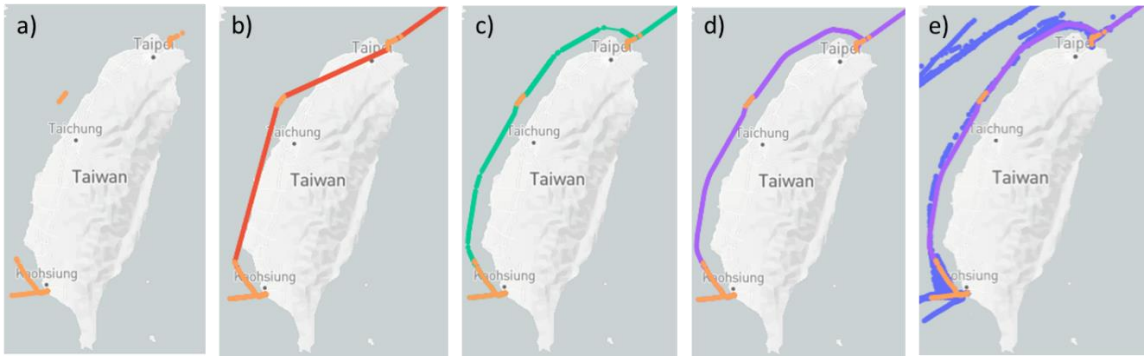

Figure 3.5. Example of AIS data rerouting: a) original AIS position data, b) upsampled/downsampled position data, c) re-routed position data to avoid land, d) re-spaced position data to maintain consistent sampling frequency, e) comparison of re-routed/re-spaced positions (purple) with historical positions for same vessel during a different transit (blue)

In the example shown in Figure 3.5, the resulting re-routed points were compared with AIS data for the same vessel transiting a similar route at a different period of time and the re-routed points with the observed similar transit routes shows generally good agreement as seen in Figure 5d. It should be noted that while this approach provides a more complete position dataset and ensures that points do not fall within land masses, it cannot account for all possible AIS data gaps. For example, this approach cannot recreate the behavior of the vessel during large data gaps or with substantial changes in course between available data points. When large gaps in AIS data are present, the re-routed points may not

accurately reflect the exact transit path of the vessel. The impact of these inexact position points requires further study. As will be discussed in the following section, the spatial and temporal resolution of the metocean data combined with the generalizations of the sea state characterization applied in the fatigue assessment likely mitigate the impact of the approximation in interpolating the transit route.

The resulting processed vessel position data is then inserted into the Digital Twin vessel position data model replacing the original data to be used in further analyses.

3.2.3 Wave Condition Data Model

The Digital Twin wave condition model maintains the virtual representation of the physical environment that is required for the fatigue damage assessment. For this application, the wave condition data is also stored and managed in a cloud-based SQL database.

3.2.3.1 Metocean Hindcast Data

The vessel-specific wave conditions that a ship has experienced during a given service period can be constructed based on either onboard wave measurements (such as through installed wave radar) [75] or metocean parameters generated from numerical hindcast models [76,77]. Equipment for direct measurement, such as wave radars, are expensive and therefore have limited installment on commercial vessels. Therefore, in this study, the vessel-specific wave conditions are determined using publicly available metocean hindcast data. The use of metocean hindcast data in vessel structural analysis is fairly limited in the literature [64–67,78]. The results from these studies have demonstrated that the stress spectra generated from metocean, hydrodynamic, and structural models show favorable agreement with the stress spectra generated from direct measurement using strain gauges. This motivates further investigation of its application in a Digital Twin to monitor vessel fatigue.

Metocean hindcast are numerical atmospheric and ocean response models that are run for a historical period to generate the wave spectra at selected points and time steps. These models can be computationally expensive to run for a large number of points and time steps; however, several organizations provide global datasets for extended periods of time. One of these sources is the global NOAA NWS NCEP WaveWatchIII ® (WWIII) [76] metocean hindcast data, which has been used by several studies to perform stress or fatigue estimation [61,62,78] and is adopted for generating vessel-specific wave conditions in this study. Metocean hindcast data has been found to be a reliable estimate of actual metocean conditions, particularly in deep water [79]. However, the WWIII model assumptions limit its applicability in shallow water, especially near shore [80]. The WWIII model resolution also limits its ability to fully resolve storm conditions, such as hurricanes and typhoons [80]. Other publicly available sources of metocean data include ECMWF ERA5 data [81]. Comparisons were made between these hindcast models by Stopa and Cheung, and the outputs were found to be in good agreement with each other as well as with wave buoy and altimeter data [82].

The ideal wave condition representation is a two-dimensional directional wave spectrum, which describes the wave system variance for all frequencies and directions. While this data is generated by the WWIII model at each location and time step, the full dataset is not typically available due to the large number of parameters. In the case of the WWIII 30-year hindcast phase 2, 2D wave spectra data are only provided for approximately 2000 locations [80]. A reduced dataset is provided for all locations giving the bulk spectral parameters for the wave system, including the significant wave height (H_s), primary wave direction (D_p) and the peak wave period (T_p). The global WWIII data has a 3-hour time resolution and a 0.5°x0.5° spatial resolution.

In the production Digital Twin, the WWIII output files from the NOAA NCEP FTP site are retrieved and processed daily by a virtual machine, which then stores the resulting parameters in a cloud-based SQL database. This then becomes the source of the metocean data for the Digital Twin application.

3.2.3.2 Vessel-Specific Wave Condition Data

To obtain the wave condition along a specific vessel route, interpolation of the bulk spectral parameters is performed over both space and time. In Adland et al., the metocean data from the ECMWF ERA5 model is combined with vessel AIS data by matching the coordinates and timestamps within a specified threshold (0.25° and one hour), however this resulted in a number of the vessel position points not having corresponding metocean data [69]. In Zhang et al., a trilinear approach is applied to derive the parameters from several metocean data sources, where linear interpolation is applied to fit the timestamp of the AIS data point and bilinear interpolation is applied based on the latitude and longitude of the AIS data point [70]. In this study, an interpolation approach is applied utilizing a trained Kriging model. As part of the wave condition data model, a software tool has been developed to retrieve a selection of the required bulk spectral parameters from the SQL database based on a given vessel's position data and timestamp. To provide sufficient data to train the Kriging model, for each point on the vessel's route, a grid of metocean data points that surrounds that route point in both space and time is retrieved. This grid of selected points is 1.5° x 1.5° in space and 6 hours in time, which equates to 48 training points for each Kriging model for each bulk parameter as shown in Figure 3.6. The interpolation approach uses 3D ordinary Kriging with a linear variogram model [83].

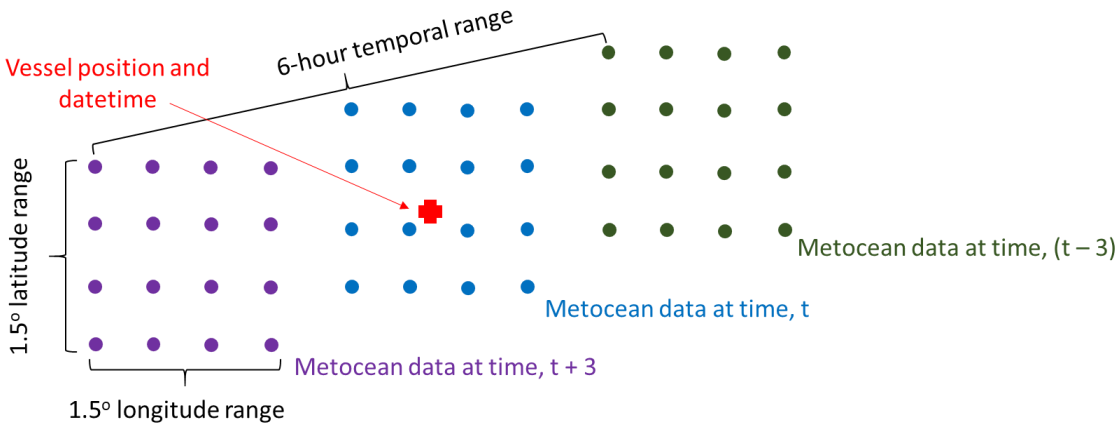

Figure 3.6. Kriging model training data grid

This metocean data is then used to train Kriging models along the ship's route to infer the bulk spectral parameters at each position's location and timestamp. An example of the significant wave height Kriging model result for a spatial region at a fixed time is given in the following figure. The points in the figure represent the training data with the gradient showing the significant wave heights for the region of interest estimated from the resultant trained Kriging model.

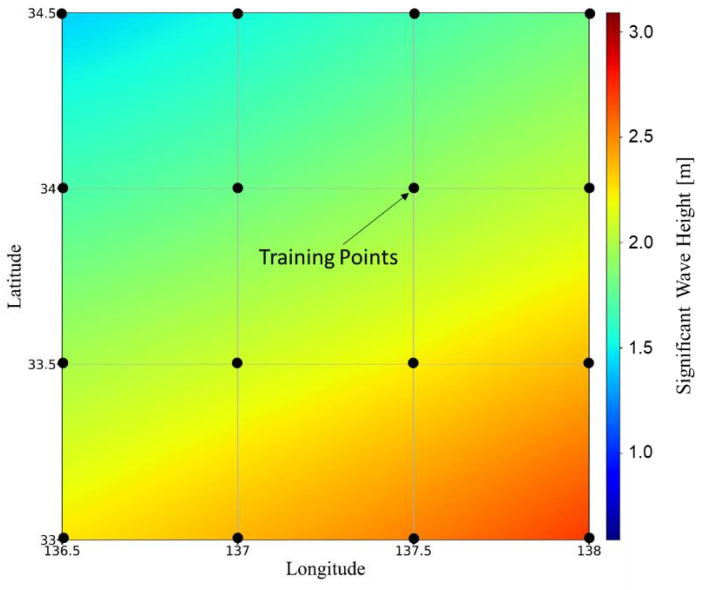

Figure 3.7. Metocean data Kriging model for significant wave height

The results from the Kriging model are used to create the Digital Twin wave condition data model, which is a SQL database table containing the vessel's position and time stamp along with the corresponding bulk spectral parameters. This data model is then used as the primary input in the fatigue analysis.

3.2.4 Fatigue Analysis Models

After developing the Digital Twin vessel position and wave condition data models for the vessel-specific experienced wave conditions, the resulting fatigue damage can be estimated using the fatigue analysis computational models. As previously mentioned, since fatigue damage cannot be directly observed, it must be inferred from the observed data using the Digital Twin. In this proposed vessel-specific approach, several options to the traditional design fatigue method are applied to enable real-time tracking of fatigue damage using the vessel-specific wave condition data. This process uses several computational models maintained in the Digital Twin virtual representation. Both the traditional design approach and the proposed vessel-specific approach are discussed in this section.

3.2.4.1 Spectral Fatigue Analysis

Spectral fatigue analysis is an S-N curve-based approach used for determining the fatigue life of a vessel during design. During design, the operational life of the vessel is considered as many spatiotemporal segments each comprised of a set of operational parameters, including the wave condition (e.g. significant wave height and wave period) and vessel operational condition (e.g. speed, relative heading, and loading) which impact the ships short-term structural response. This analysis involves the combination of several of the Digital Twin computational models, where the outputs of one computational model are used as inputs for the other computational models.

First, the Digital Twin hydrodynamic seakeeping model is implemented. This model is developed from the vessel drawings for representing the vessel hull form. Once the vessel hull form is modeled, a frequency-domain, 2D strip theory code was used to estimate the set of vessel-specific response amplitude operators (RAOs) which are a set of transfer functions to obtain vessel motion, pressure, and global loads as a function of the operational parameters. The resulting RAOs account for the range of vessel operational conditions which the vessel may encounter. These RAOs are stored in a database for use by the other Digital Twin models.

Next, the Digital Twin full ship finite element (FE) structural analysis model is implemented. The RAOs generated from the seakeeping model are mapped to the FE model and the stress response at the selected representative critical areas is stored for the specified ranges of the operational parameters. The resulting stress transfer functions, $H_\sigma(\omega|\theta)$, for each selected structural location are stored for future use.

Finally, the resulting stress transfer functions from the FE model are used as input for the fatigue damage accumulation model. The fatigue damage model is based on a spectral approach which assumes that variation of stress is a narrow-banded random Gaussian process. Based on this assumption, the short-term probability distributions for the stress ranges and the resulting fatigue damage corresponding to the range of possible wave conditions is determined. The probabilities for range of wave conditions over a specified period of time can be characterized using a wave scatter diagram (WSD), which gives the probability distribution of binned wave height and wave period combinations. An illustrative example

based on collected vessel data is shown in Figure 3.8. Similarly, an example wave rosette, which gives the wave heading probability relative to the vessel orientation, shown in Figure 8. During design, a uniformly distributed wave heading is generally assumed, however as can be seen data from actual vessel operation does not follow this design assumption.

Wave Scatter Diagram

		Wave Period (s)											Sum Over All Periods
		3.5	4.5	5.5	6.5	7.5	8.5	9.5	10.5	11.5	12.5	13.5	
Wave Height (m)	0.5	0.142478	0.028637	0.016543	0.016185	0.009474	0.012214	0.019864	0.017707	0.009367	0.003060	0.002870	0.278398
	1.5	0.033769	0.054859	0.062566	0.060212	0.044090	0.029510	0.023514	0.021094	0.014224	0.005901	0.003981	0.353719
	2.5	0.000880	0.017239	0.045903	0.042328	0.032987	0.021687	0.013488	0.010915	0.006040	0.002897	0.002084	0.196450
	3.5	0.000000	0.001545	0.011170	0.023307	0.024018	0.014571	0.010069					
	4.5	0.000025	0.000000	0.000922	0.006294	0.013747	0.009358	0.004404					
	5.5	0.000000	0.000000	0.000000	0.001302	0.004660	0.004990	0.003773					
	6.5	0.000000	0.000000	0.000000	0.000000	0.000714	0.001915	0.002674					
	7.5	0.000000	0.000000	0.000000	0.000000	0.000083	0.000445	0.000411					
	8.5	0.000000	0.000000	0.000000	0.000000	0.000000	0.000048	0.000000					
	9.5	0.000000	0.000000	0.000000	0.000036	0.000000	0.000000	0.000057					
	10.5	0.000043	0.000000	0.000000	0.000000	0.000031	0.000000	0.000000					
	11.5	0.000015	0.000028	0.000000	0.000000	0.000022	0.000000	0.000050					
	12.5	0.000001	0.000103	0.000035	0.000062	0.000029	0.000000	0.000000					
	13.5	0.000203	0.000009	0.000017	0.000000	0.000063	0.000055	0.000000					
	14.5	0.000132	0.000000	0.000025	0.000000	0.000000	0.000000	0.000000					
Sum Over All Heights		0.177546	0.102420	0.137180	0.149726	0.129918	0.094793	0.078303					

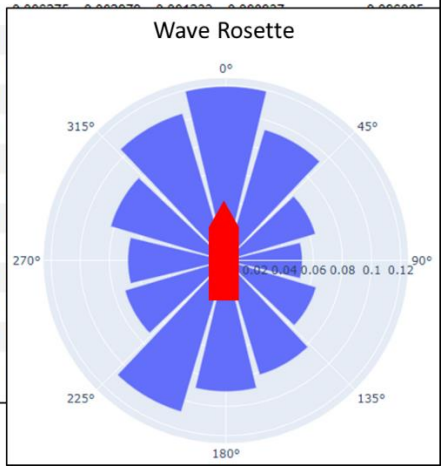

Figure 3.8. Sample wave scatter diagram and wave rosette

The total accumulated fatigue damage is then calculated as a weighted linear summation based on the probabilities of each wave condition as given in the wave scatter diagram (i.e. each cell in the WSD). The mathematical formulation of this approach is given below.

From the stress transfer functions, the resulting stress energy spectrum is determined by scaling the wave energy spectrum, $S_\eta(\omega|H_s,T_z)$, which supplies useful information about the characteristics of the ocean wave system and is given as:

$$S_\sigma(\omega|H_s,T_z,\theta) = |H_\sigma(\omega|\theta)|^2 S_\eta(\omega|H_s,T_z) \tag{3.1}$$

where

$S_\eta(\omega|H_s,T_z)$ = wave energy spectra

H_s = significant wave height, in meters

ω = circular wave frequency, in radians/sec

T_z = average zero up-crossing wave period, in seconds

In standard practice for ship design, idealized wave spectra are used instead of determining the specific wave spectra at a given location and time since this is unknown at the time of vessel design. For a Digital Twin application, the actual encountered wave spectra could be estimated from the bulk spectral parameters provided in the metocean hindcast dataset and used instead of an idealized form. However, this presents an operational trade-off for the performance of the Digital Twin. In selecting an idealized form, the vessel response to the range of possible sea states can be pre-calculated, substantially reducing the computational time. In this Chapter, to achieve this improved computational performance, the Digital Twin implements the idealized Bretschneider wave spectrum [84] which is typically applied for open ocean areas with fully developed seas. Future work will examine the impact of this assumption by comparing with the results obtained from deriving the wave spectra for each vessel location during its historical voyages. The Bretschneider wave spectra is given as:

$$S_\eta(\omega|H_s,T_z) = \frac{H_s^2}{4\pi}\left(\frac{2\pi}{T_z}\right)^4 \omega^{-5} exp\left[-\frac{1}{\pi}\left(\frac{2\pi}{T_z}\right)^4 \omega^{-4}\right] \tag{3.2}$$

Since the ship is generally moving with a forward velocity, the wave spectrum must be defined from the ship's reference frame rather than a stationary reference frame. In the ship's reference frame, the wave spectrum needs to account for the transformation of the spectral frequency components due to the Doppler effect determined based on the ship's forward speed, V, and wave encounter angle, θ. The resulting Doppler effect is accounted for with the term $(\omega - V\omega^2 \cos\alpha\,/g)^n$. It can also be noted that energy equivalence implies that the stationary reference frame, $S(\omega)d\omega$, is equivalent to the vessel reference frame, $S(\omega_e)d\omega_e$.

To account for short-crested sea conditions that result in kinetic energy spread, a cosine-squared approach is used to account for this spreading using a term, α, assumed from +90 to -90 degrees on either side of the wave heading. The n^{th} spectral moment, m_n, is then given as:

$$m_n = \int_{\theta-90}^{\theta+90} \left(\frac{2}{\pi}\right) cos^2(\alpha-\theta)\left(\int_0^\infty (\omega - V\omega^2\cos\alpha\,/g)^n S_\sigma(\omega|H_s,T_z,\alpha)d\omega\right)d\alpha \tag{3.3}$$

The Rayleigh probability density describing the short-term stress range distribution is then given as:

$$g(s) = \frac{s}{4m_0} exp\left[-\left(\frac{s}{2\sqrt{2m_0}}\right)^2\right] \tag{3.4}$$

A corresponding short-term stress range distribution can then be defined for each short-term wave condition (i.e. each cell in the WSD) and the cumulative distribution is considered as the weighted sum over all the combinations of wave conditions and heading directions.

Once the resulting stress distribution is determined, the resulting fatigue damage accumulation can be calculated. The approach used to determine fatigue damage during vessel design is Palmgren-Miner's rule, which assumes that the cumulative damage, *D*, resulting from a group of variable stress cycles is the sum of the damage inflicted by each stress range. Thus the damage incurred by the i^{th} wave condition, assuming a S-N curve of the form $N = AS^{-m}$ is given as:

$$D_i = \left(\frac{T}{A}\right) \int_0^{\infty} (k_t k_{ms} k_h s)^m f_{0i} p_i g(s)_i ds \tag{3.5}$$

where

D_i = damage incurred in the *i*-th wave condition

k_h = factor for high tensile steel

k_t = factor for thickness effect

k_{ms} = factor for mean stress effect

m, *A* = physical parameters describing the S-N curve

T = duration of wave condition, in seconds

p_i = joint probability of H_s and T_z

f_{0i} = zero-up-crossing frequency of stress response, H_z

s = specific value of stress range from the short term stress-range distribution given in Eq. 4

The total accumulated fatigue damage can then be estimated by considering the sum of all the individual fatigue damage for the *i*-th wave condition weighted by the probability of that wave condition and heading as given by the wave scatter diagram and wave rosette. A closed form expressed for the total accumulated fatigue damage based on an analytical distribution for the stress range, *g*(s), is given in Eq. 3.6. Failure is defined as the total accumulated fatigue damage, *D*, exceeding a critical value, η, equal to unity which corresponds to the generation of a through-thickness crack at the considered critical area. The full details of the expression can be found in [68].

$$D = \left(\frac{T}{A}\right)\left(2\sqrt{2}\right)^{m}\Gamma\left(\frac{m}{2}+1\right)\sum_{i=1}^{M}\lambda(m,\varepsilon_i)\mu_i f_{0i} p_i (k_h k_t k_{ms}\sigma_i)^m \leq \eta \quad (3.6)$$

where

Γ = complete gamma function with the argument (m/2 + 1)

$\sigma_i = \sqrt{m_0}$ for the i-th considered sea state

λ = rainflow factor of Wirsching

μ_i = endurance factor for bi-linear S-N curves

p_i = probability of the i-th considered sea state

Some limitations of the Palmgren-Miner approach for determining fatigue damage accumulation include, conservatism arising from the code S-N curves, the simplified failure criterion of D exceeding unity, and the accounting for initial flaws. However, as this approach is the current standard in ship design, its use in the Digital Twin provides the decision-makers with a common and consistent output that can be easily compared with the original design assumptions. Thus, the selection of approach in this case is to maximize the interpretability of the Digital Twin for the end user. This Digital Twin use case can be considered to be monitoring the vessel load exposure/fatigue damage accumulation compared with the original design assumptions and providing decision-makers with relative indicators of how the actual vessel is operating against this baseline. It should be noted, that as Digital Twins become more commonplace, alternate fatigue damage approaches and failure criteria, such as fracture mechanics (which can consider initial defects and overcome some of the limitations of the Palmgren-Miner approach), could be implemented in this framework.

For fatigue assessment during the design phase, the probabilities for the various wave conditions the vessel may experience are given by the wave scatter diagram for unrestricted services and equal heading probability wave rosette [68]. These are based on the wave conditions in the North Atlantic and are typically assumed as conservative estimation of experienced wave conditions. In this study, they are adopted as the reference wave condition to compare against the vessel-specific variations.

3.2.4.2 Vessel-Specific Fatigue Procedure Options

The design methodology is inherently conservative as the actual operating conditions are likely to be less severe than the environment assumed during design. By utilizing the vessel-specific position data and corresponding wave data models, the short-term response and corresponding fatigue damage can be calculated based on the wave conditions experienced during vessel-specific operations. For the application of the proposed Digital Twin approach for monitoring

fatigue damage, the virtual representation should include the following computational models: the hydrodynamic model, the full-ship FEA model, and the spectral fatigue analysis model. These models should be kept up to date with the current structural condition of the vessel, including any structural modifications, degradation, and repairs. For example, the steel thicknesses of the structural elements in the full-ship FEA model are updated based on periodic thickness measurements. Additionally, the Digital Twin also maintains a fatigue damage accumulation data model, which is the database that tracks the states of fatigue damage over time for each critical area of interest. Once the necessary Digital Twin models are established, the vessel-specific methodology is employed to update these models based on the collected vessel wave condition data. Three options of the fatigue analysis procedure are investigated in this section to incorporate the vessel-specific wave conditions in the Digital Twin.

In the first option, the vessel-specific fatigue damage is calculated using Eq. 3.6 with the probabilities of the wave conditions and headings taken from the wave scatter diagram and wave rosette based on the entire history of the vessel's operation up to the present instead of using the reference wave scatter diagram and wave rosette. The result of this analysis is a weighted fatigue damage accumulation rate. This fatigue rate represents the amount of fatigue damage occurring per unit of time and can then be applied over a specified duration, T, which is taken as the age of the vessel multiplied by an operational time factor, to account for the periods when the vessel was in port. Because this approach only provides a resultant weighted fatigue rate over the time duration considered, it does not give any insight into the day-to-day fatigue damage accumulation which may be very beneficial to supporting operational decisions.

To provide more insight into variability of fatigue damage accumulation during the vessel's operation, the second approach option is based on a selected updating period (e.g. day, week, month, etc.). For the updating period, the corresponding wave scatter diagram and wave rosette are developed based on all of the available positions and corresponding metocean hindcast data for this period. The fatigue damage for the updating period is then calculated using Eq. 3.6 and the corresponding wave condition probabilities for the updating period. The total accumulated fatigue damage is then determined as the cumulative sum of the fatigue damage calculated for each updating period. This approach provides additional insight compared to the first vessel-specific approach by showing the fluctuation in the fatigue damage accumulation as a function of the vessel's operation within the scope of the update period. However, as the updating period is reduced, this approach can be more computationally expensive than the other approach options in terms of calculation time.

The third approach option takes advantage of the processed AIS position data that is achieved by the procedure developed in Section 3.2.2 to provide a more computationally efficient estimate of the accumulated fatigue damage while also providing insight into the variations in fatigue damage during the vessel's operation. Since the vessel position data and corresponding metocean hindcast data cover the extent of the vessel's transit with a constant resolution, instead of generating a corresponding WSD and wave rosette, it is assumed that each wave condition experienced by the vessel is

captured and thus the fatigue damage for each encountered sea state can be directly determined and the total accumulated fatigue damage can be determined as a cumulative sum. For computational efficiency, the fatigue damage for each wave condition, D_i, is pre-calculated for a unit time interval (e.g. T = 1 hour).

$$D_i = \left(\frac{T}{A}\right)\left(2\sqrt{2}\right)^m \Gamma\left(\frac{m}{2}+1\right)\lambda(m,\varepsilon_i)\mu_i f_{0i}(k_h k_t k_{ms}\sigma_i)^m \tag{3.7}$$

where the parameters are defined as in Eq. 3.5 and Eq. 3.6.

These pre-calculated damage values can then be efficiently assigned to each row of the vessel position and wave condition data from the Digital Twin wave condition data model. The total accumulated fatigue damage, D, is then taken as the cumulative sum of all the D_i values for all rows of the data table. The key assumption being made in this approach is that the sea state remains stationary on the time order of the position sampling frequency. This assumption is reasonable as the sampling frequency used in this study is 1 hour and it has been observed that the typical range of time a sea state statistics remain stationary ranges from 30 minutes to 10 hours, and the standard time between registering sea states is typically taken as three hours [85].

One of the challenges that arises when considering the vessel-specific approach is handling the uncertainty introduced by gaps in the data, particularly the vessel position information. In the first and second approach options presented above, the generation of the wave scatter diagram and wave rosette for the selected time interval can be based on all the vessel-specific data that is available. The resulting wave scatter diagram and wave rosette are then applied in the procedure for that entire time interval, effectively ignoring the data gaps and assuming that the available data is sufficiently representative of the sea state probabilities experienced by the vessel for the given time period. This assumption may be problematic in that it may potentially bias the long-term distribution if the missing data is not missing at random. This concern is addressed by the upsampling/downsampling and rerouting approach proposed in this Chapter. By using the available data to infer the missing position data, this provides a more comprehensive input dataset for the fatigue analysis.

For each of these methodology options, the resultant fatigue damage is estimated daily in following the update of the wave condition data model. These results are then used to update the Digital Twin fatigue damage accumulation models. This process is automated so that as new input data is retrieved, the fatigue damage accumulation is assessed, and the models are updated. After the model updates, one of the most important aspects of the Digital Twin is the communication of the results to decision-makers. In this approach, plots of the overall fatigue damage accumulation and daily fatigue damage rate and displayed along with plots of the vessel's route. Thresholds can also be set on the daily fatigue damage rate to provide automated alerts when a high fatigue rate is observed. This could be used to trigger recommendations such as immediate inspections or creating target inspection plans for future repair availability periods.

3.2.5 Future Fatigue Damage Prognosis

The Digital Twin implemented above can also be used to predict the future fatigue damage and the remaining fatigue life for a specific vessel. The fatigue damage estimate is affected by numerous factors such as vessel routing, wave conditions, operational time, etc. These factors are not deterministic but have large uncertainties which makes stochastic methods, such as Monte Carlo simulation, necessary for predicting fatigue damage.

3.2.5.1 Monte Carlo Fatigue Prognosis Model

The Digital Twin Monte Carlo fatigue simulation model applies the uncertainty of future wave conditions that a vessel may experience to observe the impact on fatigue damage prediction. Monte Carlo simulation relies on repeated random sampling of the stochastic inputs and parameters to obtain numerical results regarding the uncertainty of system performance. The data generated from the simulation can provide insight through statistical analysis and help make decisions given the uncertainty estimate in the analysis output. An outline of the Monte Carlo simulation process for vessel-specific fatigue damage prediction is shown in Figure 3.9.

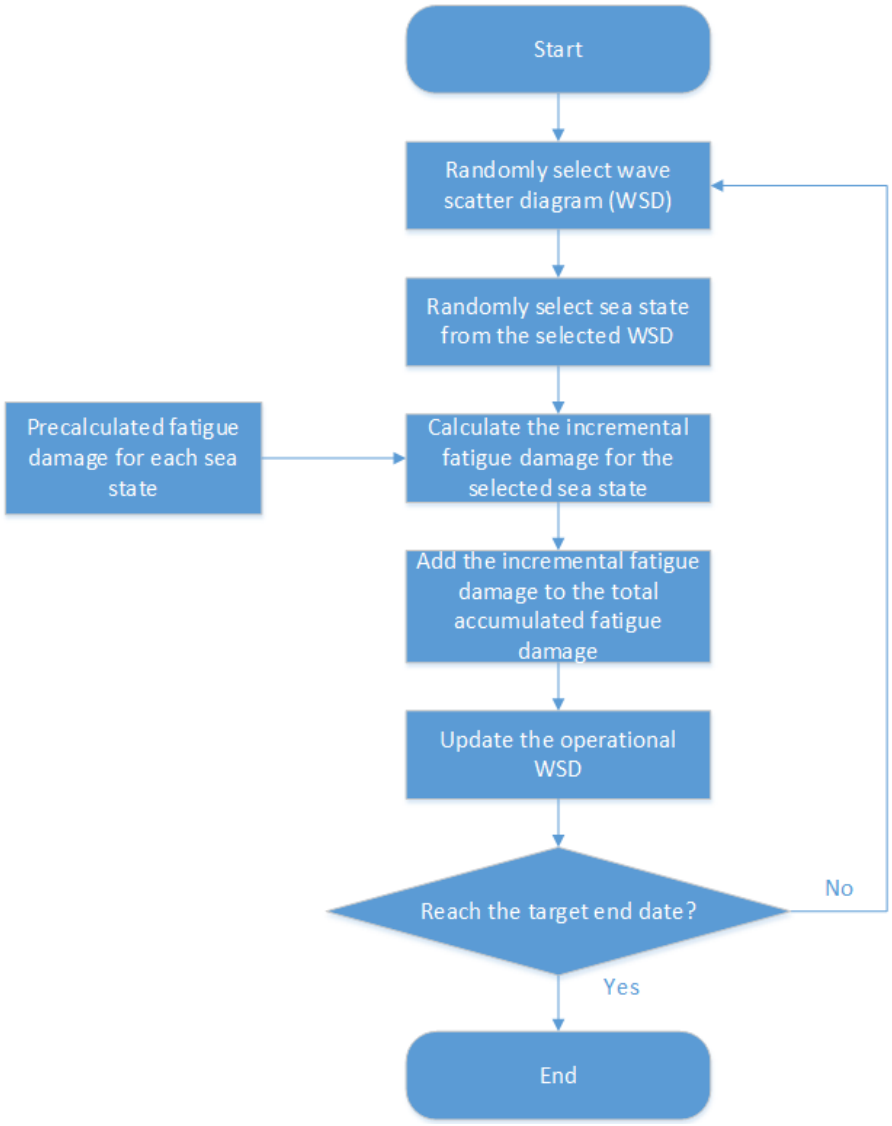

Figure 3.9. Monte Carlo simulation process for fatigue prognosis

The Monte Carlo simulation process shown in Figure 3.9 focuses on the variability of the future fatigue damage accumulation based on the uncertain expectation of future sea state exposure. In the first two steps of the process, a random sea state is selected from a random WSD based on the expected future sea state exposure due to vessel operation, described further in Section 3.2.5.2. After selecting the random sea state from the selected WSD, the Monte Carlo prognosis model applies the same fatigue damage approach used in the third methodology option presented in Section 3.2.4.2. In this option, the short-term fatigue damage is pre-calculated using the spectral fatigue analysis approach, which provides the incremental fatigue damage for each possible encountered sea state characterized by the significant wave height, zero crossing wave period, and relative wave direction to the vessel. This approach is necessary as the Monte Carlo simulation is computationally unaffordable for a long-term fatigue calculation, since the period being analyzed may require simulating millions of short-term fatigue calculations. To eliminate the repetitive short-term fatigue calculation and reduce

the computational time, the fatigue damage for all the sea states are pre-calculated and stored in the model. After calculating the fatigue damage for the selected sea state, this is accumulated in the total fatigue damage, and the process is repeated until the end condition is met.

3.2.5.2 Future Wave Condition Variability

Fatigue prediction requires assumptions to be made about the future operation of the vessel to define the variability in the future wave conditions. In the proposed methodology, future wave conditions can be described using three possible wave scatter diagrams, shown in Table 3.1.

Table 3.1. Wave scatter diagrams

Wave Scatter Diagram (WSD)	**Description**
WSD 1	Vessel-specific historical wave conditions that the vessel has experienced
WSD 2	Route-specific wave conditions based on the planned future routes and wave statistics for these routes/areas
WSD 3	Wave conditions for unrestricted services (the reference wave condition)

In Table 3.1, WSD1 is based on the vessel's historical operation and experienced wave conditions. The applicability of this wave scatter diagram is based on two conditions, first is the age of the vessel and the second is if the operational profile of the vessel is expected to remain the same in the future. If the vessel age is low, the wave statistics determined from historical operation may not be representative of the range of possible wave conditions the vessel may experience in the future, particularly the occurrence of extreme events that have a low probability of occurrence. Use of WSD1 for fatigue analysis in this case may result in a potentially less conservative estimate of the remaining fatigue life as a result. To address this, use of WSD2 relies on the knowledge of future operational planning and the wave statistics for certain routes and areas. By using knowledge of the vessel's past and anticipated future operation, historical wave data from a global wave database can be used to generate a corresponding wave scatter diagram based on decades of wave condition data. As this wave scatter diagram is more likely to capture the probabilities of extreme wave events, the fatigue results are likely more conservative than WSD1 for fatigue damage prognosis. The use of WSD1 and WSD2 are also based on the assumption that the vessel will operate in a known region. If the vessel changes routes in the future, WSD1 and WSD2 are likely no longer representative of the future wave conditions the vessel will experience. In this case, the design reference wave condition WSD3 is the most conservative option but as previously discussed this may overestimate the future fatigue damage.

Since none of the defined wave scatter diagrams may be appropriate based on the current knowledge of the vessel's future operations, the proposed methodology uses a weighted combination of the possible wave scatter diagrams, with the weights selected based on the knowledge of the vessel and the assumptions made about its future operation. Weights are assigned to each wave scatter diagram which correspond to the probability of selecting a wave condition from that wave scatter diagram during the Monte Carlo simulation.

Assuming future route planning information is not available, WSD2 (route-based wave conditions) is not defined and its weight is set to zero. This results in the approach using a combination of only WSD1 (historically experienced wave conditions) and WSD3 (the reference WSD for unrestricted services) to predict the fatigue damage. There are many possible approaches for setting the respective weights for WSD1 and WSD3. In this approach, the weights are set by the age of the vessel as given in Eq. 3.8.

$$P1 = \frac{Vessel\ Age}{Service\ Life} \tag{3.8}$$

where P1 is the probability of selecting the historical vessel-specific wave scatter diagram, WSD1. Thus, the probability of selecting the historical vessel-specific wave scatter diagram is proportional to the vessel's relative age versus its intended service life. The reasoning for this is, as the vessel is older, the historical wave scatter diagram is based on more vessel-specific wave conditions and is likely more representative of its future operation. Additionally, with more years of data, the rare wave condition events are more likely to have been accounted for. When the vessel is young, WSD1 may not be representative and due to the increased uncertainty of future wave conditions, a more conservative approach (e.g. WSD3 for unrestricted services) should be dominant. After defining the weight for WSD1, the probability of selecting the wave condition for unrestricted services P_3 is then determined as $P_3 = 1 - P_1$ since WSD2 is not used in this study and P2 is taken as zero.

3.2.5.3 Monte Carlo Simulation

After setting the probabilities for the respective candidate wave scatter diagrams, the Monte Carlo simulation is performed according to the process shown in Figure 3.9. In each simulation fatigue damage is incrementally calculated for a three-hour wave condition exposure. The damage is accumulated until the simulation reaches its termination condition, typically a target end date in the future.

In each iteration, first the wave scatter diagram to be used for that iteration is selected based on the probabilities determined in the previous section. From the selected wave scatter diagram, a wave condition (i.e. a significant wave height and wave period) is selected from the wave scatter diagram according to its joint probability P_i, where P_i is defined as the probability of occurrence of each sea state in the WSD is proportional to the number of occurrences in each sea state bin of the WSD as shown in Eq. 3.9 below, where n_{bin} is the total number of sea-state bins, N_i is the number of

occurrences for sea state *i*. Then, the same sampling approach can be used to randomly select the wave heading based on the relative wave heading probability to the ship's heading.

$$P_i = \frac{\mathrm{Ni}}{\sum_{i=1}^{n_{bin}} \mathrm{Ni}} \tag{3.9}$$

For the selected sea state, the pre-calculated short-term fatigue damage is retrieved and added to the accumulated fatigue damage for the current simulation. The process is then repeated until the end condition is reached. This process is then repeated for a fixed number of simulations to obtain the distribution of possible fatigue damage accumulation as a function of the future wave condition variability.

These results are then stored in the Digital Twin and displayed through visualizations to decision-makers. As the vessel operates, the fatigue prognosis can also be continuously updated to reflect the change in the operational conditions and the impact of that on the forecasted fatigue life.

3.3 Case Study

To investigate the impact of vessel-specific wave conditions on the accumulated fatigue damage, a case study is conducted with a container carrier trading between Asia and North America. The vessel particulars are given in Table 3.2. A Digital Twin was constructed comprised of the data models and analysis models as described in Section 3.2.1.

Table 3.2 Vessel particulars

Parameter	Description
Ship type	Container ship
Ship length	276 (m)
Ship beam	40 (m)
Gross tonnage	64,500 (tons)
Deadweight (at max draft)	66,500 (tons)
Draught (avg)	9.8 (m)
Speed (avg/max)	13.9 (knots) / 26 (knots)

3.3.1 Representative Critical Areas

For monitoring fatigue, the Digital Twin tracks the damage accumulation at selected representative critical areas. For example, representative connections within the midship region can be selected to investigate the wave condition's impact

on the accumulated fatigue damage. These example representative connections are listed in Table 3.3 and shown in Figure 3.10. Representative critical areas for a midship section. For this case study, representative critical area 1 (RC1) was selected to investigate the impact of the vessel-specific wave conditions on the accumulated fatigue damage. This procedure can be used for any other critical area of a vessel, by simply adding the models for that critical connection to the Digital Twin.

Table 3.3. Representative critical areas

Representative connection (RC)	Description
RC 1	Connection of Deck Longitudinal and Transverse Bulkhead
RC 2	Connection of Side Shell Longitudinal and Transverse Bulkhead
RC 3	Connection of Bottom Longitudinal and Transverse Bulkhead at Side
RC 4	Connection of Bottom Longitudinal and Transverse Bulkhead at Center

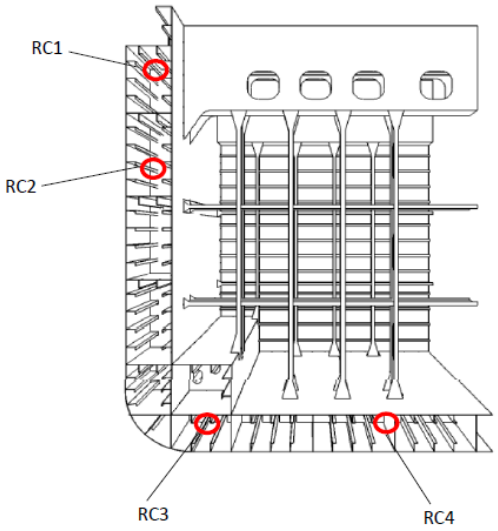

Figure 3.10. Representative critical areas for a midship section

3.3.2 Vessel Route and Wave Condition Determination

The vessel's AIS data from 2013 to 2019 was collected from the global fleet database and stored in the Digital Twin vessel position data model. Then the proposed route upsampling/downsampling and re-routing approach from Section 3.2.2.2 was applied and the position data model was updated.

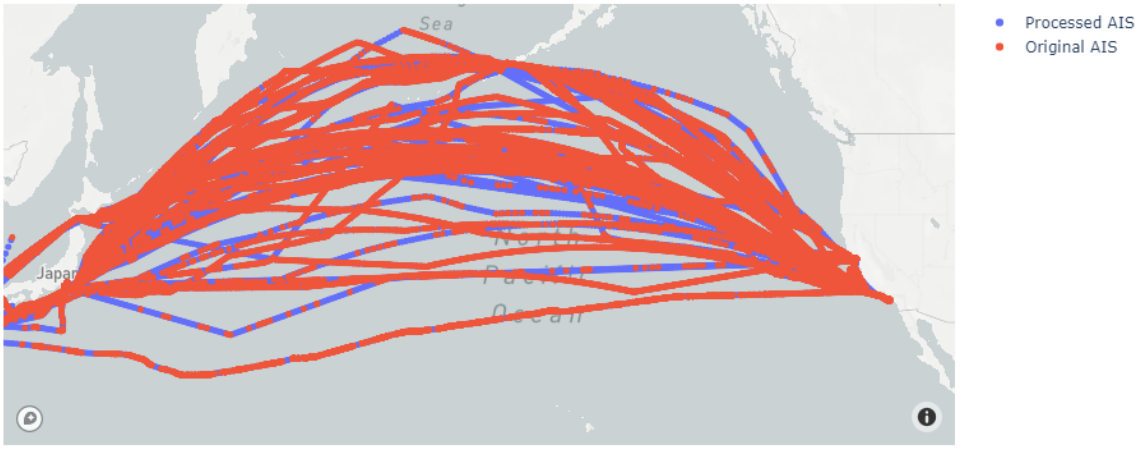

Figure 3.11. Containership route history: original and processed position data (AIS data provided by Spire Global, Inc)

A summary of the original and processed data is provided in Table 3.4. The most noticeable outcome of the upsampling/downsampling and rerouting process is the significant reduction (79%) in the number of position points while increasing the overall coverage at the selected data fidelity (i.e. 1-hour frequency) to 100%. This provides the benefit of ensuring that the sea states experienced by the vessel during operation are adequately captured while reducing the overall computational burden that results from the greater volume of data in the original AIS dataset. Another important outcome of the proposed approach is the determination of the percentage of time the vessel is non-operational (i.e. in port, moored, anchored, etc.). This can be determined by using the vessel status code provided in the AIS data. However, since this code is manually entered by the ship's crew, it was observed that there were substantial periods of time where the vessel was clearly non-operational (e.g. in port with no movement), as such the percentage of time the vessel was non-operational may be underestimated based on the status code alone. An alternate approach is to use the reported vessel speed over ground as the basis for determining non-operational time, where it is assumed the vessel is non-operational when it is not moving. Due to variations in the reported speed due to GPS drift, which is the difference between the actual position and the position recorded by the GPS, especially when stationary, a maximum vessel speed threshold of 0.2 knots was applied to obtain a possible range of non-operational time. This non-operational time percentage is applied during the fatigue analysis to prevent overestimation of the fatigue damage accumulation.

Table 3.4. AIS data processing results

Position Dataset	Time Range	Number of Position Points	Temporal Coverage Percentage	Non-Operational Time Percentage
Original AIS	01-01-2013 to 05-31-2019	271,094	66.7%	21%
Processed AIS	01-01-2013 to 05-31-2019	56,206	100%	22%

3.3.3 Fatigue Damage Accumulation Estimate

Spectral-based fatigue analysis was then performed using the vessel-specific wave conditions applying both the reference wave condition and proposed approach. The fatigue damage under the reference wave condition was also calculated to compare the relative accumulated fatigue damages for each approach.

Figure 3.12 shows the accumulated fatigue damage for RC1 under the vessel-specific wave conditions applying each of the three vessel-specific procedure options in Section 3.2.4.2. Figure 3.13 shows the normalized daily fatigue rate for RC1 again considering each of the three vessel-specific procedure options. The normalized rate is determined as the calculated fatigue rate determined from the vessel-specific wave conditions divided by the fatigue damage determined using the reference wave condition.

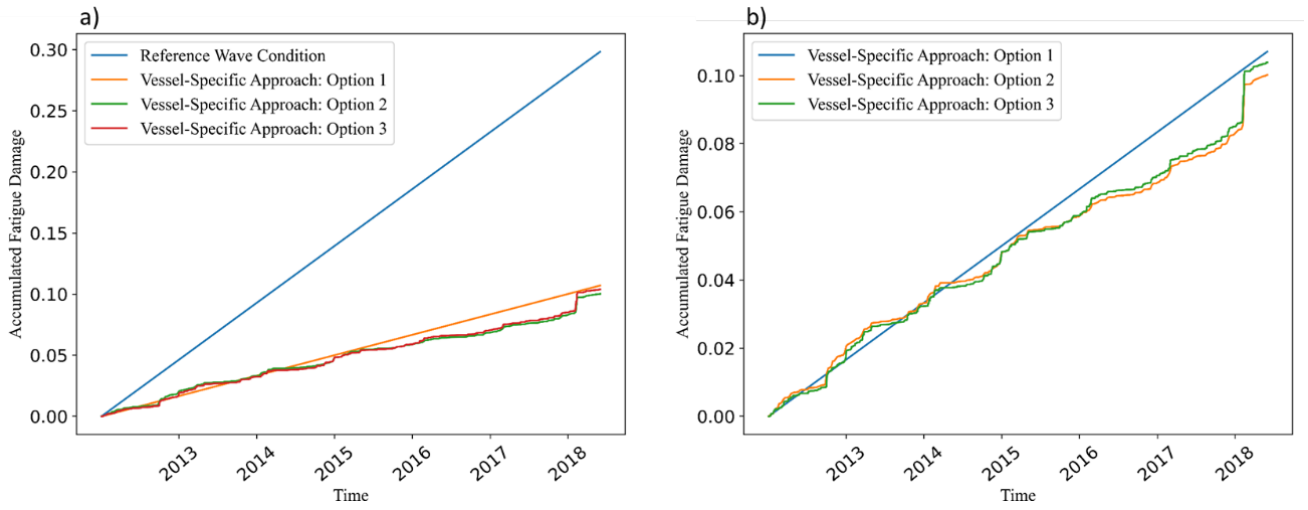

Figure 3.12. Accumulated fatigue damage for RC1 under vessel-specific wave conditions: a) Comparison of vessel-specific approaches with the reference wave condition, b) Comparison of only the vessel-specific approaches

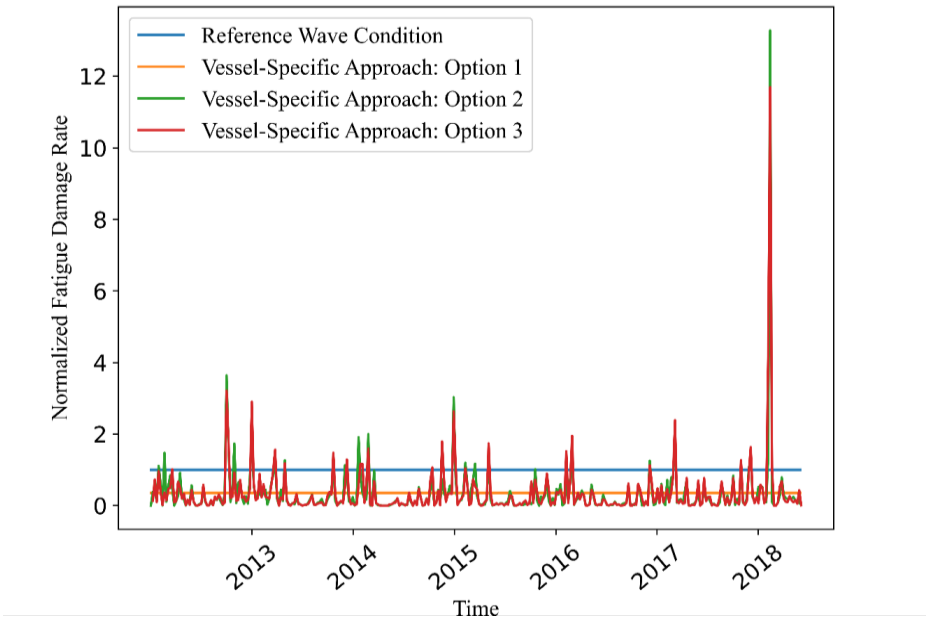

Figure 3.13. Normalized fatigue damage rate for RC1 under vessel-specific wave conditions

The first observation in Figure 3.12 is that the vessel-specific approaches show significantly reduced fatigue damage accumulation compared with the design reference condition. As mentioned earlier, this is expected since the reference wave condition is intended to be highly conservative. For RC1, the consideration of the vessel-specific wave conditions results in a 65% reduction in the estimate of fatigue damage accumulation compared to the reference wave condition for the 6.5-year period of the study.

Similarly, when examining the normalized fatigue damage rates in Figure 3.13, it can be observed that for a majority of the operational time the vessel-specific fatigue rate is far less than the fatigue rate determined from the reference wave condition. However, it can also be observed that there are clear instances where the vessel-specific fatigue rate exceeds the reference condition. A closer examination reveals a cyclical response with higher vessel-specific fatigue rates occurring during the winter months (November to February) each year. This corresponds with the winter monsoon season and the resulting more severe sea states. This information can be useful to the vessel operator both for operational decision-making and availability planning. Additionally, in the event of a large exceedance such as the one observed in early 2019, inspections could be conducted in easily accessible areas to confirm that no damage resulted from the event.

The comparison of the three vessel-specific methodology options show close alignment with each other regarding accumulated fatigue damage. While there are some differences, the present accumulated fatigue damage only shows a maximum difference of 3.6% for all of the approach options. This suggests that for this case study, the original AIS data coverage used in the first two approach options is sufficient to generate wave scatter diagrams and wave rosettes that compare closely with the wave conditions captured by the processed AIS position data used in the third approach option.

3.3.4 Fatigue Prognosis Results

After completing the setup of the Digital Twin for monitoring the fatigue damage accumulation, the fatigue prognosis model was implemented using the methodology presented in Section 3.2.5 for the selected critical area, RC1.

As previously discussed, the future route is assumed to be unknown and the fatigue prognosis is calculated based on the weighted combination of the vessel-specific wave scatter diagram and the design reference wave scatter diagram. Based on the vessel's current age of 6.5 years and intended service life of 20 years, the vessel-specific wave scatter diagram is given a probability of being selected as 32.5% and the reference wave condition is given a probability of being selected as 67.5%.

The Monte Carlo fatigue prognosis model was then run to simulate 50,000 possible fatigue damage accumulation results for the next 13.5 years which reaches the end of the ship's design service life. From these 50,000 runs, the distribution of fatigue damage based on the variability in the assumed future wave conditions can be determined. The results of this simulation are combined with the results for the Digital Twin fatigue damage accumulation model to show the estimated fatigue damage over the life of the vessel. The results are shown in Figure 15.

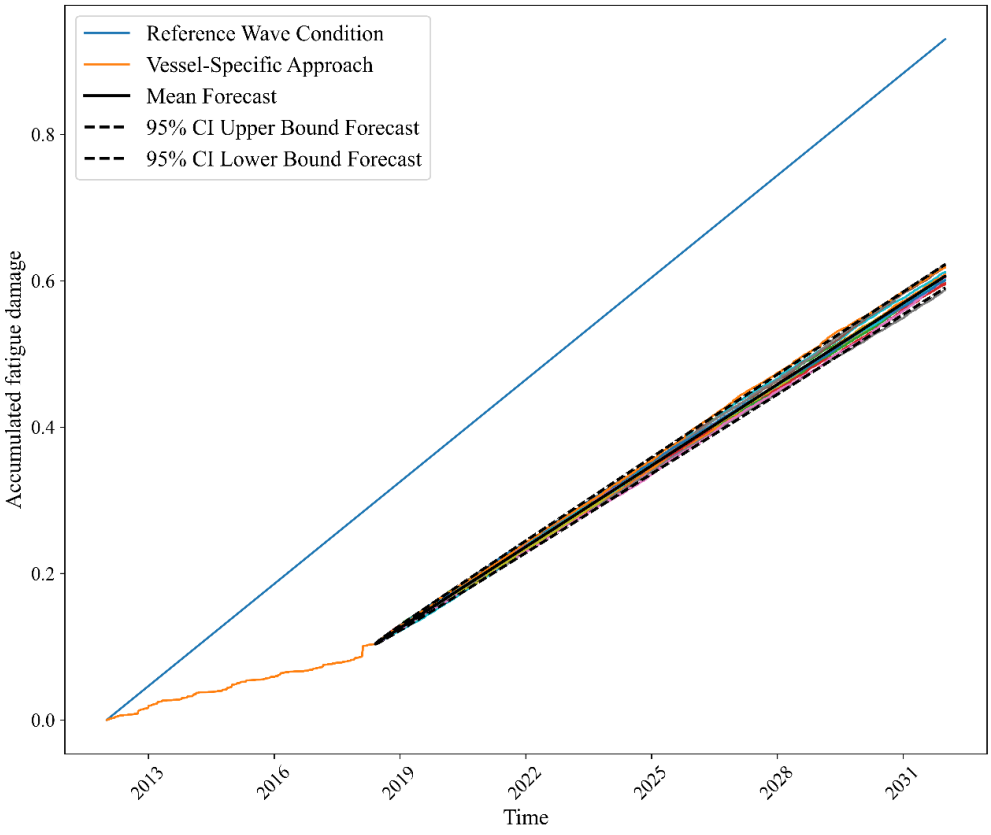

Figure 3.14. Future fatigue damage prognosis for critical area RC1

It can be seen in Figure 3.14 that due to the wave scatter diagram weighting favoring the reference wave conditions, the forecasted fatigue damage rate more closely follows the reference wave condition. The resulting distribution of possible fatigue damage at the end of the vessel's service life can also be determined. This distribution, given the assumptions made about the vessel's future operational conditions, can be used to estimate a probability of failure. For this approach, failure is defined as the accumulated fatigue damage exceeding a value of 1, which corresponds to the presence of a through-thickness crack. In this case study, at the end of the vessel's design service life, the probability of failure is determined to be infinitesimally small.

The simulation can be extended to run until the failure condition is reached to estimate the remaining useful life (RUL). Using the same Monte Carlo fatigue prognosis model, the estimated remaining useful life was calculated. The mean RUL when considering the weighted combination of the reference wave conditions and vessel-specific wave conditions was 24.23 years. For comparison, the simulation was also run using only the reference condition which resulted in a RUL mean value estimate of 19.28 years and only the vessel-specific wave condition which had a RUL mean value estimate of 52.47 years. This further highlights the possible conservatism in the reference wave condition compared to vessel-specific operations, as the vessel-specific wave conditions result in a RUL more than double the RUL estimated from the reference wave condition and weighted combination wave condition. This insight could support potential life extension or fleet balancing if certain routes are found to result in greater fatigue accumulation.

As the vessel ages, the forecasted fatigue damage rate will be more heavily influenced by its historical operation. Additionally, if assumptions were made about its future operational routes, the corresponding wave data for those routes could also be incorporated. As discussed earlier, the assumptions made about the future wave conditions for this case study are likely conservative and this is appropriate given the limited vessel-specific data and the assumed lack of knowledge about the future vessel operations and the presence of other uncertainties that are not accounted for (e.g. computational model uncertainties, S-N curve parameter uncertainty, corrosion effects, mean stress effects, etc.). As more vessel-specific data is collected, such as steel thickness gauging measurements, vessel hydrostatic loading information, etc. these can be incorporated into the Digital Twin to continue to reduce the uncertainty and refine the fatigue damage estimation and forecasting.

3.3.5 Future Work

As highlighted in this Chapter, challenges introduced by gaps in the data and requirements for calculation speed resulted in several simplifying assumptions being made in the Digital Twin model and additional sources of uncertainty that were not quantified. Further, as sensor data becomes available from monitored vessels, validation of the various steps of the fatigue monitoring process should be performed. Validation should be considered in four key steps: (1) validation of metocean model data with actual vessel encountered wave conditions, (2) validation of vessel global response to the

encountered wave conditions, (3) validation of stress calculated at the representative critical areas, and (4) validation of fatigue damage accumulation prediction. Additionally, within each step there are also other sources of uncertainties that could be included, and model fidelity decisions that can be examined to quantify the impact of these assumptions.

Future development of the Digital Twin approach should also incorporate the influence of high-frequency phenomena such as springing and whipping. During ship structural design, springing and whipping are considered separate from the primary design process. A typical procedure would involve applying specialized software programs to evaluate slamming, springing, and whipping. The resultant fatigue damage from these effects is then added to the fatigue calculated in the primary design process. Extension of the design approach to consider the encountered sea state conditions of the monitored vessel could be used to estimate these effects in the Digital Twin.

The proposed approach also focuses primarily on load monitoring for the Digital Twin. For a complete assessment of risk, the uncertainties introduced by the presence of anomalous conditions on the hull structure that might impact the fatigue damage accumulation should also be considered. This is partially handled in the proposed approach through updates to the finite element model. Plate thickness measurements from periodic hull gauging campaigns is used to update the properties of the finite element model to reflect the impact of general corrosion on the hull structure. The updated finite element model can then be used to update the corresponding stress transfer functions used in the fatigue damage calculation. The presence of local anomalies (such as corrosion pitting and grooving) are not directly accounted for in the discussed approach but can be represented separately via a Digital Twin condition model which manages and visualizes the results from visual and non-destructive testing inspections. These inspection results can be overlaid with the results from engineering analysis, such as the presented approach for fatigue damage monitoring, to provide decision-makers with the necessary data to make inspection, maintenance, and repair decisions.

3.4 Summary

This Chapter developed a Digital Twin approach for vessel-specific fatigue damage accumulation monitoring and prognosis using publicly available position and wave condition data. The Digital Twin was characterized by a combination of data and computational models that provide a lower cost alternative for tracking the impact of a vessel's operation on its fatigue damage accumulation compared to sensor-based approaches. Three options of the fatigue analysis methodology for the vessel-specific approach were presented and compared. The Digital Twin automates the end-to-end vessel-specific fatigue damage monitoring process allowing for a scalable solution that could then be applied to monitor a fleet of vessels.

The application of the Digital Twin approach was demonstrated through a case study of a containership that had been in operation for 6.5 years. The Digital Twin data and computational models were established for the selected vessel. The impact of the vessel specific wave conditions on the accumulated fatigue damage were characterized by comparison with

the fatigue damage estimation based on the design reference wave conditions. The results showed that the fatigue damage estimated from the vessel-specific wave conditions is significantly less than the damage estimated for the same period during design. Additionally, the daily fatigue damage rate is tracked to identify periods of time that may have resulted in more severe fatigue damage compared to the assumed design fatigue rate. Tracking fatigue damage in a Digital Twin may provide ship owners with assistance in decision making related to ship operations, maintenance, and life extension.

There are still a number of uncertainties related to the fatigue damage prediction that should be addressed. These include model uncertainties, such as S-N curve parameters, computational model uncertainties (e.g. FEA and hydrodynamic models), and uncertainties related to the structural condition such as the presence of workmanship issues and impact of corrosion. For practical applications, the impact of the assumption of the form of the wave spectra will be investigated in a future study through comparisons with the results derived from a derived wave spectrum from the metocean data. Additionally, as in-service data becomes available, the proposed approach needs to be validated by comparison using on-board sensors to monitor both vessel response and strain at known critical areas, and future work is needed to further develop the Digital Twin as a decision support tool to support the life-cycle management of ship structures. Even with the current uncertainties that are not quantified, the Digital Twin approach still can provide a valuable role in providing guidance for vessel-specific operational or maintenance related concerns.

Once set up, the Digital Twin can be continuously updated as the vessel position and wave condition data become available. This vessel-specific monitoring can serve owners, operators, and classification societies by providing insights that support operational decision making and guide future inspection and survey planning, leading to enhanced vessel safety and readiness while potentially reducing operational costs.

CHAPTER 4

BAYESIAN MODEL UPDATING WITH SUMMARIZED STATISTICAL AND RELIABILITY DATA

4.1 Introduction

Decision making in engineering applications often relies on the use of mathematical or computational models to predict the behavior of complex engineering systems. When these complex engineering systems are modeled as Digital Twins the decision making relies on the data models and computational models that comprise the virtual representation as described in Chapter 2 and Chapter 3. The resulting engineering analysis is affected by both aleatory uncertainty (natural variability) and epistemic uncertainty (lack of knowledge regarding the variables or the models). The epistemic uncertainty can further be classified into statistical uncertainty and model uncertainty to represent the lack of knowledge in variables and models respectively. The model uncertainty is related to model approximations as well as the uncertainty in the model parameters. It is important that the model parameters be calibrated based on the available information so that the model predictions accurately reflect the physical reality. This updating process is informed by data and requires that all available information be properly incorporated into the modeling and simulation.

The model calibration data may be available in many different forms, including but not limited to, experimental and operational data, inspection reports, health monitoring data, engineering plans, rules and standards, and expert opinion. These heterogeneous sources of information can lead to significant challenges for model calibration, as the data may often be imprecise, uncertain, ambiguous, and/or incomplete. Additional challenges may arise as the data may not be provided in a traditional format, such as point or interval data [86], but instead may be provided in abstracted formats such as sample statistics (e.g. mean, variance, median, max, etc.), probability or frequency data, or reliability data.

The term “abstracted data” in this Chapter refers to the case where raw data has been reduced to a simplified representation of portions or the entirety of the raw dataset. There are several sources of abstracted data in practical applications [87,88]. For example, instead of receiving the full data of all the outcomes of an experiment, sometimes the only information provided from testing may be in the form of summary statistics of the observed sample distribution (e.g., mean, variance etc.) or the observed frequencies for categorical data. In some cases, the performance of a population of components or system may be given as reliability data [89] or summarized results from acceptance testing [90], both of which can be considered as forms of abstracted data. Sometimes, experts may provide their point or interval estimates of moments, frequencies, or probability ranges. This calibration process can be further complicated if data is provided simultaneously in several of these heterogeneous abstracted forms.

The incorporation of abstracted data in inference is not a new concern. Early work focused on the use of abstracted data for distribution parameter estimation of random variables, particularly in cases where the estimation based on the

original raw data might be biased due to data inconsistencies, such as outliers [91–93]. Additionally, an initial formulation by Pratt [94] describes the incorporation of summary statistics into Bayesian inference. Pratt also conveyed the idea that in certain situations, the resulting posterior distribution of the parameter of interest closely approximates the posterior distribution that would be obtained using the full dataset. Summary statistics with this property are defined as Bayesian sufficient statistics [95]. Much of the previous work has considered the cases where the raw data was available, but abstracted data was used instead to ensure robust inference in the presence of data inconsistencies. The focus of these past studies was primarily on the selection of the most appropriate statistics for the given problem.

More recent applications of abstracted data in the inference process include the identification and use of summary statistics for improving computational efficiency as commonly seen in methodologies such as the Approximate Bayesian Computation (ABC). ABC methods have been explored for a wide variety of applications in Bayesian inference [96–99] and were developed to circumvent the need to evaluate the likelihood function which might be analytically intractable or computationally expensive to evaluate. ABC is a simulation-based approach, where model parameters are randomly selected from a prior distribution and used to generate a sample dataset. The discrepancy between the simulated data set and the observed dataset is examined to determine if the model parameter values used to generate the simulated dataset should be accepted or rejected. The accepted model parameter values are used to generate the posterior distribution. For high-dimensional data, the probability of selecting appropriate model parameter values that generate a simulated dataset matching the observed dataset within a prescribed tolerance significantly decreases. To improve computational efficiency, low-dimensional summary statistics are used in ABC instead of the raw data. The main concern in using summary statistics is the loss of information associated with condensing the data, which may bias the discrimination between two models [98]. A sizeable amount of work in ABC has gone into determining the optimal summary statistics to minimize the information loss [100,101]. An area of research that has not currently been considered is the application of ABC when only sample summary statistics are provided instead of the raw data. However, previous efforts have shown that the computations can be particularly problematic when the considered statistic is not relevant to the current inference problem [102].

Another recent approach that has incorporated summary statistics into the inference process is maximum relative entropy (MrE). The MrE method has been proposed as a generalized framework to unify classical Bayesian inference with the concept of Maximum Entropy (MaxEnt) [103]. This has been found to be particularly useful in cases where both point data and moment data[1] are given [104]. Based on the axioms of maximum entropy [105], the optimal posterior

[1] Moment data in this case refers to information about the expected values of moments of the distribution and is a form of abstracted data.

distribution is the one that maximizes the relative entropy between the prior and posterior distributions. Observation data is incorporated into the inference process through the placement of constraints on the posterior distribution. This formulation is beneficial since it allows for the incorporation of any form of data that can be written as a constraint on the posterior distribution. While the advantage of this approach for engineering problems has been demonstrated [106], there is still some debate concerning its performance. Particularly, some studies argue that in certain situations, the MrE method conflicts with Bayes' rule [107,108] and that it can often lead to counterintuitive consequences [109]. This is perhaps most apparent when considering the sequence effects of processing different types of information, where the processing of constraints simultaneously vs. in different sequential orders could result in different posteriors. Another limitation of the MrE method is that the formulated constraints placed on the posterior are hard constraints, meaning that all posterior distributions which violate the constraint are ruled out. This can lead to difficulties if there is uncertainty in the abstracted data; the incorporation of data uncertainty is a challenge that is yet to be fully addressed in the MrE method.

The use of summary statistics in the Bayesian inference process has typically been examined as an alternative to using the raw data in order to ensure robust inference in the presence of data inconsistencies or to reduce the computational effort in inference, and the focus in both these cases has been on identifying the appropriate form of the statistics to achieve accurate inference results. This Chapter considers the case where only the abstracted data is provided and the raw data is unavailable, and we seek to incorporate this form of data in Bayesian inference.

There are several major challenges when considering the inference problem if only abstracted data is provided. These include the potential loss of information resulting from the data abstraction resulting in an insufficient statistic and the incorporation of the uncertainty associated with the probability distribution of the statistic resulting from a random sample of limited and potentially unknown sample size.

Bayesian networks provide a convenient and well-established approach for facilitating the inference of unknown or unobservable parameters, utilizing observations of random variables conditional on these unknown parameters. Therefore, this Chapter proposes a novel idea to incorporate "observations" of abstracted data through a Bayesian network representation to enable the Bayesian inference process in the presence of abstracted data. The relevant theory is developed from first principles and is suitable for practical problems. Since the proposed approach is based on a Bayesian network representation, this approach can be easily extended beyond the simple inference of distribution parameters of random variables (based on observations of that random variable) to the calibration of model parameters in physics models.

The remainder of the Chapter is organized as follows. Section 4.2 reviews Bayesian networks and inference. Section 4.3 proposes the methodology to incorporate abstracted data into the Bayesian network and presents a generalized form of Bayesian inference with abstracted data. Section 4.4 illustrates the proposed approach for inferring distribution

parameters using material yield strength data. Section 4.5 then demonstrates the use of the proposed approach for physics model calibration using manufacturing acceptance testing/component reliability data. Section 6 provides concluding remarks.

4.2 Bayesian networks and inference

In this section, we first discuss stochastic and deterministic nodes in Bayesian networks and discuss how Bayesian methods provide a convenient framework for combining prior beliefs about parameters with current evidence gained from data.

4.2.1 Bayesian networks

Bayesian networks provide a convenient framework for graphically representing probabilistic relationships among multiple variables. More specifically, a Bayesian network is a directed, acyclic graph (DAG) representation of a multivariate distribution, expressing its decomposition into a combination of marginal and conditional probabilities. An example of a DAG model is given in Figure 4.1.

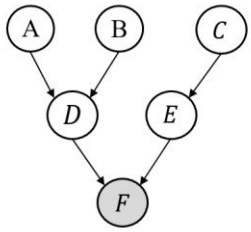

Figure 4.1. DAG model example

Each node in a Bayesian network denotes a random variable and the directed edges between nodes (arcs) are associated with conditional probabilities. If there exists a directed edge between two nodes, the upstream node is designated the parent node and the downstream node is designated the child node. The dependence between these nodes can be described mathematically by a conditional probability distribution. Based on the *directed Markov condition*, a node is independent of its non-descendant nodes when conditioned on its parent nodes, therefore the Bayesian network can be decomposed into a product of conditional and marginal probabilities using the graphical structure and the chain rule of probability [110,111]. If the random variables in a Bayesian network are denoted as $\boldsymbol{X} = \{X_1, X_2, \ldots, X_n\}$, then from the chain rule in probability theory, the joint distribution of $\boldsymbol{X}$ is given by

$$f_X(X) = \prod_{i=1}^{n} f_{X_i}\left(X_i|\mathrm{Pa}_{X_i}\right) \tag{4.1}$$

where $f_{Xi}(X_i|\text{Pa}_{Xi})$ denotes a conditional probability distribution of X_i and Pa_{Xi} denotes the parent nodes of X_i. If $f_{Xi}(X_i|\text{Pa}_{Xi}) = f_{Xi}(X_i)$, then X_i is a root node and is defined by a marginal distribution. For the example DAG given in Figure 4.1, the joint distribution of the Bayesian network can be decomposed as:

$$p(A,B,C,D,E,F) = p(F|D,E)p(D|A,B)p(A)p(B)p(E|C)p(C) \tag{4.2}$$

In directed graphical models, the direction of the arcs between nodes can also be seen as indicating causality. For example, in Figure 4.1, the arc from C to E can be regarded as signifying that C "causes" E. For many engineering applications, where the relationships between random variables are related by known physics models, this is often convenient for the construction of the graph structure. In these cases, the arc directions are established from the known causality of the data generative process being modeled.

4.2.2 Deterministic nodes in Bayesian networks

Each random variable in the graphical model corresponds to uncertainty that is to be modeled and is represented by a *stochastic node* that is probabilistically conditioned on its parent nodes. Directed graphical models can also be used to encode deterministic relationships. A node in a directed graphical model is a *deterministic node* if it is functionally dependent on its corresponding parents. A deterministic node can be considered as a special case of uncertainty where its outcome has exactly only one possible value for each possible configuration of its parent node states. In other words, if the states of the parent nodes are known, then the value of the deterministic node is also known with certainty. When deterministic nodes are present in the middle layers of a directed graphical model, they may also sometimes be referred to as hidden variables, as they exist solely to simplify the structure of the network and reduce the total number of arcs. Deterministic nodes present in a bottommost layer (i.e. they have no child nodes) of the graphical model represent a transformation and/or abstraction of their corresponding parent node uncertainty. The directed edges connecting two nodes can be either stochastic or functional depending on the child node type [112]. Arcs terminating at a stochastic child node are designated as *stochastic arcs* and arcs terminating at deterministic child nodes are designated as *functional arcs*. In this Chapter, stochastic nodes are represented by circles and deterministic nodes are represented by inverted triangles. It is emphasized that deterministic nodes are only present in the graphical model to simplify its presentation but should not be included with the stochastic nodes in the factorization of the multivariate distribution since the joint PDF of the combined stochastic and deterministic nodes does not exist.

4.2.3 Bayesian inference from observed data

Consider again a random sample of data $x_1, \ldots, x_n$ now taken from a distribution $f(x|\boldsymbol{\theta})$ for a random variable which is dependent on unknown input parameters $\boldsymbol{\theta}$ contained in a parameter space Θ. In the canonical Bayesian inference process, the goal is to estimate the posterior distribution of $\boldsymbol{\theta}$. Our existing knowledge of $\boldsymbol{\theta}$ is represented through the *prior distribution* $f'(\boldsymbol{\theta})$ and this knowledge can be updated through the information provided from the observed data $x_1, \ldots, x_n$ in

the form of the *likelihood* function, given as $f(\boldsymbol{x}|\boldsymbol{\theta})$ or $L(\boldsymbol{\theta}|\boldsymbol{x})$ or simply $L(\boldsymbol{\theta})$. Utilizing probability laws and Bayes' theorem, the *posterior distribution* is given as

$$f''(\boldsymbol{\theta}|\boldsymbol{x}) = \frac{L(\boldsymbol{\theta})f'(\boldsymbol{\theta})}{\int L(\boldsymbol{\theta})f'(\boldsymbol{\theta})d\boldsymbol{\theta}} \tag{4.3}$$

It can be seen that the denominator is the marginal distribution of the data based on the prior $f'(\boldsymbol{\theta})$ and is simply a normalization factor. Therefore, the posterior distribution can alternatively be written as

$$f''(\boldsymbol{\theta}|\boldsymbol{x}) \propto L(\boldsymbol{\theta})f'(\boldsymbol{\theta}) \tag{4.4}$$

The likelihood function can be understood as the probability of observing the given data $x_1, \ldots, x_n$ conditioned on the parameters $\boldsymbol{\theta}$. From the perspective of the Bayesian network as established in the previous section, the expression for the likelihood function can be given as

$$L(\boldsymbol{\theta}|\boldsymbol{x}) \propto f_X(X = x|\mathrm{Pa}_X) \tag{4.5}$$

where $\mathrm{Pa}_X \in \boldsymbol{\theta}$ are the parent nodes of X and $f_X(X = x|\ \mathrm{Pa}_X)$ is the PDF value at $X = x$ from the conditional probability distribution for X_i.

This formulation for the likelihood function considers data collected from a single experiment. In the case of data obtained from n different independent experiments, the final likelihood function will be the product of the n likelihood functions calculated for each individual experiment.

$$L(\boldsymbol{\theta}) \propto \prod_{i=1}^{n} f_X(X = x_i|\mathrm{Pa}_X) \tag{4.6}$$

In this Chapter, nodes in the Bayesian network which have corresponding observations are indicated by being shaded.

4.3 Incorporating abstracted data into Bayesian networks and inference

This section proposes a methodology in which abstracted data can be represented in a Bayesian network through a deterministic node. We then demonstrate how observations of the abstracted data can be utilized in exact inference in the Bayesian network using *arc reversal* [113]. Practical approaches for Bayesian inference are then addressed through approximations of the sampling distribution of the abstracted data. Concepts related to sufficient and insufficient statistics are also discussed.

4.3.1 Abstracted data as deterministic nodes in Bayesian networks

A simple Bayesian network consisting of both stochastic and deterministic nodes can be seen in Figure 4.2, where the random variables, X_1, X_2, and X_3 are conditioned on their stochastic distribution parameters, $\boldsymbol{\theta}_1$, $\boldsymbol{\theta}_2$, and $\boldsymbol{\theta}_3$ respectively. The child node Y is a deterministic node which is defined as the outcome of a mathematical function of the random variables X_1, X_2, and X_3, e.g.

$$y = h(X_1, X_2, X_3) = \frac{1}{3}(X_1 + X_2 + X_3) \tag{4.7}$$

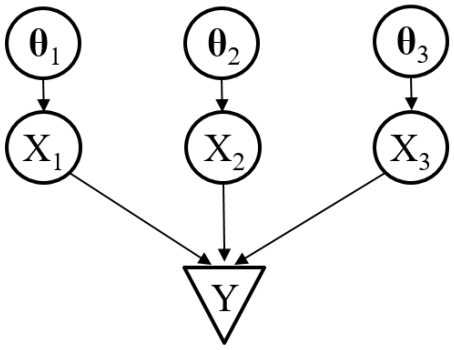

Figure 4.2. Bayesian network for simple functional relation with multiple inputs

If X_1, X_2, and X_3 have the same distribution type and distribution parameters $\boldsymbol{\theta}$, then the Bayesian network can be shown as in Figure 4.3.

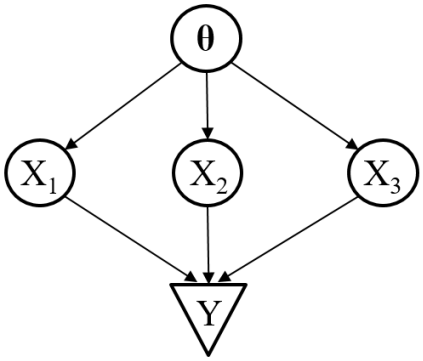

Figure 4.3. Bayesian network for simple functional relation with multiple inputs from the same distribution

The random variables, X_1, X_2, and X_3, can be thought of as independent observations from the same distribution defined by distribution parameters, $\boldsymbol{\theta}$. The deterministic node, Y, can be designated as a *statistic* and the function $g(\boldsymbol{X})$ can be designated as a *statistic function*.

4.3.2 Data abstraction and the statistics function

If the Bayesian network is generalized for a random sample of n independent observations, $x_1,\ldots, x_n$ taken from the same distribution, we can define a function $T(\boldsymbol{X})$ which is evaluated from the observations. Any real-valued function $T(\boldsymbol{X})$ is designated a *statistic*. Some examples of statistics include the sample mean, the sample variance, the sample median, and the maximum observation of a sample. The Bayesian network corresponding to the data abstraction is developed following the data generative process and is shown in Figure 4.4. For convenience, the layer of independent observations are collapsed are collapsed to a subgraph represented by plate notation.

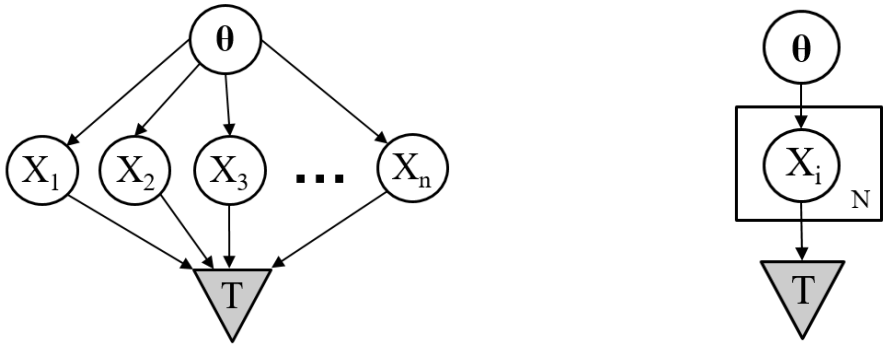

(a) (b)

Figure 4.4. a) Bayesian network for statistical function, b) Bayesian network collapsed plate notation representation of statistic function

In the Bayesian inference problem, we seek to update our knowledge of the distribution of parent nodes in the Bayesian network using observations of the child nodes. In the present case of the statistic function, the only information we know about the true value of the parent node, $\boldsymbol{\theta}$, is given by the prior distribution for $\boldsymbol{\theta}$ and the data observed. Therefore, the raw observations $x_1,\ldots, x_n$ contain all of the new, available information about the distribution parameters being inferred. For the problem discussed in this Chapter, the raw observations $x_1,\ldots, x_n$, are considered to be unavailable, and only observations of their transformed functional output, $T(\boldsymbol{X})$, are available.

The function $T(\boldsymbol{X})$ defines a form of "abstraction" of the original information, in that it takes n pieces of information and transforms it to a single piece of information which is used to summarize a key feature of the raw observations. It is apparent that this "abstraction" will never result in an information gain and almost always results in a loss of information. In the ideal case, the abstracted result contains the same amount of information as the information contained in all n observations of raw data. In this case, the statistic is defined as a *sufficient statistic*. When any information regarding the parameters of interest is lost in the "abstraction", the statistic is defined as an *insufficient statistic*.

Much effort has gone into efficiently determining sufficient statistics for inferring different parameters [102]. However, this past work has been based on the assumption that the original raw observations are available, and therefore

any statistic $T(\boldsymbol{X})$ can be determined from them. There are many cases in practical engineering applications where the raw observation data may not be available, as it has already been "abstracted" to a statistic form prior to analysis. This is the situation of interest in this Chapter. In many such cases, the mean and variance may not be sufficient statistics, and in some cases, there might not be any sufficient statistics. However, out of habit or naiveté, the data collector may believe that the abstracted form is enough. In these cases, the provided statistic is often an insufficient statistic for inferring the requisite parameters. However, even in cases of information loss associated with an insufficient statistic, the observations of $T(\boldsymbol{X})$ may still provide useful knowledge about the parent nodes and can be used to update their distributions.

In the current form of the Bayesian network, it is assumed that observations are only available for the deterministic node (i.e. the statistics function $T(\boldsymbol{X})$). Consider the resulting joint probability represented by this Bayesian network as:

$$Pr(\boldsymbol{x}, t, \boldsymbol{\theta}) = Pr(t|\boldsymbol{x})Pr(\boldsymbol{x}|\boldsymbol{\theta})Pr(\boldsymbol{\theta}) \tag{4.8}$$

where t is a realization of the statistic $T(\boldsymbol{x})$. As mentioned earlier, a deterministic node can also be thought of as a special case of uncertainty, such that the conditional probability term $Pr(t \mid \boldsymbol{x})$, is equal to 1 when $t = T(\boldsymbol{x})$ and 0 otherwise. If the value of a deterministic node was known/observed, its parent nodes would be restricted to the domain of the inverse that known value under the deterministic nodes evaluation function. This proves to be a challenge, since there is no straightforward methodology for incorporating observations of deterministic nodes for inference in this model form. Therefore, observations of T cannot be used for inference using the network in Figure 4.4, and we seek to construct an alternative model form of the Bayesian network that directly gives T as a stochastic node with a conditional distribution with respect to the parameters of interest, $\boldsymbol{\theta}$.

4.3.3 Alternative Bayesian network model form via arc reversal

The alternative model form of the Bayesian network that directly gives the conditional distribution of T with respect to the parent node, $\boldsymbol{\theta}$, can be obtained exactly via a process called *arc reversal* [113].

The structure of the original Bayesian network given in Figure 4.4, including the arcs between nodes and the corresponding arc directions, was constructed based on the data generative process. However, this is only one possible factorization of the random variables comprising the multivariate distribution. The direction of any arc in the Bayesian network can be reversed provided that there is no other path between the two nodes connected by that arc. If another path existed between the two nodes, the reversal of the arc would create a cycle.

The arc reversal process is a local operation that affects only the conditional distributions of the two nodes at the ends of the arc. The distributions for the remaining nodes in the network remain unchanged. After arc reversal, both nodes will inherit each other's parent nodes, the old child node becomes the parent node, and the old parent node becomes the child node, but there may be exceptions to this general rule when either node is deterministic [114]. The process of arc

reversal can add a considerable number of arcs, increasing the relative complexity of the model after arc reversal has been performed. Additionally, if multiple arc reversals are utilized, the order in which they are performed may impact the final resulting arc structure.

Arc reversals between two stochastic nodes is accomplished by use of Bayes Theorem. Consider the Bayesian network given in Figure 4.5(a), where we seek to perform arc reversal between the stochastic nodes *X* and *Y*. After arc reversal, node *Y* inherits node *X*'s parent node and the arc between node *X* and *Y* switches direction. The resulting conditional distributions for each node in the alternative model form are a result of the application of Bayes Theorem, and the resulting Bayesian network is shown in Fig. 5(b).

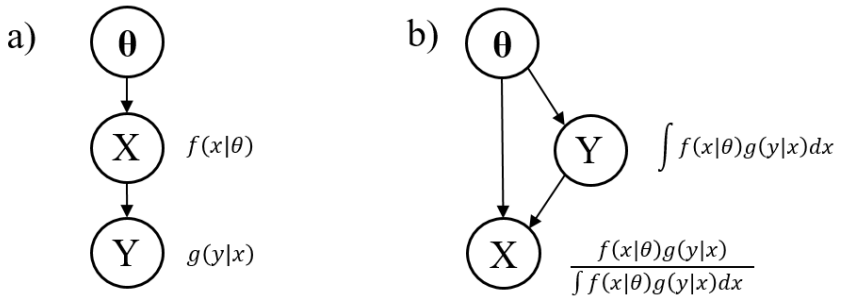

Figure 4.5. Arc reversal between two stochastic nodes: a) Original network b) Transformed network after arc reversal

The arc reversal between a stochastic and deterministic node differs from arc reversal between two stochastic nodes in that a joint distribution of the two variables does not exist, so Bayes Theorem cannot be used directly [114]. After arc reversal, the density is transferred from the stochastic node to the deterministic node. This procedure is the well-known transformation technique for deriving the distribution of a variable which is a function of a single random variable [32]. Consider the Bayesian network given in Figure 4.6(a), where the Bayesian network given in Figure 4.6(a), where *Y* is now a deterministic node given by $Y = h(X)$, where *h* is assumed to be an invertible and differentiable function. The Bayesian network resulting from the arc reversal is shown in Fig. 6(b).

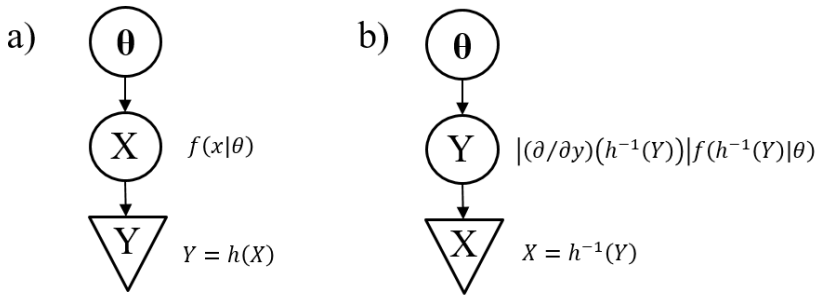

Figure 4.6. Arc reversal between a stochastic and deterministic node: a) Original network b) Transformed network after arc reversal

It can be seen in this case, that although both nodes inherit each other's parent nodes, node *X* loses $\boldsymbol{\theta}$ as a parent node. It can also be seen that node *X* is now a deterministic node. Both of these results are a consequence of the assumed invertibility of the function *h*. If the function is not invertible but has known zeros, the arc reversal process will result in node *X* as a stochastic node with possible values as the known function zeros. For example, the function $y = g(X) = x^2$ is not invertible, but has two simple zeros, $x = \pm\sqrt{y}$. If in this example, the arc between node *X* and node *Y* was reversed, node *X* would be a stochastic node with possible values $\sqrt{y}$ and $-\sqrt{y}$ with a probability $f(\sqrt{y})/\left(f(-\sqrt{y}) + f(\sqrt{y})\right)$ and $f(-\sqrt{y})/\left(f(-\sqrt{y}) + f(\sqrt{y})\right)$ respectively. If the function is not invertible and has no easily determined zeros or is not differentiable, then the distributions for the nodes after arc reversal will not have closed form solutions [114].

The concept of arc reversal for both stochastic and deterministic nodes can then be extended to the case of the statistics function. Consider the simple statistic given by the sum of two random samples from a distribution. The Bayesian network consistent with the data generative process is as shown in Figure 4.7(a). It is desired that the statistic, *T*, be a stochastic node that is conditional only on the parameters of interest, $\boldsymbol{\theta}$. To achieve such a Bayesian network, two arc reversals are required. The first arc reversal is between X_2 and *T*. Since *T* is a deterministic node and the function is invertible and differentiable, X_2 becomes a deterministic node as shown in Figure 4.7(b) and loses its parent node, $\boldsymbol{\theta}$. The first arc reversal also results in *T* becoming a stochastic node with $\boldsymbol{\theta}$ as one of its parent nodes fitting the desired model form. The second arc reversal is between node X_1 and node *T*, so that *T* will be conditional solely on the parameters of interest, $\boldsymbol{\theta}$. The Bayesian network resulting from the second arc reversal is shown in Figure 4.7(c).

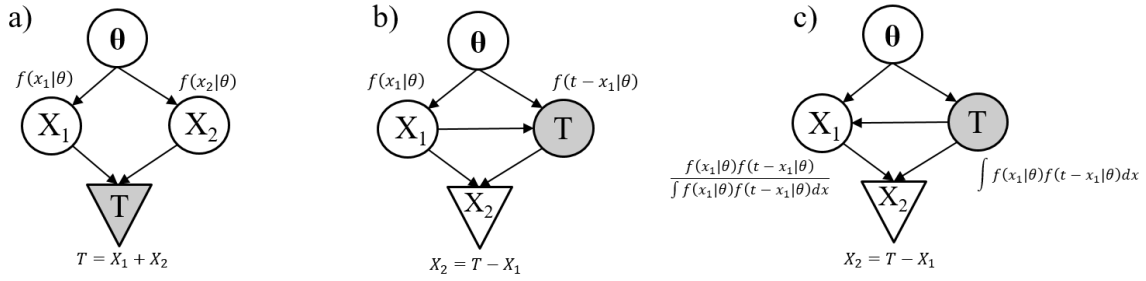

Figure 4.7. Arc reversal for summation statistic: a) Original network b) Transformed network after first arc reversal c) Transformed network after second arc reversal

Thus, it can be seen that the final resulting Bayesian network matches our goal model form. It can also be seen that the resulting conditional distribution describing the stochastic node *T* is the convolution formula. In other words, arc reversal allows the construction of a mathematically equivalent Bayesian network enabling inference based on observed abstracted data.

This procedure for arc reversal can be further extended to any number of samples of *X*, and any statistic function $T(\boldsymbol{X})$ to obtain the desired Bayesian network model form required for inference. The resulting generalized Bayesian network

for a statistic function is given in Figure 4.8, with the plate notation being utilized to simplify the representation of the subgraph of the *X*'s.

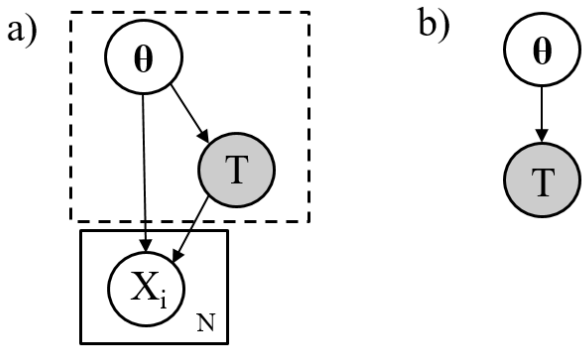

Figure 4.8. Bayesian network after arc reversal for observations of statistic *T:* a) Complete Bayesian network after arc reversal, b) Simplified Bayesian network after removing barren nodes

The resulting joint probability distribution for the complete Bayesian network can then be written as:

$$Pr(\boldsymbol{x}, t, \boldsymbol{\theta}) = Pr(\boldsymbol{x}|t, \boldsymbol{\theta})Pr(t|\boldsymbol{\theta})Pr(\boldsymbol{\theta}) \tag{4.9}$$

where *T* is now represented by a stochastic node conditioned on the parent node, $\boldsymbol{\theta}$, and observations of this node can be utilized for inference.

For the currently considered problem, the *X*'s are unobserved and barren, thus only the Bayesian network shown inside the dashed box will be utilized for performing Bayesian inference of the of the parameters of interest, $\boldsymbol{\theta}$, thus we may only need to consider the Bayesian network given in Fig. 8(b) when performing inference in practical problems.

Most importantly, the arc reversal process also gives the exact form of the conditional distribution of *T* to be used in inference, $f_T(t|\boldsymbol{\theta})$. This resulting conditional distribution is typically called the sampling distribution or finite-sample distribution, due to the fact that it is derived from a random sample of finite size *n*. However, as can be seen even for the simple example of the sum of two random variables, the determination of the exact sampling distribution via the arc reversal process is *np*-hard and quickly becomes computationally expensive for a large number of individual *X* values. Furthermore, if the statistic function, $T(\boldsymbol{X})$, is such that it is not invertible or differentiable, then there may not be a closed form expression for the sampling distribution of *T* after arc reversal. Thus, for any practical applications, sampling distribution for *T*, $f_T(t|\boldsymbol{\theta})$, must be determined using approximate methods.

4.3.4 Approximation of the Sampling Distribution, $f_T(t \mid \theta)$

The sampling distribution $f_T(t|\boldsymbol{\theta})$ is dependent on the underlying distribution of the parent node, $f_\theta(\boldsymbol{\theta})$, the form of the statistic function, $T(\boldsymbol{X})$, and the sample size, *n*. As shown in the previous section, the exact form of the sampling

distribution can be determined analytically using the arc reversal procedure when considering a graphical model. Alternative analytical methods to the arc reversal methods used to obtain the sampling distribution include the cumulative-distribution-function technique and the moment-generating-function technique [115]. A large amount of theoretical work has been devoted to the derivation of the sampling distributions of various common statistics [116–119]. However, as noted, the exact form of the sampling distribution, $f_T(t|\boldsymbol{\theta})$, may be analytically intractable or too computationally expensive to determine. For practical applications it must be determined using alternative methods, including sampling-based approximations and assumed parametric distributions.

By utilizing the conditional relationships of the known data generative process, it is always possible to use sampling-based methods for the approximating arc reversal process in estimating the probability density function (pdf) coinciding with the density transfer from the stochastic nodes to the deterministic node. Values from the sampling distribution are generated synthetically using Monte Carlo simulations for assumed values of the parameters of interest, $\boldsymbol{\theta}$, where several thousand sets of random samples are drawn and the resulting statistic is calculated from each set of samples [120,121]. These samples can then be used to construct an empirical CDF, or approximate the pdf using kernel density estimation [122]. However, even this approximation method may also become computationally expensive when utilized for inference for complex Bayesian networks.

Another possible approach is to approximate the sampling distribution using an assumed parametric distribution form and analytically defined distribution parameters relating to the parameters of interest. It has also been found that in many cases, due to the Central Limit Theorem, the normal distribution will in many cases give a fairly good approximation for the sampling distribution even when the sample size n is small so long as the parent distribution is not highly skewed or multimodal [123]. For example, the normal approximation well approximates the sampling distribution of sample mean for any distribution type provided that the sample size is sufficiently large [124]. The normal distribution is also often used for the sampling distribution of sample proportions, where the first two moments are derived from the binomial distribution. From the Rule of Sample Proportions, the distribution of a proportion, p, will be approximately normally distributed given that both $n \, x \, p \geq 10$ and $n \, x \, (1 - p) \geq 10$ [125].

The numerical examples presented later in this Chapter demonstrate a variety of these methods for approximating the sampling distribution when performing inference.

4.3.5 Bayesian inference with abstracted data

As shown in the section 4.3.3, the arc reversal can be used to transform the Bayesian network to the desired form which gives the abstracted data T as a random variable conditional on the parent nodes. Once the abstracted data T is represented as a stochastic node in this Bayesian network form, observations of the abstracted data form can be incorporated in the inference process. After this transformation, the resulting likelihood can be written as

$$L(\boldsymbol{\theta}|\boldsymbol{t}) \propto f_T(T = t|\mathrm{Pa}_T) \tag{4.10}$$

where the parent nodes $\mathrm{Pa}_T \in \boldsymbol{\theta}$. Given the sampling distribution for the statistic T corresponding to the abstracted data either by exact analytical methods or approximate methods, the likelihood of observed abstracted data can be calculated.

If multiple independent statistic values are given, then the combined likelihood can be calculated similar to Eq. 4.6.

$$L(\boldsymbol{\theta}|\boldsymbol{t}) \propto \prod_{i=1}^{n} f_T(T = t_i|\mathrm{Pa}_T) \tag{4.11}$$

The generalized form of the likelihood function which may consider abstracted data may then be combined with the prior to determine the posterior distributions of the parameters $\boldsymbol{\theta}$. As indicated in Eq. 4.4, the product of the likelihood and prior are only proportional to but not equal to the posterior distribution. This is due to the normalization term $\int L(\boldsymbol{\theta}) f'(\boldsymbol{\theta}) d\boldsymbol{\theta}$ in the denominator which may often be challenging to calculate due to the multi-dimensional integration required. Therefore, an inference algorithm is required to evaluate the posterior distribution. Exact inference is often computationally expensive for large networks; thus sampling-based methods are used to approximate the posterior distribution [126–128].

4.3.6 Simultaneous vs sequential inference

Having formally defined the generalized likelihood function for abstracted data and discussed how this method can be used for Bayesian inference, the ramifications of this methodology on simultaneous and sequential inference are discussed here. When provided with multiple sets of independent data, there is the option of performing the inference simultaneously with all of the provided data or sequentially, as when considering data which are received sequentially in time. This is particularly meaningful in the context of comparisons of the proposed methodology with entropy approaches such as MrE when handling abstracted data.

In the MrE approach, the observed data, whether it is raw data or abstracted data, is included through the application of constraints on the posterior distribution. When the optimization process is performed to infer the posterior, all the distributions that do not satisfy the given constraint are ruled out. For multiple sets of data, multiple constraints will be defined. Constraints are called *commuting* [104] when there is no difference between whether they are handled simultaneously or sequentially. However, generally constraints do not commute and therefore the resulting final posterior in the MrE approach depends on whether they are considered simultaneously or sequentially.

For traditional Bayesian inference, the resulting posterior is the same regardless of whether the data is handled simultaneously or sequentially, due to the assumption that the observations are independent to each other. For the case of

multiple observations of abstracted data, if the corresponding raw data $\boldsymbol{x}_1$ and $\boldsymbol{x}_2$ are unknown and only $T(\boldsymbol{x}_1)$ and $T(\boldsymbol{x}_2)$ are given, then the sequential and simultaneous inference using the abstracted data will also be the same provided that $T(\boldsymbol{x}_1)$ and $T(\boldsymbol{x}_2)$ are independent.

Now consider the case where both point data and abstracted data are provided. If collected independently, this is equivalent to being provided with observation data for two different branches of the Bayesian network, where the parameter(s) to be inferred, $\boldsymbol{\theta}$, is the shared node. When considering simultaneous or sequential inference, we can consider three possible cases: (1) simultaneous update with both traditional point data and the abstracted data, (2) sequential updating, first with the point data and then with the abstracted data, and (3) sequential updating, first with the abstracted data and then with the point data. The selection of the inference case may be dependent on the order in which the data was received, and we seek to determine the final posteriors resulting from these three different cases. It was shown by Ling [129] that for a Bayesian network of the form given in Figure 4.9, all three of these cases will result in identical posterior distributions. This is advantageous when compared to the MrE approach, where for non-commuting constraints, sequential updating will result in a different posterior than simultaneous updating, and the order in which constraints are applied must be carefully selected.

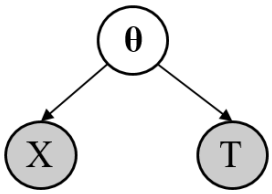

Figure 4.9. Bayesian network for observations of both point data and abstracted data

4.3.7 Inference of uniform distribution parameters given sample mean data

The following illustrative example demonstrates the value of incorporating available abstracted data into the inference process, while also showing the unavoidable information loss compared to inference with the original raw data. We consider several types summary statistic data calculated from samples drawn from a uniform distribution. Eighty synthetically generated raw data points were obtained from the distribution $X \sim U(500, 800)$. The 80 samples were split into four groups of 20 samples each, from which the sample mean, standard deviation, 5^{th} percentile, and 95^{th} percentile were obtained for each group. It is also assumed that distribution type is known, but the distribution parameters (i.e. the upper and lower bounds) are unknown.

The first inference considers the case where only the sample mean data and corresponding sample sizes are provided, and the upper and lower bounds of the uniform distribution are then inferred. The corresponding Bayesian network for the first inference case is shown in Figure 4.10, considering the network both before and after the arc reversal. Since the

first inference case assumes that only the sample mean data is available, the Bayesian network shown within the dashed box in Fig. 10(b) is used for performing inference.

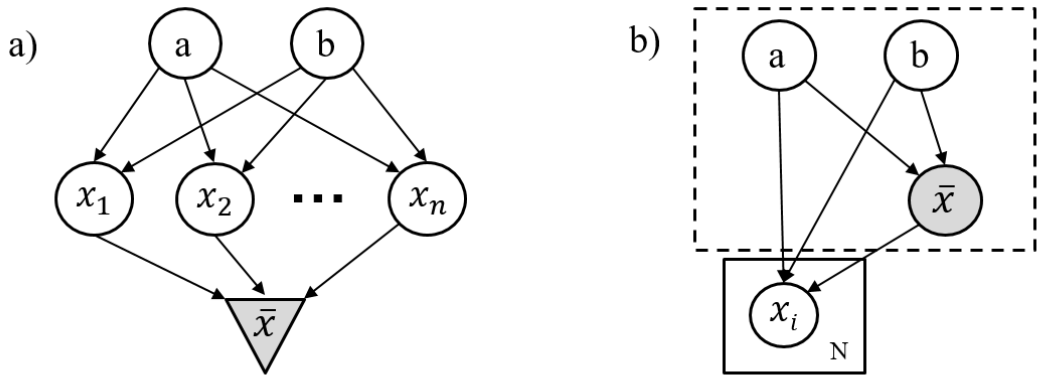

Figure 4.10. Bayesian networks for uniform distribution parameter inference using sample mean data: a) Bayesian network before arc reversal, b) Bayesian network after arc reversal

The sampling distribution, which conditions the observed sample means on the parameters of interest, results from the shown arc reversal. The distribution corresponding to the mean of *n* independent random variables, each with a uniform distribution on (*a*, *b*) is given by the Bates distribution [130], with probability density function given by:

$$f_{\bar{X}}(\bar{x}; n, a, b) = \begin{cases} \sum_{k=0}^{n} (-1)^k \binom{n}{k} \left(\frac{x-a}{b-a} - k/n\right)^{n-1} sgn\left(\frac{x-a}{b-a} - k/n\right) & if\ x \in [a, b] \\ 0 & otherwise \end{cases} \tag{4.12}$$

As the sample size is increased, due to the Central Limit Theorem, the sampling distribution for the sample mean can also be well approximated by a normal distribution:

$$\bar{X} \sim N\left(\mu, {\sigma^2}/{n}\right) \tag{4.13}$$

where μ and σ are the true population mean and standard deviation respectively, and *n* is the sample size used to calculate the sample mean. For a uniform distribution, μ and σ can easily be derived from the upper and lower bounds.

$$\bar{X} \sim N\left(\frac{a+b}{2}, \frac{(b-a)^2}{12n}\right) \tag{4.14}$$

where *a* and *b* are the lower and upper bounds respectively.

The second and third inference cases consider the availability of additional abstracted data which can be utilized along with the sample means during inference. The second case introduces the availability of sample standard deviation data

and the third case further includes the availability of sample 5th and 95th percentile data. The Bayesian network corresponding to the third case is shown in Figure 4.11.

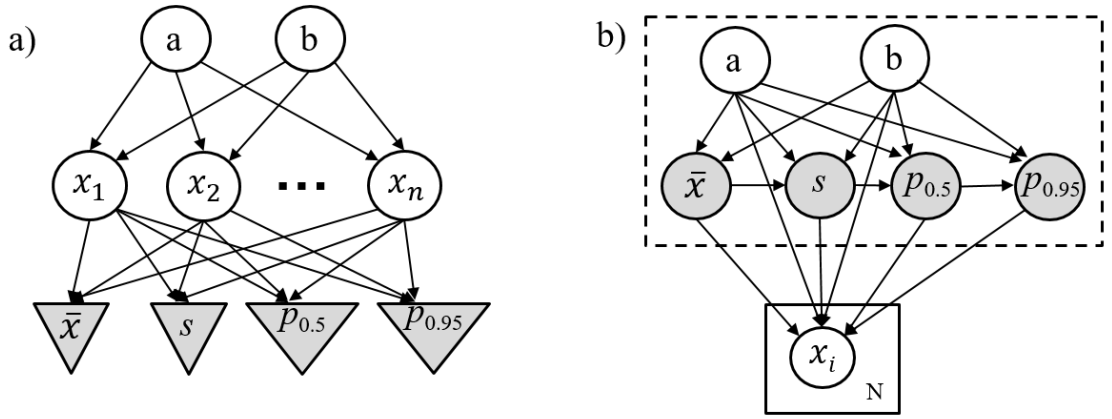

Figure 4.11. Bayesian networks for uniform distribution parameter inference using sample mean, standard deviation, and percentile data: a) Bayesian network before arc reversal, b) Bayesian network after arc reversal

The inclusion of observations of additional forms of abstracted data in the inference process adds additional considerations to the development of the required sampling distribution. It can be seen in Figure 4.11(b) that the arc reversal has resulted in a conditional relationship between the observed abstracted data that must also be accounted for. Unlike the first inference case, there is no closed form solution that can be derived for the joint sampling distribution of the sample mean, standard deviation, and percentile data. Therefore, the joint sampling distribution for all of the observed abstracted data forms must be approximated. Using a sampling-based approach, the sampling distribution can be approximated for different values of distribution parameters *a* and *b*, by simulating the data generative process shown in Figure 4.11(a) and constructing the multivariate sampling distribution using kernel density estimation [39].

The final case considers that the entirety of the raw data is available, and the inference process is then repeated. The results of all inference processes are shown in Figure 4.12.

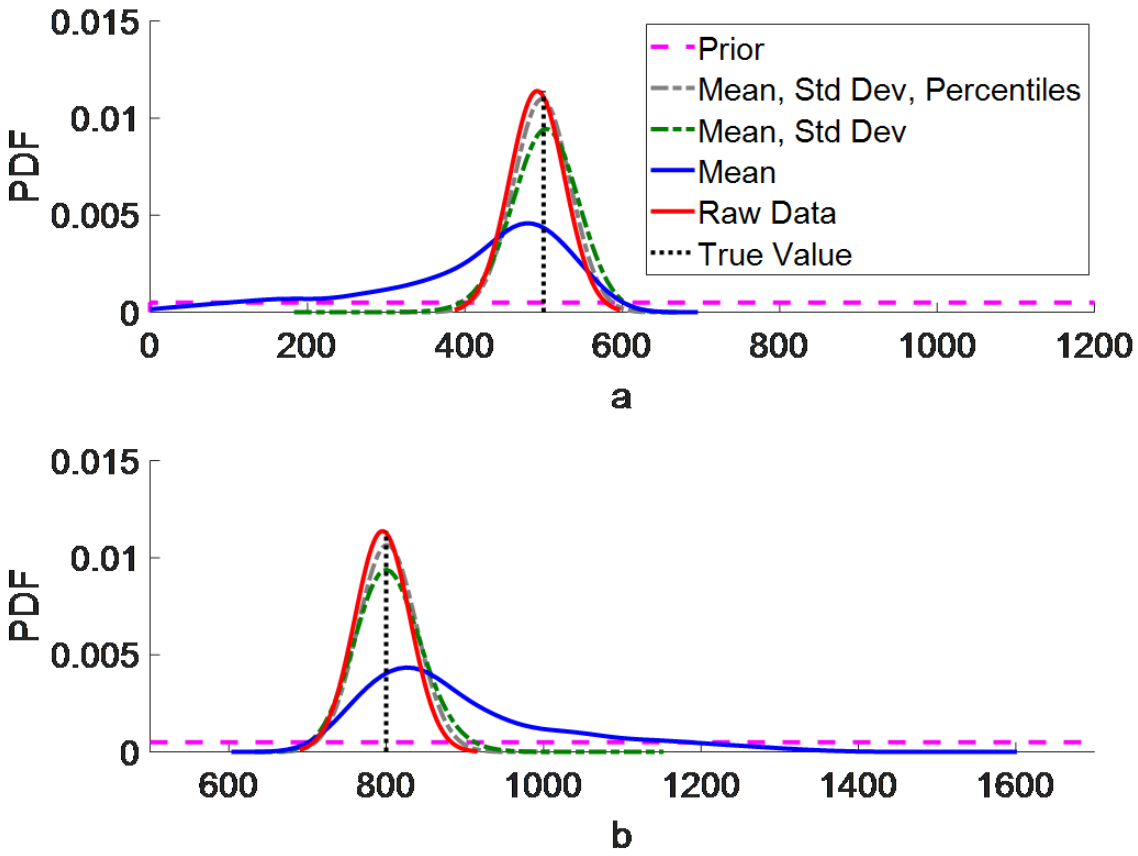

Figure 4.12. Posterior distributions of the lower and upper bound parameters for a uniform distribution

It can be seen that for this example, although the sample mean is an insufficient statistic for inferring the upper and lower bounds, the resulting posterior obtained from the abstracted data still provides a meaningful inference of the parameters. It is also clear that the loss of information resulting from the abstraction leads to greater uncertainty in the posterior when compared to the posterior obtained from the raw data. However, as observations of additional summary statistics are considered, the loss of information is reduced and the posterior resulting from the abstracted data converges to that resulting from the original raw data. It may be possible to characterize information loss resulting from data abstraction with respect to the inference of the parameters of interest through global sensitivity analysis (GSA). This will be considered in future work.

4.4 Application to sample mean data for material yield stress

Consider the case of material yield stress data under tensile test obtained by a steel mill over a four year period, but instead of reporting the raw data, the summary statistics for the means of the samples and corresponding sample sizes for all the tests performed were given instead. We note that in the case of a normal distribution with unknown variance, the sample mean alone is an insufficient statistic for inferring the distribution variance [124], and therefore some information

regarding the distribution has been lost in the transformation from the raw data to the abstracted form. We seek to infer the distribution parameters for the yield stress by using the proposed approach.

Table 4.1. Sample mean data

Sample	Sample Mean (MPa)	Sample Size
1	376	737
2	393	24
3	377	2189
4	386	767
5	371	11396
6	348	2497
7	383	940
8	364	102
9	377	4237
10	389	2252
11	388	24
12	393	19
13	352	2989
14	388	1513
15	385	23

Past work [131,132] has shown that the lognormal distribution is appropriate to represent the distribution of yield stress. Therefore, $\sigma_y \sim LN(\lambda, \zeta)$ where $\boldsymbol{\theta} = \{\lambda, \zeta\}$ are the unknown parameters to determine using Bayesian inference. Suppose non-informative priors are selected for both λ and ζ with parameters based on these previous studies.

4.4.1 Hierarchical Bayesian model

When considering real-world data, the observed data are often naturally clustered. Although these clusters may be sampled at random and consist of random sampling within the cluster, this often induces dependencies between the observations. When considering abstracted data, clustering may be even more common, since data is usually abstracted in groupings based on natural breaks in the data collection process. In the example of yield strength data, this may arise from taking means from samples corresponding to different manufacturing batches. The dependencies introduced by this

clustering can be considered using a hierarchical Bayesian model [133], which allows the model parameters to vary by group/cluster. For the present example, the overall distribution of the material yield stress is expected to follow the lognormal distribution, but it is assumed that the observed means were obtained from clustered data based on manufacturing batches. Each manufacturing batch is assumed have a unique mean, μ_{batch}, corresponding to aleatory uncertainty in the inputs to the manufacturing process. The variability of the batch means can be accounted for in the Bayesian network through the consideration of a hierarchical Bayesian model, where each of the observed sample means, $\bar{x}$, is assumed to come from a unique batch, where for each batch, $\mu_{batch} \sim N(\mu_x, \sigma_{batch})$. The additional unknown standard deviation parameter, σ_{batch}, is also calibrated. The corresponding Bayesian network is shown in Figure 4.13, with Figure 4.13(a) showing the original Bayesian network corresponding to data generative process and Figure 4.13(b) showing the required model form which results from the arc reversal process and gives $\bar{x}$ as a stochastic node. Given the desired form of the Bayesian network (Figure 4.13(b)), since we only have the observations of the abstracted data, we only requires the Bayesian network shown inside the dashed box for performing inference.

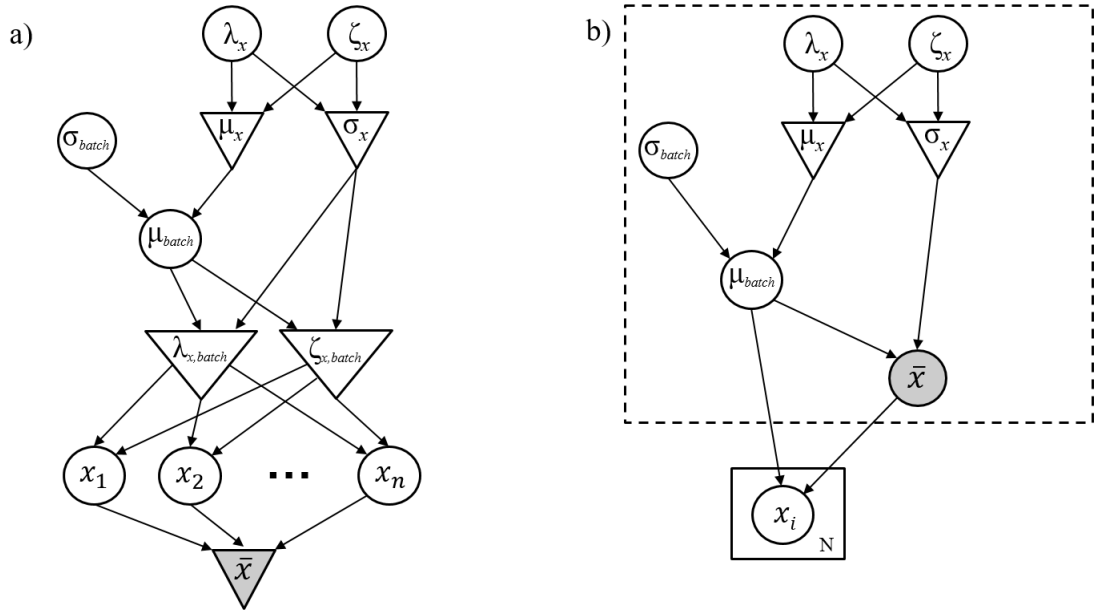

Figure 4.13. Bayesian network for yield strength distribution with consideration of random effects: a) Bayesian network before arc reversal, b) Bayesian network after arc reversal

The complexity of the Bayesian network and the large number of samples makes it computationally inefficient to derive the exact analytical form for the sampling distribution via the arc reversal process. Instead, given the transformed Bayesian network in Figure 4.13(b), it is then necessary to determine an approximation for sampling distribution of $\bar{x}$ given the unknown parameters, λ_x, ζ_x, and σ_{batch}. As noted in the previous example, the sampling distribution for the sample mean can be well approximated by a normal distribution provided a sufficiently large sample size. Therefore, the conditional sampling distribution given a value of μ_{batch} can be approximated by:

$$\bar{X}|\mu_{batch}, \boldsymbol{\theta} \sim N\left(\mu_{batch}, {\sigma_x}^2/n\right) \tag{4.15}$$

where $\boldsymbol{\theta} = \{\lambda_x, \zeta_x, \sigma_{batch}\}$. Since μ_{batch} is also a random variable conditioned on the parameters of interest, we can find the unconditional distribution of $\bar{x}|\boldsymbol{\theta}$ by integrating out the unknown parameter μ_{batch}.

$$p_{\bar{X}|\boldsymbol{\theta}}(\bar{x}) = \int p_{\bar{X}|\mu_{batch},\boldsymbol{\theta}}(\bar{x}|\mu_{batch}, \boldsymbol{\theta}) p_{\mu_{batch}|\boldsymbol{\theta}}(\mu_{batch}|\boldsymbol{\theta}) d\mu_{batch} \tag{4.16}$$

The first two moments of the unconditional distribution, $p_{\bar{X}|\boldsymbol{\theta}}(\bar{x})$, are given as:

$$\begin{aligned} E_{\bar{X}|\boldsymbol{\theta}}[\bar{X}|\boldsymbol{\theta}] &= E_{\mu_{batch}|\boldsymbol{\theta}}\left[E_{\bar{X}|\mu_{batch},\boldsymbol{\theta}}[\bar{X}|\mu_{batch}, \boldsymbol{\theta}]\right] \\ &= \mu_x \end{aligned} \tag{4.17}$$

$$\begin{aligned} Var_{\bar{X}|\boldsymbol{\theta}}(\bar{X}|\boldsymbol{\theta}) &= E_{\mu_{batch}|\boldsymbol{\theta}}\left[Var_{\bar{X}|\mu_{batch},\boldsymbol{\theta}}(\bar{X}|\mu_{batch}, \boldsymbol{\theta})\right] \\ &\quad + Var_{\mu_{batch}|\boldsymbol{\theta}}\left(E_{\bar{X}|\mu_{batch},\boldsymbol{\theta}}[\bar{X}|\mu_{batch}, \boldsymbol{\theta}]\right) \\ &= {\sigma_x^2}/n + \sigma_{batch}^2 \end{aligned} \tag{4.18}$$

Since the distribution of $\bar{X}|\mu_{batch}, \boldsymbol{\theta}$ is Gaussian and the distribution of $\mu_{batch}|\boldsymbol{\theta}$ is also Gaussian, the resulting unconditional distribution, $\bar{X}|\boldsymbol{\theta}$, will also be Gaussian with distribution parameters as given in Eq. 4.17 and Eq. 4.18. Therefore, the resulting sampling distribution is then given by:

$$\bar{X} \sim N\left(\mu_x, {\sigma_x^2}/n + \sigma_{batch}^2\right) \tag{4.19}$$

Using the deterministic relationship between the parameters (μ_x, σ_x) and (λ_x, ζ_x), it is simple to extend this sampling distribution to be solely a function of the parameters of interest, λ_x, ζ_x, and σ_{batch}, as shown in Fig. 13(b).

Bayesian inference was performed and the resulting posteriors for the distribution parameters are shown in Figure 4.15.

4.4.2 Unknown sample size

It is important to note at this point that the approximation of the sampling distribution for *T* required that the sample sizes of the data from which statistic was abstracted be known. This is due to the sampling distribution of *T* being dependent on the data sample size *n*. For the current example, the sampling distribution variance for the sample mean is a function of the sample size, *n*, and is given by

$$\sigma_{\bar{x}}^2 = \frac{\sigma_x^2}{n} + \sigma_{batch}^2 \tag{4.20}$$

In many cases, the sample sizes for the abstracted data may also be unknown. Furthermore, when the data includes multiple observations of the abstracted data, each observation may have a unique unknown sample size. The epistemic uncertainty regarding each of these sample sizes can also be represented in the transformed Bayesian network through stochastic nodes, as shown in Figure 4.14, and these additional nodes corresponding to the sample size are also calibrated.

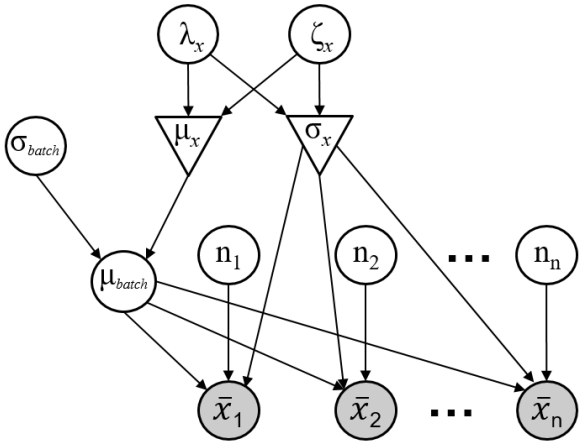

Figure 4.14. Bayesian network (after arc reversal) for abstracted data with unknown sample sizes

Repeating the previous example but now assuming that the sample sizes are unknown, the Bayesian inference results of the yield stress distribution parameters, are shown in Figure 4.15. The posteriors for the sample sizes when they are considered unknown are not included since they are not the parameters of interest.

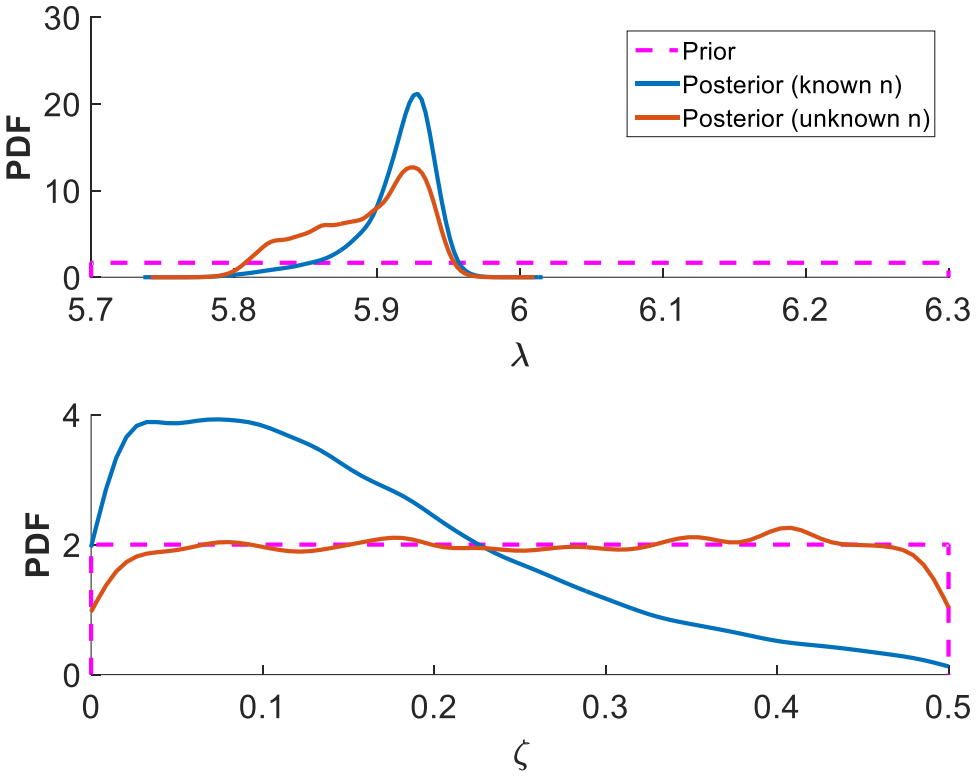

Figure 4.15. Prior and posterior distributions for yield strength parameters using mean data considering known and unknown sample sizes

For the Bayesian updating of model parameters using abstracted data, the issue of identifiability may also be present, which is clearly demonstrated in the above example. Including the unknown sample sizes in the Bayesian network renders both the scale parameter, ζ, and sample sizes, n_i, as unidentifiable. Information can still be obtained regarding the distribution location parameter, λ, but with greater uncertainty.

4.4.3 Simultaneous inference with abstracted and raw data

It was noted earlier, that since the proposed approach incorporates abstracted data into the overall Bayesian network, observations of both raw data and abstracted data can be considered either simultaneously or sequentially in the inference process, and the result will be identical. This may be very beneficial when data is received over a period of time, since it is not necessary to perform an update with all of the collected data, but to simply update the current posteriors using the most recent observed data, either raw data, abstracted data, or both.

Table 4.2. Raw yield strength data

Sample	Raw values (MPa)
1	360.6
2	360.0
3	406.2
4	385.5
5	362.4

To consider this, some additional raw data measurements are considered as given in Table 4.2. Two inference cases are then considered, the first is a sequential inference process which first considers the inference with the abstracted data, followed by inference with the raw data. The second case considers the simultaneous update using both the raw and abstracted data. The results are shown in Figure 4.16. As expected, the proposed method gives identical results for both the simultaneous and sequential updating cases.

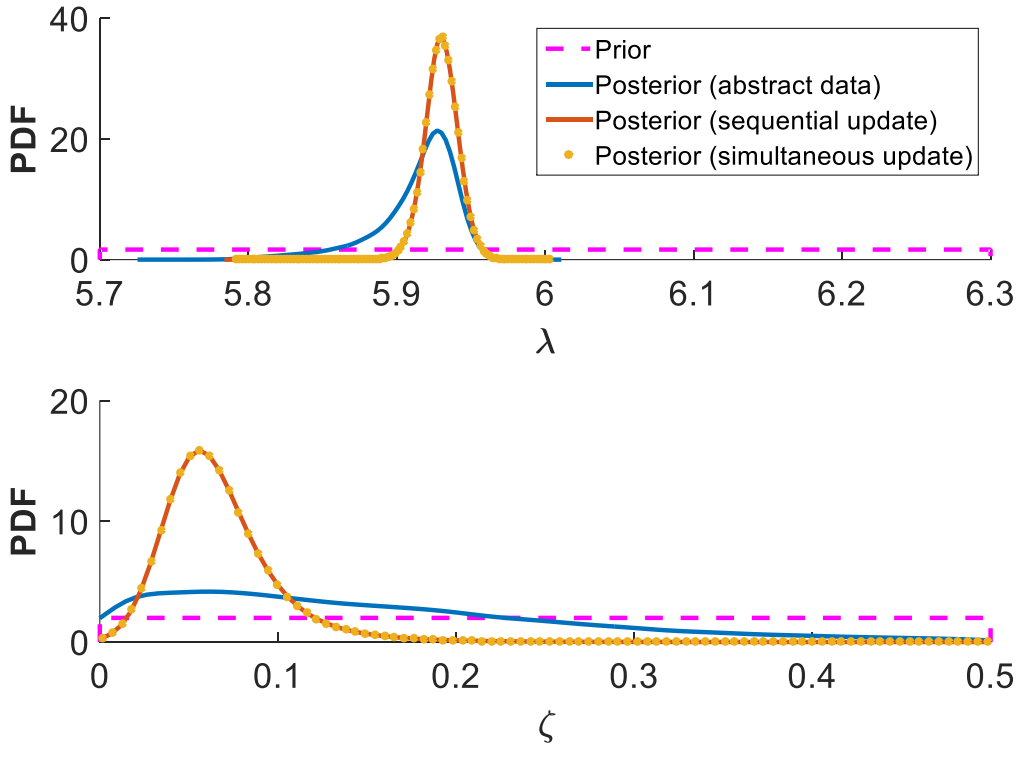

Figure 4.16. Posterior distributions considering sequential or simultaneous inference with both raw and abstracted data

4.5 Application to Reliability Data

To demonstrate the application and generality of this approach, this section presents a practical example and applies the proposed inference methodology for reliability data as a form of abstracted data.

4.5.1 Reliability data

One method of determining the reliability of a system is by performing *n* independent tests and recording whether the system's performance exceeds some set threshold value. The reliability of the system is the ratio of the number of tests which did not exceed the threshold over the total number of tests. This can be considered as a form of abstracted data as defined in this Chapter since the raw system performance values are logically classified as pass/fail according to a threshold value and these pass/fail counts are further reduced into a single proportion giving the sample reliability.

In this case there are two possible forms of abstracted data that could be considered as the data generative process naturally gives the counts of pass/fail components as an intermediate step in the calculation of the overall sample reliability. If the sample reliability data is given and the corresponding sample size is known, the intermediate form of abstracted data (i.e. the number of pass and fail data) could be determined and alternatively used in the inference process. We will instead consider the case where the reliability data is presented with an unknown sample size, and use the proposed methodology to infer the system parameters using the sampling distribution, $T(\boldsymbol{x})$, corresponding to the reliability data.

4.5.2 Sampling distribution for reliability data

The sampling distribution $T(\boldsymbol{x})$ for reliability data is a discrete probability mass function (PMF). For a given sample size, *n*, there are only *n* discrete outcomes, however, as *n* becomes large, the discrete PMF can typically be approximated by a continuous PDF. As reliability data is very near the upper bound, the Rule of Sample Proportions does not apply and a normal approximation of the sampling distribution is not appropriate. Some other authors have suggested that the probabilistic characteristics of p can be described by the beta distribution [134] or inflated beta distribution [135].

For this example, a truncated four-parameter beta approximation will be considered, where the parameters of the four-parameter beta distribution are determined from the Pearson system, utilizing the first four moments of the sampling distribution. A four-parameter beta is used to approximate the skewness of the sampling distribution as the true value of the reliability approaches the upper bound at one. Since the four parameter beta distribution approximation is not necessarily bounded between zero and one, to ensure that the distribution is consistent, it is truncated at both bounds of zero and one. The first four moments for the sampling distribution of the reliability necessary for finding the parameters of the four-parameter beta distribution can be analytically derived from the binomial distribution and are given as:

$$E[\hat{p}] = p \tag{4.21}$$

$$V[\hat{p}] = \frac{p(1-p)}{n} \tag{4.22}$$

$$Skew[\hat{p}] = \frac{1-2p}{n\sigma_{\hat{p}}} \tag{4.23}$$

$$Kur[\hat{p}] = \frac{6p^2 - 6p + 1}{np(1-p)} \tag{4.24}$$

4.5.3 Application problem: micro-cantilever beam

Abstracted data in the form of reliability data obtained from quality testing of a manufactured product is considered for the Bayesian model calibration in this section. In particular, calibration of the Young's modulus using an analytical model for a cantilever beam is considered. A thick micro-cantilever beam subjected to a point load *P* is considered (Figure 4.17) [136].

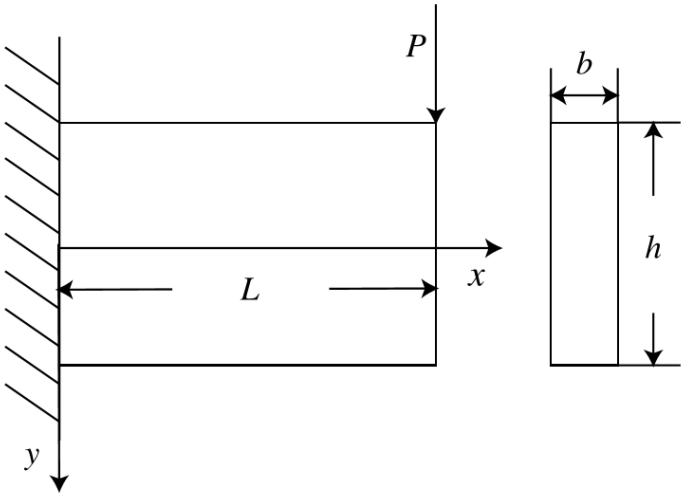

Figure 4.17. A thick cantilever beam subjected to a point load at the free end

From the Euler-Bernoulli beam theory, the static vertical deflection u_y at any point can be determined from the following equation:

$$u_y = \frac{P(3L-x)x^2}{6EI} \tag{4.25}$$

The formulation for beam deflection given in Eq. 4.25 does not account for shear deformation. A more accurate solution for the deflection u_y is given by the Timoshenko beam equation:

$$u_y = \frac{P}{6EI}\left[(4+5\nu)\frac{h^2 x}{4} + (3L - x)x^2\right] \tag{4.26}$$

For the sake of illustration in this example, it is assumed that Eq. 4.25 represents the prediction/calibration model for the deflection u_y and that Eq. 4.26 represents the reality. It is assumed that the beam dimensions and the applied load are subject to known variability due to manufacturing tolerances and their distributions are given in the following table.

Table 4.3. Parameter Distriutions

Parameter	**Distribution**	**Mean**	**Std. Dev.**
b	Normal	1 μm	0.1 μm
h	Normal	400 μm	0.1 μm
L	Normal	400 μm	0.1 μm
P	Normal	2.5 μN	0.2 μN

Synthetic reliability data is generated from Eq. 4.26 including the parameter distributions in Table 4.3, Young's Modulus of E = 200 GPa, and a critical value of the vertical deflection, $u_{y,crit}$ = 7.05 x 10^{-5} μm. Note that the Young's Modulus value and the "true" solution in Eq. 4.26 are assumed to be unknown in this model calibration example. The Euler–Bernoulli beam solution in Eq. 4.25 is assumed to be the only available physics model, and the synthetic data are used to calibrate E using Eq. 4.25. It is also noted that due to the difference in physics represented by the "true" model in Eq. 4.26 and the assumed form in Eq. 4.25, that the discrepancy function will be given by:

$$\delta_{true} = \frac{P}{6EI}(4+5\nu)\frac{h^2 x}{4} \tag{4.27}$$

However, this form of the model discrepancy is assumed to be unknown and is instead represented simply by an unknown constant which is also calibrated along with the Young's Modulus. E.

In this example, synthetic data is generated via Monte Carlo sampling for a fixed sample size to give estimates of the reliability. The synthetic data is given in Table 4.4.

Table 4.4. Reliability data (synthetic)

Sample Set	**Sample Reliability**
1	0.9940

4.5.4 Bayesian model calibration results

The corresponding Bayesian network before and after arc reversal is shown in Figure 4.18. The transformed Bayesian network, Figure 4.18(b), also includes a stochastic node corresponding to the sample size corresponding to the observed reliability data which is assumed to be unknown. Again, due to the complexity of the model, the sampling distribution is determined by approximation using the method described in Section 4.5. And for practical applications we only require the Bayesian network contained within the dashed box for performing inference.

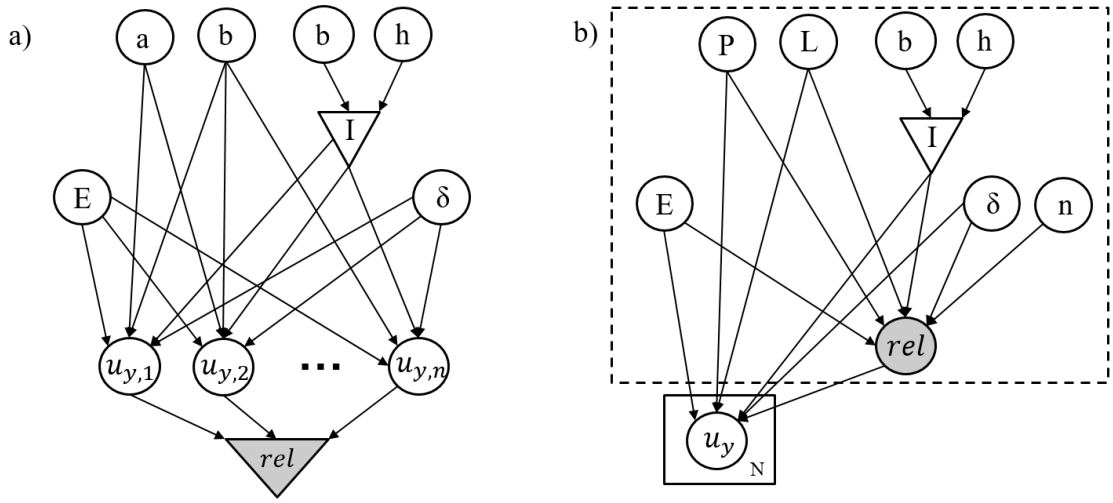

Figure 4.18. Bayesian network for reliability data: a) Bayesian network before arc reversal, b) Bayesian network after arc reversal

For each proposed sample of the Young's modulus, model discrepancy, and sample size, the corresponding system reliability given these sample values was determined using the First-Order Reliability Method (FORM) [137]. The likelihood of observing the reliability data given in Table 4.4 can then be calculated from the sampling distribution as approximated by the four-parameter Beta distribution with moments as given in Eq. 4.21 - 4.24. Note that *p* in those equations corresponds to the reliability value determined from the FORM analysis.

Using the synthetic probability of failure data shown in Table 4.4, Young's Modulus and model discrepancy were updated based on the reliability data observation and the results are shown in Figure 4.19.

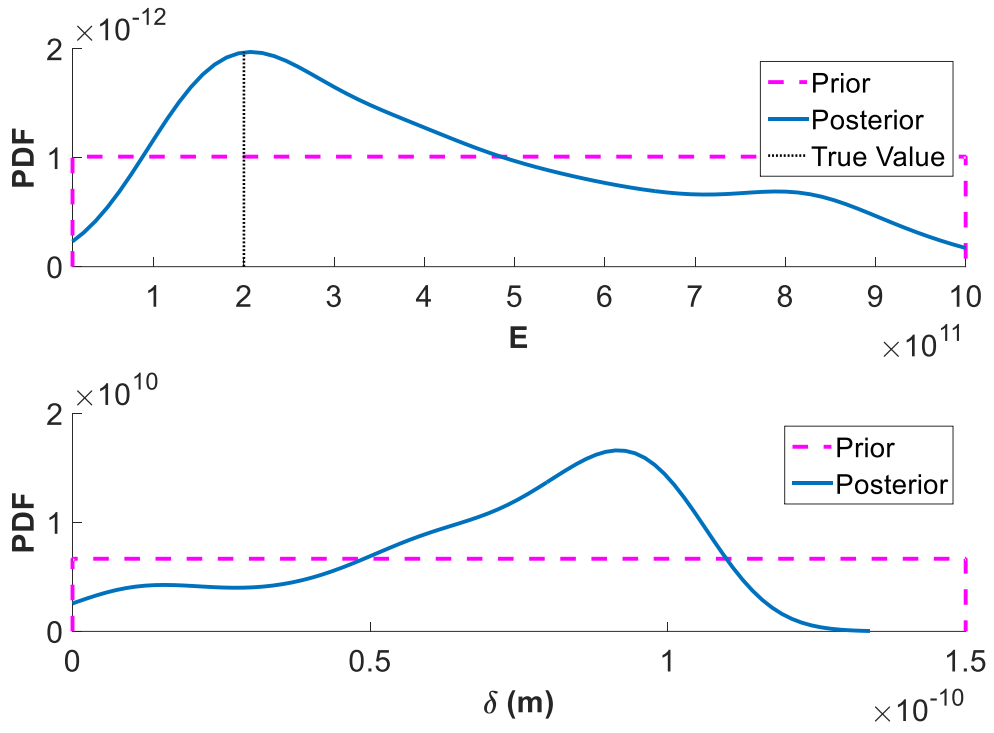

Figure 4.19. Prior and posterior distributions for the Young's Modulus, *E*, and model discrepancy, δ

Since the quantification of model discrepancy is not the goal of this Chapter, we assumed for illustration purpose, the model discrepancy as an unknown constant. The treatment of the model discrepancy as an unknown constant is just one way of considering model discrepancy. Other alternative treatments of model discrepancy are possible, such as: (1) a Gaussian random variable with unknown distribution parameters; (2) a Gaussian random variable with input dependent distribution parameters; (3) a Gaussian process with a square exponential covariance function. Further details and comparisons on the incorporation of these different options for representing model discrepancy can be found in [136].

4.6 Application in Digital Twins

A critical component of the Digital Twin is the interconnection of the physical reality of interest and the virtual representation. This interconnection allows observations of the physical reality to update the state variables and model parameters of the data models and computational models that comprise the virtual representation. When we incorporate uncertain data in the Digital Twin update process, we can choose to model these state variables and model parameters as distributions as opposed to deterministic values. When these state variables and model parameters are described by distributions, we can define the resulting as a probabilistic Digital Twin.

The update process for a probabilistic Digital Twin is conceptually the same as the Bayesian model updating process described in Section 4.2 and both the state variables and model parameters can be considered as a Bayesian network. This

is a useful form for the Digital Twin update process because it allows the Digital Twin to maximize the value of the available data, even when the observed data may be uncertain or abstracted in some way. Data for updating the Digital Twin may be available both during the initial Digital Twin implementation and calibration, as well as during the continuous updating process during the Digital Twin's operation.

An example of this type of Digital Twin application is a Digital Twin to monitor the condition of a structure to support inspection planning and identify potential impending failures. This Digital Twin would include computational models to describe the different degradation mechanisms that could impact the structural integrity over time, including fatigue and corrosion. Determining criticality of the structural components within this model also requires a detailed understanding of the associated asset-specific associated failure criteria. During the initial calibration of the Digital Twin during the implementation, knowledge of the material properties corresponding to the specific instance of the structure under consideration is extremely valuable. As described in Section 4.4, material property data obtained from steel mills and other manufacturers are often provided as statistical data for a batch of material tests instead of providing each individual test value. Using the methodology described in this Chapter, the material test data for the manufacturer of the material used in the structural components of interest could be used to update the probabilistic Digital Twin, specifically updating the material parameters associated with the failure criterion being evaluated in the degradation models.

4.7 Summary

When considering the interconnection of the physical reality with the Digital Twin virtual representation, updating the Digital Twin data models and computational models must make use of all the available data regarding the state of the system of interest. However, there are many situations in engineering practice where the raw data may not be available but is instead presented in an abstracted or summarized format. This potentially stems from the fact that it may generally be assumed that the mean and variance are enough to adequately summarize the data, when this is often not the case. This Chapter presents a methodology for incorporating such abstracted data in the Bayesian inference process. The general concept of data abstraction is presented through the incorporation of the statistic function, $T(\boldsymbol{X})$, which is defined as the result of any mathematical function of a finite sample of independent data observations. The resulting abstracted data is represented as a deterministic node in a Bayesian network when the network is developed in a form consistent with the data generative process. A novel approach is then proposed that leverages the process of arc reversal to rearrange the Bayesian network such that the deterministic node is transformed into a stochastic node conditioned on the parameters of interest thereby allowing observations of this node, such as abstracted data, to be used in the Bayesian inference process. Following the arc reversal process, the corresponding conditional distribution for $T(\boldsymbol{X})$, $f_T(\boldsymbol{t}|\boldsymbol{\theta})$, also called the sampling distribution, is given exactly. However, in many cases, the sampling distribution for $T(\boldsymbol{X})$ may not be analytically tractable and must be determined using approximate methods. Once the sampling distribution for $T(\boldsymbol{X})$ is calculated, the

corresponding likelihood of the observed abstracted data can be calculated. This enables available information in the form of abstracted data to be used in the Bayesian inference process through well-established techniques, such as Markov Chain Monte Carlo (MCMC).

Since the proposed methodology leverages Bayesian networks for abstracted data, Bayesian inference can easily be performed for combinations of raw data and abstracted data. The most common forms of abstracted data are the summary statistics which are typically calculated for a data set. These include the mean, standard deviation, median, maximum, minimum, and quartiles. A synthetic example using a uniform distribution was used to demonstrate how one or more types of abstracted data can be used together to infer the parameters of interest. Next, a practical common example of parameter estimation was presented considering mean yield stress data provided by a steel mill. While the mean data alone was an insufficient statistic, it was demonstrated that the distribution parameters could still be updated but not to the extent when raw observations are available. Furthermore, it was shown that in cases where the corresponding sample sizes are not provided, information regarding the distribution location parameter can still be inferred, but with greater uncertainty.

This approach was then extended to the case of reliability data, which can also be considered as an abstracted data form, as it condenses the individual pass/fail results to a single probability value. This example also demonstrated how through a Bayesian network, the observations of abstracted data can be used to calibrate model parameters in more complex physics-based models.

The proposed methodology provides a flexible and general approach for performing Bayesian inference with abstracted data and describes how this can be applied during the Digital Twin updating process. This methodology is particularly useful in cases when the provided statistic is insufficient, as was demonstrated in the case of the yield stress data with only the sample means provided. When compared to existing methods such as MrE and approximate Bayesian computation, the proposed inference framework is more flexible, in that it enables the direct incorporation of the uncertainty associated with the sampling distribution (i.e. the standard error) into the inference process. This flexibility is also apparent in the consideration of sequential and simultaneous updating, where MrE may give different results dependent on the order in which constraints are applied, while the Bayesian network approach is indifferent to sequential or simultaneous updating.

CHAPTER 5

BAYESIAN INFERENCE WITH UNCERTAINTY IN CATEGORICAL DATA

5.1 Introduction

Epistemic uncertainty in observed data can also occur when the observations of the system result in uncertain and/or ambiguous interpretations. In Chapter 4, the values of the observed data, while abstracted, were accepted with certainty in the Bayesian inference process. In some instances, the observed evidence cannot be provided in such certain terms with respect to the possible states of the system as defined by the formal model. Instead, this evidence must be interpreted to the form of the ideal representation, for instance, the form defined by the data models and computational models comprising the Digital Twin as described in Chapter 2 and Chapter 3. The Digital Twin model parameters need to be calibrated/updated based on all of the available information so that the model predictions accurately reflect the physical reality.

The data for model updating in a Digital Twin may be available from different sources, including but not limited to, experimental and operational data, inspection reports, health monitoring data, engineering plans, rules and standards, and expert opinion. These different kinds of data are available in different formats (numerical, categorical, image, text, etc.). These heterogeneous sources of information can lead to significant challenges for Bayesian inference, especially when the data is imprecise, uncertain, ambiguous, and/or incomplete [138]. One particular data format is considered in this Chapter, namely categorical data, which may result from a machine learning-based classification model that is applied to interpret and classify the original, raw observed data. In such cases, the uncertainty in the machine learning model results should also be considered in the downstream analysis.

It is recognized that any attempt to model the physical reality requires the idealization of that reality based on some level of abstraction. Reality is then represented in this idealized form by assigning values to the model variables based on the interpretation of the data collected from the physical reality. Due to the abstraction of reality, the evidence collected about that reality must be transformed into data consistent with the idealized representation. The process by which the data is transformed to be consistent with the idealized representation given evidence about reality is called the interpretation process and is shown in Figure 5.1.

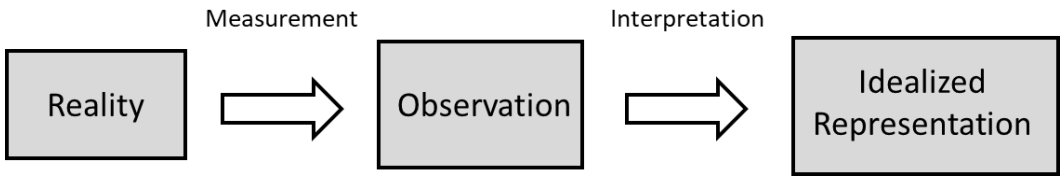

Figure 5.1. Data abstraction process

Considering this data abstraction process, the incorporation of classification data from machine learning models into Bayesian inference can be seen as analogous to the incorporation of expert opinion data. The combination of expert knowledge has been raised as an important factor in developing an effective Bayesian inference process [139]. In this sense, several data inputs are collected and synthesized by a single source and a procedure is developed to present this data in a form consistent with the idealized model representation. For an expert, this process is based on experience and judgement, and for a computer-based classification model, it is based on the relationship between the inputs and the output learned from the training dataset. With complex systems and data, an expert's opinion may also implicitly include a level of confidence in their assessment as it would be unrealistic to expect precise probability values to be provided by an expert. Accuracy and bias arising from the elicitation of expert opinions for use in Bayesian inference has been extensively studied [140–143]. Similarly, classification models often report accuracy measures which can be used to evaluate the confidence in the classification model's output. The confusion matrix and related metrics such as accuracy, sensitivity, recall and F1 score describe the overall performance of the classification model [144]. Confusion matrices present percentages of correctly classified and mis-classified results so that the overall performance of the classification model can be evaluated. While a confusion matrix can provide insight into the classification model's overall performance considering all the model testing data, it does not provide any insight about how confident the model is in being correct for an individual observation. To evaluate the confidence in each individual classification model prediction, a separate confidence measure is required.

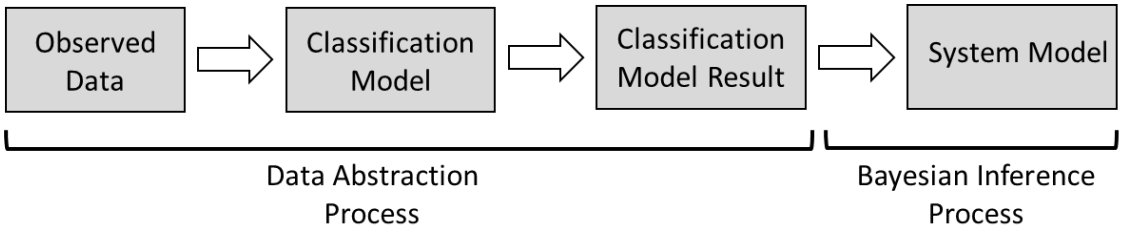

Figure 5.2 Process of incorporating observed data in the system model via a classification model abstraction

Bayesian inference provides a convenient and well-established approach for facilitating the inference of unknown or unobservable parameters, utilizing observations of other variables that are conditional on these unknown parameters. From a Bayesian perspective, analysis of multivariate continuous data has been well studied [145–147]. However, classification model results provide categorical/nominal or ordinal data which have been comparatively less pursued in the literature [148,149]. The incorporation of uncertainty in observed categorical data is even more limited. Zhang et al. [143] addressed the incorporation of confidence in the classification of linguistic data through the use of Dempster-Shafer theory combined with a Bayesian network.

This Chapter proposes a novel idea to incorporate "observations" in the form of classification model results to enable the Bayesian inference process in the presence of uncertainty in the classification model results. The relevant theory is developed from first principles and is suitable for practical problems.

Contributions of this Chapter include a proposed methodology for incorporating the classification model results in Bayesian inference while accounting for classification model output uncertainty. A confidence measure is assigned for each individual classification model result, which is then incorporated in the Bayesian inference procedure. This approach is then demonstrated for a model calibration problem and a practical damage diagnosis example.

The remainder of the Chapter is organized as follows. Section 5.2 reviews Bayesian networks and inference, and Section 5.3 proposes the methodology to incorporate classification model results and the corresponding confidence measures into the Bayesian network; thus it develops a generalized form of Bayesian inference with uncertain categorical data. Section 5.4 illustrates the proposed approach for inferring system model parameters using the classic Iris petal classification problem. Section 5.5 then demonstrates the use of the proposed approach for a practical engineering application using image classification of visual inspection data on corrosion damage. Section 5.6 provides concluding remarks.

5.2 Bayesian inference

5.2.1 Bayesian inference from observed data

Consider a random sample of observed data $x_1, \ldots, x_n$ taken from a distribution $f(x|\boldsymbol{\theta})$ of a random variable which is dependent on unknown parameters $\boldsymbol{\theta}$ contained in a parameter space Θ. In the canonical Bayesian inference process, the goal is to estimate the posterior distribution of $\boldsymbol{\theta}$ which reflects the information obtained from the observed values of $\boldsymbol{x}$. The existing knowledge of $\boldsymbol{\theta}$ (before considering the observed data) is represented through the *prior distribution* $f'(\boldsymbol{\theta})$. The information provided by the observed data $x_1, \ldots, x_n$ is used to compute the *likelihood* function, given as $f(\boldsymbol{x}|\boldsymbol{\theta})$ or simply $L(\boldsymbol{\theta})$. Utilizing probability laws and Bayes' theorem, the *posterior distribution* is given as

$$f''(\boldsymbol{\theta}|\boldsymbol{x}) = \frac{L(\boldsymbol{\theta})f'(\boldsymbol{\theta})}{\int L(\boldsymbol{\theta})f'(\boldsymbol{\theta})d\boldsymbol{\theta}} \tag{5.1}$$

The denominator is simply a normalization factor. Therefore, the posterior distribution can alternatively be written as

$$f''(\boldsymbol{\theta}|\boldsymbol{x}) \propto L(\boldsymbol{\theta})f'(\boldsymbol{\theta}) \tag{5.2}$$

The likelihood function can be understood as the probability of observing the given data $x_1, \ldots, x_n$ conditioned on the parameters $\boldsymbol{\theta}$. The expression for the likelihood function can be written as

$$L(\boldsymbol{\theta}|\boldsymbol{x}) \propto f_X(X = x|\boldsymbol{\theta}) \tag{5.3}$$

where $\text{Pa}_X \in \boldsymbol{\theta}$ are the parent nodes of X and $f_X(X = x|\ \text{Pa}_X)$ is the PDF value at $X = x$ from the conditional probability distribution for X_i.

This formulation for the likelihood function considers data collected from a single experiment. In the case of numerical data obtained from *n* different independent experiments, the final likelihood function will be the product of the *n* likelihood functions calculated for each individual experiment.

$$L(\boldsymbol{\theta}) \propto \prod_{i=1}^{n} f_X(X = x_i|\theta) \tag{5.4}$$

Note that this form of the likelihood assumes that the observations of X are independent. However, this might not always be the case, especially in considerations for Digital Twins, where observations may occur over a period of time (for the same system and response quantity) and therefore have some dependence on one another. In such cases, the likelihood function would need to be adjusted to reflect the likelihood of the joint observation taking into account the dependence between observations [150].

This canonical Bayesian inference process by which observed data is used to determine a posterior distribution of parameters of interest may use generalized observed data, *D*, and can occur in a variety of forms including numerical, categorical, linguistic, etc. [138,143,149]. This data may also be precise, imprecise, or abstracted in some form, such as summary statistics [138,151].

5.2.2 Bayesian inference with uncertain categorical evidence

In the previous section, the likelihood function $L(\boldsymbol{\theta})$ is the probability of observing data, D, conditional on $\boldsymbol{\theta}$, a realization of the distribution, $f(\boldsymbol{\theta})$. In practice, the observed data may deviate from their true values due to random noise, measurement error, and other errors in the data collection process. This deviation of the observed value from the true value may be modeled explicitly as an observation error model, or the uncertainty resulting from the observation errors may be simply included in the overall model uncertainty.

In the case of categorical data, the uncertainty arising from a deviation of the observed data from the true data can be represented as $f(D'|D)$, where D' is the true data, D is the observed data, and $f(D'|D)$ is the probability that D' is the true data when D is observed. Using Jeffrey's rule of probability kinematics [152], the posterior distribution can be constructed as a sum of weighted posterior distributions corresponding to individual data points, as

$$f''(\boldsymbol{\theta}|D) = \sum_{D'} f''(\boldsymbol{\theta}|D')f(D'|D) \tag{5.5}$$

This representation of the variability of the true values around the observation, *f(D'|D)*, is known as Berkson error [153,154]. This formulation is appropriate when the true data, *D'*, is only conditional on the observed data, *D*. However, this is rarely the case since *f(D'|D)* will often depend implicitly on the underlying distribution of *D'*. Alternatively, the relationship between the true data and observed data can be expressed as Classical error [154], which represents the variability of the observed values around the true value, *f(D| D').* To apply this Classical error term in a manner that is consistent with probability calculus, it is applied to the likelihood function such that the law of total probability is satisfied as shown in Eq. 5.6:

$$L(\boldsymbol{\theta}|D) = \sum_{D'} L(\boldsymbol{\theta}|D')f(D|D') \tag{5.6}$$

This concept of modification of the posterior or likelihood to account for model and data uncertainty has been considered in the literature. In Sankararaman and Mahadevan, a model reliability metric is applied to modify the model calibration posterior based on the probability that the model is valid [155]. In Agostinelli and Greco, a form of the likelihood is proposed with a set of weights that are applied to down-weight the likelihood of single term components that corresponded to anomalous values [156].

Consider now the case of a classification model that is being used to evaluate a set of inputs and generate a categorical output observation, *D*. This output *D* is then to be incorporated into a subsequent Bayesian analysis as described above. For illustration of this case, consider a common structural health monitoring problem of identifying the presence of fatigue cracks in a structure. For a given inspection using an NDI technique, the detection of a crack can be considered a form of binary classification, where the two classes are no crack detected or crack detected. The inference regarding the presence or absence of a crack can then be incorporated into a fracture mechanics model for quantitative diagnosis or prognosis [157–159]. However, when incorporating this observation, uncertainties in the accuracy of the classification model might result in the observed value, *D*, deviating from its true value, *D'*. This potential deviation should be accounted for in the Bayesian process through the incorporation of the modified likelihood function given in Eq. 5.6.

5.2.3 Confidence measures

To apply this Classical error term in the case of classification model results, we must first define the variability term, *f(D| D'),* which describes the probability that the observed data has occurred given an assumed true value.

Overall classification model performance is typically provided as a confusion matrix, which indicates for the test data the number of correct and incorrect classifications for each categorical value as shown in Figure 5.3.

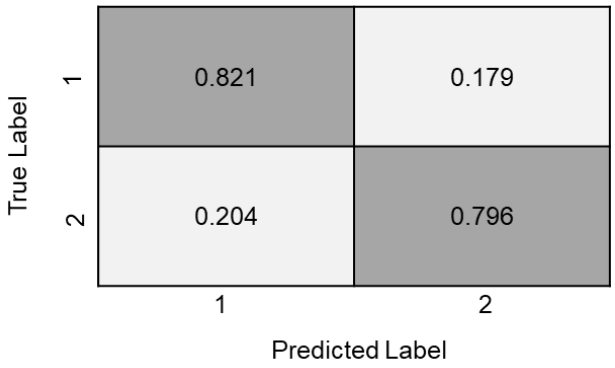

Figure 5.3 Confusion Matrix

In the absence of any additional data, the confusion matrix could be used as the basis for determining the Classical error term, *f(D|D').* However, in many instances, the classification model also provides additional information about the individual classification result accuracy along with each classification value, which should be incorporated.

To illustrate this concept, consider a simple two-class classification problem, where the class of the output is determined based on a single representative parameter and a specified threshold. This is shown in Figure 5.4 where the solid line represents the distribution of the parameter for Class 1 and the dotted line represents the distribution of the parameter for Class 2.

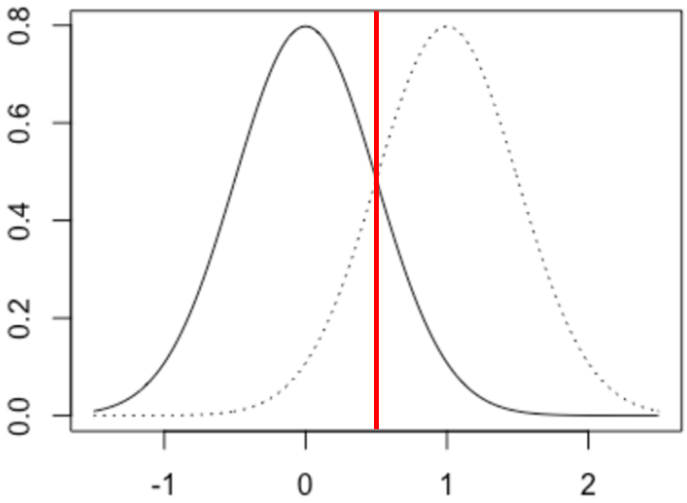

Figure 5.4. Single parameter classification

It can be observed from the distributions in Figure 5.4 and the selected threshold that there is a non-zero probability for misclassification where the distribution for Class 2 falls to the left of the threshold and the distribution of Class 1 falls

to the right of the threshold. In general, this probability for misclassification could be directly calculated and represented as a confusion matrix as shown in Figure 5.3.

However, even if we consider a single observation of the parameter to be classified, we observe that we have information available to us in addition to whether the observed parameter value falls to the left or right of the threshold. First, we know the distance of the parameter value from the threshold and second, we can determine the likelihood value of the parameter for both class distributions. Thus once the observed class is assigned, we can use this additional information to also assign a measure of confidence in the observed value being correct with respect to an assumed true value. For example, we will have greater confidence that the observed value is of a given class the farther away from the threshold the observed parameter value is. If we express this confidence in the form of a value from 0 to 1, it can be incorporated as the Classical error term, $f(D|D')$.

For the simple two class example given above, we could consider the ratio of the likelihoods for the observed parameter considering the distributions of Class 1 and Class 2. This likelihood ratio of two scenarios is also known as the "Bayes factor" and is used in applications such as facilitating the calculation of uncertainty in damage detection [159], which is similar in concept to classification (i.e., two classes: damage and no damage).

We then seek to incorporate this form of the confidence measure into the Bayesian formulation for system model calibration/updating. To describe this process, we will use the Bayes factor confidence measure described above. Given an observation of the parameter, x_i, and the associated distributions of parameter X for Class 1 and Class 2 $\{f_{Xj}(x_j), j = 1, 2\}$, we can calculate the likelihood for each class as

$$L_j(\boldsymbol{\theta}|\boldsymbol{x}) \propto f_{Xj}(X = x|\mathrm{Pa}_X) \tag{5.7}$$

The confidence measure, C_j, for each class, j, can then be given as the following ratio.

$$C_j(\boldsymbol{x}) = \frac{L_j(\boldsymbol{\theta}|\boldsymbol{x})}{L_1(\boldsymbol{\theta}|\boldsymbol{x}) + L_2(\boldsymbol{\theta}|\boldsymbol{x})} \tag{5.8}$$

It can be seen from the above equation that the confidence measure C_j falls between 0 and 1, and $C_1(x) + C_2(x) = 1$. This confidence measure can then be incorporated as the Classical error term, $f(D|D')$ in Eq. 5.8. Then the posterior distribution can be written as:

$$\begin{aligned} f''(\boldsymbol{\theta}|D) \propto \big[&C_1(\boldsymbol{x})L_1(\boldsymbol{\theta}|\boldsymbol{D}') + \big(1 - C_1(\boldsymbol{x})\big)L_2(\boldsymbol{\theta}|\boldsymbol{D}') + C_2(\boldsymbol{x})L_2(\boldsymbol{\theta}|\boldsymbol{D}') \\ &+ \big(1 - C_2(\boldsymbol{x})\big)L_2(\boldsymbol{\theta}|\boldsymbol{D}')\big] f'(\boldsymbol{\theta}) \end{aligned} \tag{5.9}$$

The confidence measure given in Eq. 5.10 can be similarly determined using alternate distance measures, such as classification probability, or the SVM decision function. The choice of the confidence measure is typically determined

based on the available data and the form of the classification model. Some examples of confidence measures include the Bayes factor [159], classifier prediction probability [160], or the decision function used by support vector machine (SVM) models [161].

5.2.4 Generalization to multi-classification model results

The approach described above only applies to binary class comparisons and needs to be generalized for the case of multi-class problems. This can be accomplished by considering the pairwise comparison of all the classes. In this approach the posterior is determined for each pairwise combination of classes, in which the confidence measure is determined as described above and the confidence measure is only applied to the two classes under consideration. All the other classes are simply assigned a confidence measure of 1. This will result in a posterior distribution for each pairwise combination which must then be aggregated to determine the final posterior distribution. This is accomplished by determining a weighting function for the posterior distributions.

To determine this weighted posterior, we first note that as the classification model approaches perfect classification (e.g. no misclassifications), the confidence measure for the observed class approaches a value of 1 since we can be perfectly confident that the observed value is the same as the assumed true value. This assumption also is held for all other classes except for the pairwise classes under consideration. Therefore, we are most interested in the posteriors that deviate from this base case. This deviation from the base case can be determined using the Jensen-Shannon divergence which is based on the Kullback-Leibler divergence [162].

$$JSD_k(P_k||Q) = \frac{1}{2}D(P_k||M) + \frac{1}{2}D(Q||M) \tag{5.10}$$

where $M = \frac{1}{2}(P_k + Q)$

In this application, P_k is the posterior distribution for pairwise class combination, k, and Q is the unweighted posterior. We will define the weighting function for posterior k, W_k, as:

$$W_k = \frac{JSD_k}{\sum_m JSD_m} \tag{5.11}$$

Therefore, the final posterior can be given as:

$$f''(\boldsymbol{\theta}|\boldsymbol{D}) \propto \sum_k W_k \, f_k''(\boldsymbol{\theta}|\boldsymbol{D}) \tag{5.12}$$

where $f_k''(\boldsymbol{\theta}|\boldsymbol{x})$ is the posterior corresponding to pairwise combination k.

5.3 Application to Iris flower classification data

The following illustrative example uses the well-known Iris flower dataset [163] to demonstrate the value of incorporating the classification model confidence measure into the Bayesian analysis process. The objective of this example is to infer the Iris class ratios of a given population solely based on the classification results obtained from the trained classification model. A corresponding confidence measure for each observation from the classification model is also taken into account to address the uncertainty in the classification model result for each observed member from the population.

The Iris flower data set is one of the most commonly used examples in the field of machine learning and was introduced in the 1936 paper by Fisher [163]. The data set considered here consists of 50 samples from each of three species of *Iris* (*Iris setosa*, *Iris virginica*, and *Iris versicolor*). The samples are described by four features including the length and the width of the sepals and petals in centimeters. For the purposes of this illustrative example, only two of the Iris dataset features will be used, sepal length and sepal width. The distributions of these parameters for the three flower classes can be seen in Figure 5.5.

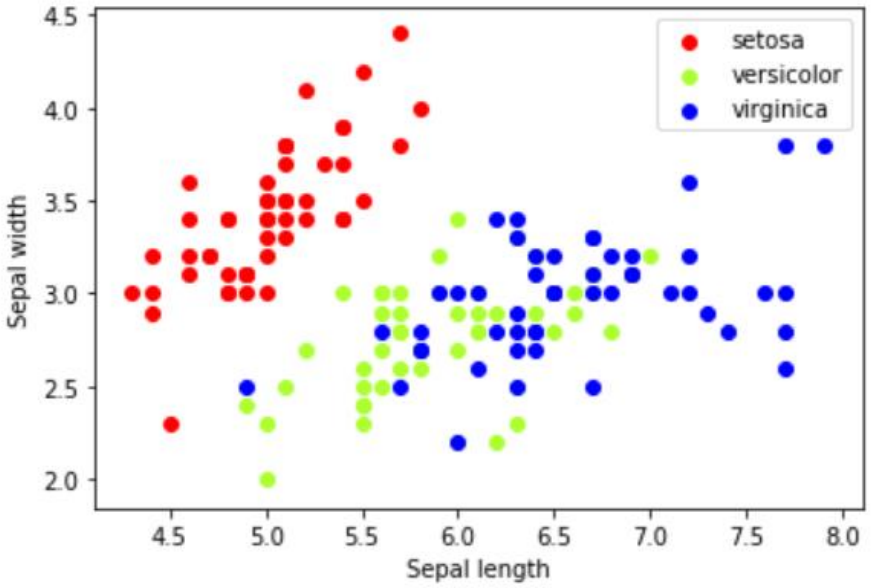

Figure 5.5. Flower class sepal length and sepal width distributions

It can be seen from Figure 5.5 that while the *setosa* class is easily distinguished using these two features, the *versicolor* and *virginica* classes have substantial overlap in their distributions that will pose a challenge for a classification model to confidently determine the class membership of flowers belonging to these two classes.

In this illustrative example, a simple system model was created to represent a population of Iris flowers with some pre-determined ratio of Iris classes: 20% *setosa*, 10% *versicolor*, and 70% *virginica*. Using these defined ratios, 100

population members were randomly generated as one of the three flower classes. For each generated population member, the corresponding features of sepal length and sepal width are generated by selecting randomly from multivariate normal distributions fit to the original Iris feature dataset for each Iris flower class. These synthetically generated sepal length and sepal width values can then be evaluated by a trained classification model to predict the class of each population member.

To demonstrate the methodology for a variety of different confidence measures, three different trained classifier models were used to predict the flower class based on the synthetically generated feature data. These included logistic regression, support vector machines, and random forest classifiers. These classification models were trained using the original Iris feature dataset and then applied to the sample data. Since the "true" class was known for the synthetically generated samples, the overall performance of each classifier could be presented as a confusion matrix as shown in Figure 5.6.

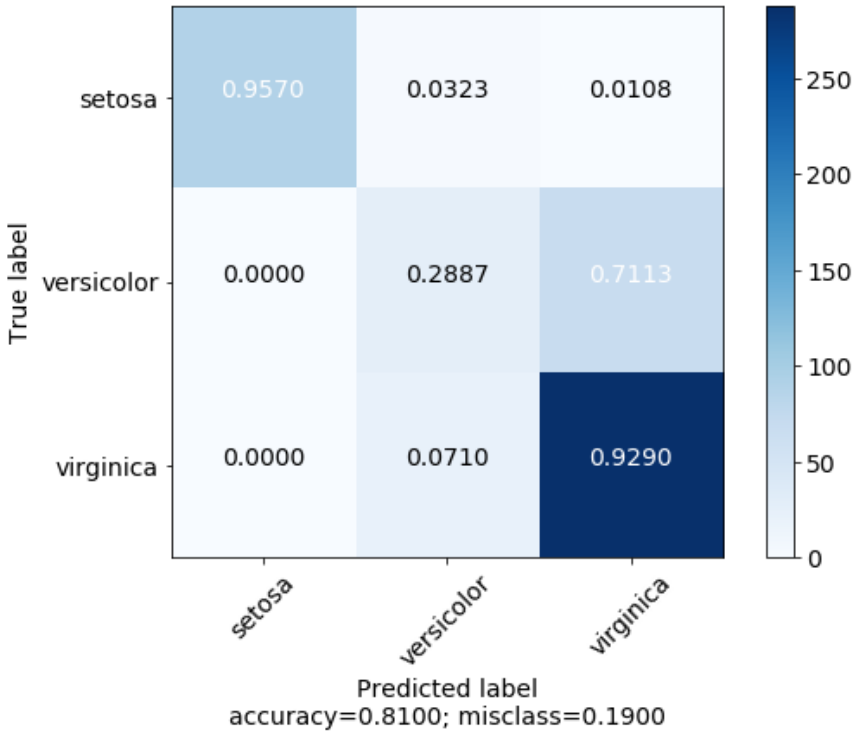

Figure 5.6 Sample confusion matrices for a logistic regression classifier model

It can be seen in the above confusion matrices that the performance of each classification model is approximately the same, with accuracy around 80% and a misclassification rate around 20%. Additionally, it can be seen that generally the class *setosa* is well predicted by each of the classification models, while most of the misclassification occurs between class *versicolor* and class *virginica*, which is consistent with the overlap in the parameter distributions shown in Figure 5.5. While the performance of the individual classification models can be improved with additional training, those efforts

were not undertaken here as the purpose of this study was to demonstrate how the uncertainty in these classification results can be incorporated in the Bayesian inference process.

For each of these classification models, an associated form of the confidence measure was selected. These included the Bayes factor for the logistic regression model, classification prediction probability for the random forest model, and the support vector decision function for the SVM classifier.

After generating the classification model result data and the corresponding confidence measures, this data could then be incorporated into the Bayesian inference process to estimate the flower species ratio. The Bayesian inference process employed in this work used sampling importance resampling (SIR) [128]. In this approach, sample particles are generated from a prior distribution, which in this case is taken as a uniform random distribution between 0 and 1, which corresponds to the naive potential range of the ratio, θ, for each flower species, i.

$$\theta_i \sim U[0,1] \tag{5.13}$$

It can also be noted that these sample particles are correlated since the total of all the species ratios must sum to 1.

$$\theta_{setosa} + \theta_{versicolor} + \theta_{virginica} = 1 \tag{5.14}$$

Then, as discussed in Section 5.2.2, each particle is then assigned a weighted likelihood which incorporates the corresponding confidence measure for each observed classification. These particles are then resampled based on their respective calculated weights to obtain the posterior distributions. For comparison, the traditional approach not incorporating the classification model confidence measures was also run and the resulting posteriors were also determined. The resulting posteriors are shown in Figure 5.7 - Figure 5.9.

Table 5.1. True and observed ratios for synthetic data

	Setosa	**Versicolor**	**Virginica**
True Ratios	22%	12%	66%
Observed Ratios	22%	28%	50%

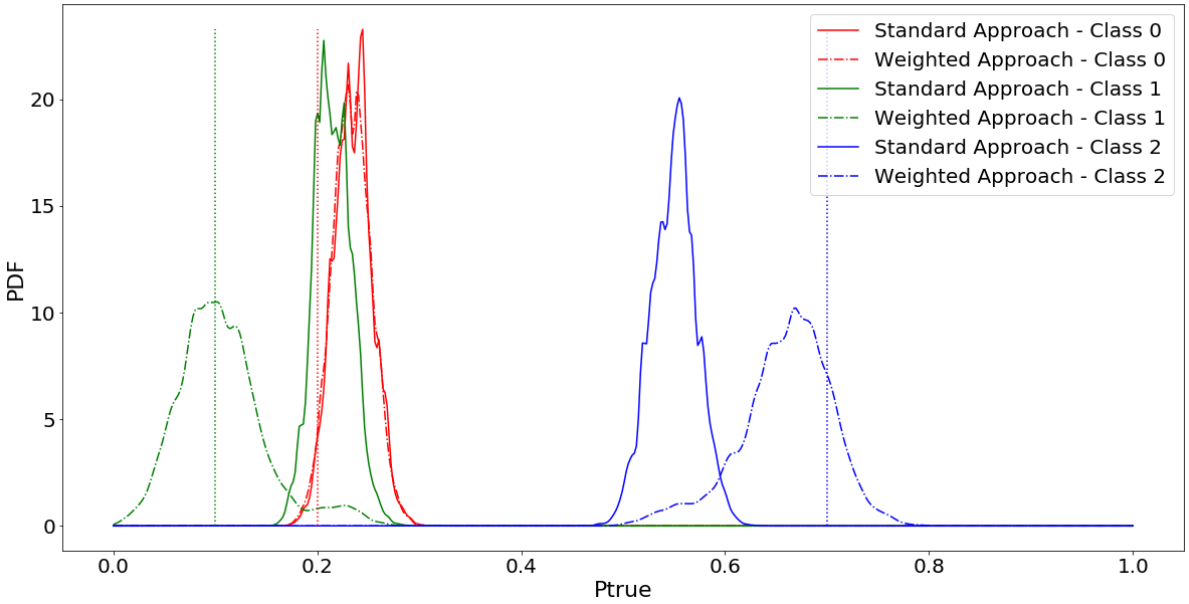

Figure 5.7. Posterior distributions for flower class ratios (logistic regression classifier)

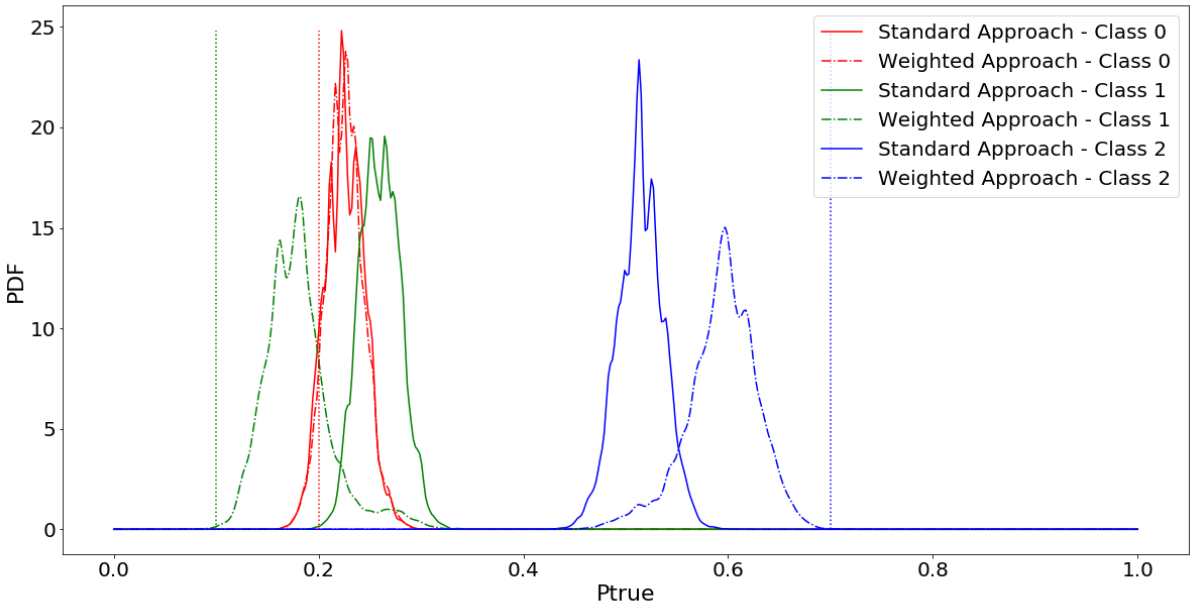

Figure 5.8. Posterior distributions for flower class ratios (random forest classifier)

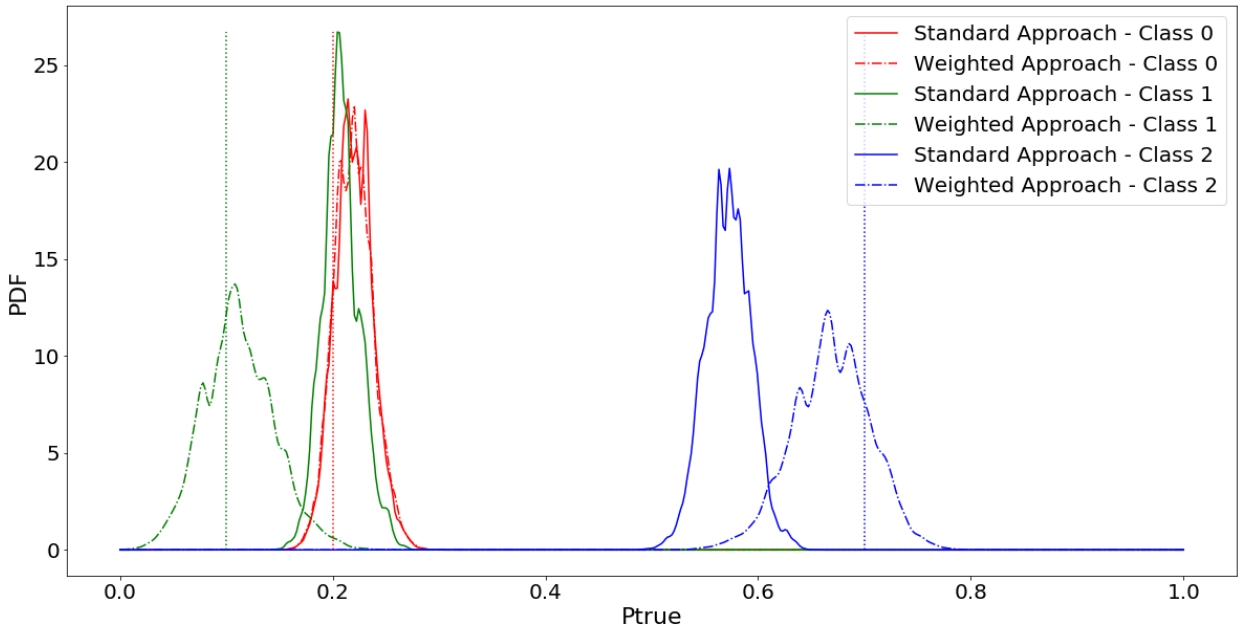

Figure 5.9. Posterior distributions for flower class ratios (support vector machine classifier)

As can be seen in Figure 5.7 - Figure 5.9, when inferring the flower species ratio using solely the observed classification data, the posterior distributions converge to the observed ratios as expected. When the classification model is effective with limited misclassification, the traditional approach would be sufficient. However, as can be seen in Table 5.1, the observed ratio does not match the true ratio due to the mediocre performance of the classification models. The classification model results are unable to consistently distinguish between the classes *versicolor* and *virginica*, as shown by the large discrepancies between the true and observed ratios in Table 5.1. Thus, when incorporating these results in the Bayesian inference of the overall population ratios, the posterior distributions (solid lines) for class *versicolor* and class *virginica* are biased. However, after incorporating the corresponding classification confidence measures, this bias begins to be corrected as the posteriors (dashed lines) shift closer to the true ratios indicated by the vertical dotted lines. It can also be observed in Figure 5.7 - Figure 5.9 that along with this shift in the central mass of the posterior is a corresponding increase in the overall variance of the posterior as well. This results from the additional uncertainty in the classification results informed by the confidence measure.

This simple example demonstrates the results of incorporating various confidence measures along with the classification results in Bayesian inference. In instances where the classification model performs well, the incorporation of the confidence measure has little to no impact on the resulting posteriors when compared with the traditional Bayesian inference methodology. But in instances where there is lower confidence in the classification prediction, the incorporation of the corresponding classification model confidence measure results in posteriors that more closely reflect the true system parameter values, albeit with greater variance reflecting the increased uncertainty in the posterior.

5.4 Application to coating condition image classification data

Material degradation due to corrosion is a dangerous and expensive issue for marine and offshore structures. A NACE study in 2002 estimated the annual cost of corrosion for the shipping industry in the United states as $2.7 billion [164].

To protect against corrosion, protective coatings are often applied to the steel surface at the time of vessel construction. However, these coatings can degrade or become damaged during the vessel's service. In order to maximize the service life of the asset and manage the overall lifecycle cost, it is critical to maintain and repair coatings in the early stages of coating degradation to prevent corrosion from occurring due to coating deterioration. Therefore, accurate and consistent assessment of coating conditions is important.

Coating conditions can be graded as "GOOD", "FAIR" or "POOR" according to the IACS Recommendation 87 [165]. Inspection intervals are then set according to the graded condition, with a worse condition leading to increased inspection frequency and higher costs. Tanks with coating graded in the FAIR or POOR conditions are required by IACS to be inspected annually [165], while those graded in GOOD condition need to be inspected about every 30 months on average.

Table 5.2. Coating condition grading criteria [166]

	Coating Condition		
Considered Area	**GOOD**	**FAIR**	**POOR**
Area under consideration(1)	Spot rusting without visible coating failures is < 3% of the area.	Breakdown of coating or rust penetration is ≥ 3% but < 20% of the area. Hard rust scale is < 10% of the area.	Breakdown of coating or rust penetration is ≥ 20% of the area. Hard rust scale is ≥ 10% of the area.

Notes:

(1). % is the percentage calculated on basis of the area under consideration or of the "critical structural area". Spot rusting is rusting in spots without visible failure of coating.

The typical practice for determining the coating condition grade is by visual inspection of a marine vessel compartment by trained inspectors. The overall percentage of area with coating failure is estimated and the corresponding coating condition grade is determined. To assist with this process, recognized organizations provide assessment scales, such as the one shown in Figure 5.10 to help determine the percentage and coating condition grade [166]. However, this determination is still highly subjective and can vary from inspector to inspector.

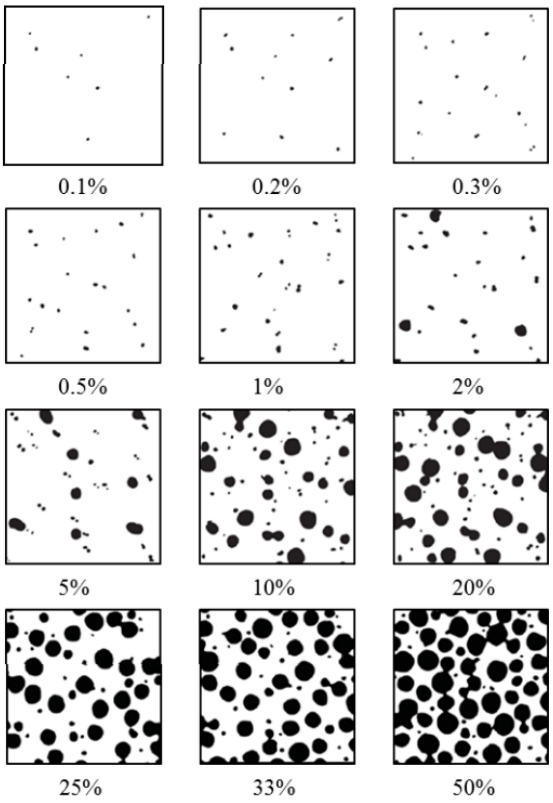

Figure 5.10 Coating breakdown diagrams [166]

To address the need for greater consistency in the grading of coating conditions, an image recognition tool was developed by the American Bureau of Shipping (ABS) and SoftServe [167]. Due to the complexity of this problem, instead of attempting to train a model to directly classify an image as one of the coating condition grades described above, a segmentation approach was implemented. In this approach, two Artificial Neural Network (ANN) models were developed and trained first to distinguish separate structural components and then to distinguish the coating breakdown at the pixel level. This results in separate classifications for each pixel as either having coating breakdown or not. Then based on all the classified pixels, the percentage areas for different coating conditions are calculated for the entire image and the coating condition grade is assigned.

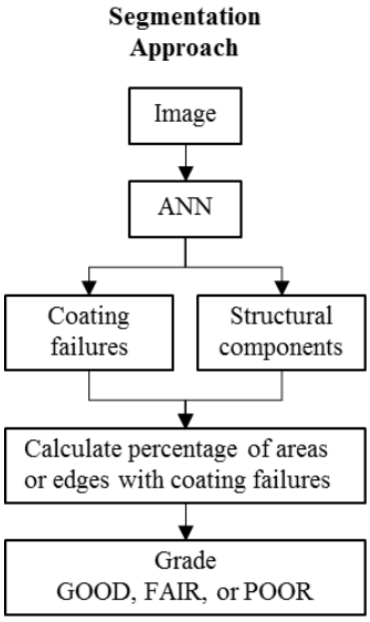

Figure 5.11 Segmentation approach for grading coating condition [167]

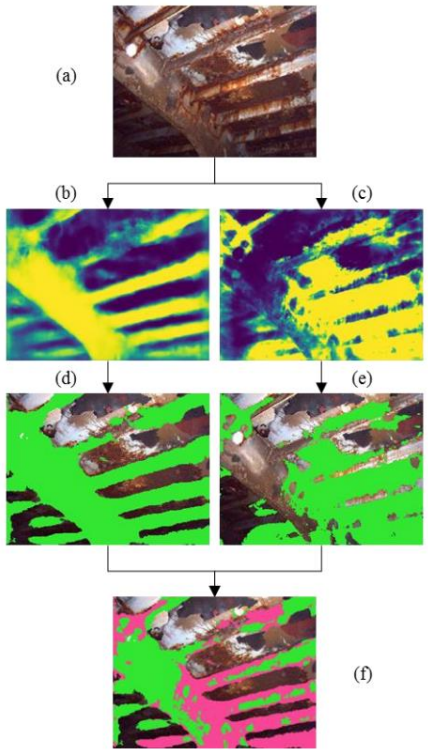

Figure 5.12 Coating condition assessment by segmentation [167]**. (a) Input image; (b) Stiffener segmentation heat map; (c) Coating failures segmentation heat map; (d) Predicted mask (green color) of stiffeners; (e) Predicted mask (pink color) of coating failures on stiffeners; (f) Overlay of coating failure prediction mask (pink color) on stiffener prediction mask (green color)**

As can be seen in Figure 5.12, the first step of the segmentation process is the generation of a heat map that represents the raw probability for each pixel top belong to each class. This heat map is then converted to a binary mask using a pre-defined threshold of 0.5. One challenge that has been identified is for the model to make judgements in cases near the boundary of two conditions. For example, as given in Table 5.2, the boundary between GOOD and FAIR is 3% of the surface area. Areas where the classification of the coating condition is near the pre-defined threshold represent a reduced confidence in the coating condition and the subsequent uncertainty in the resulting coating condition grade. To address this challenge, the proposed approach in this Chapter for incorporating the classification model confidence measure is applied here in assessing the coating condition grade for an input image.

To accomplish this task, an input image is selected with coating breakdown near the boundary of GOOD and FAIR coating conditions. The segmentation ANN model is run and the resulting probabilities for all the pixels are determined and converted to the binary classification mask. The percentage of area experiencing coating breakdown is then determined using Bayesian inference, with the pixel classifications as the observed classification data and the pixel probabilities as the classification confidence measure.

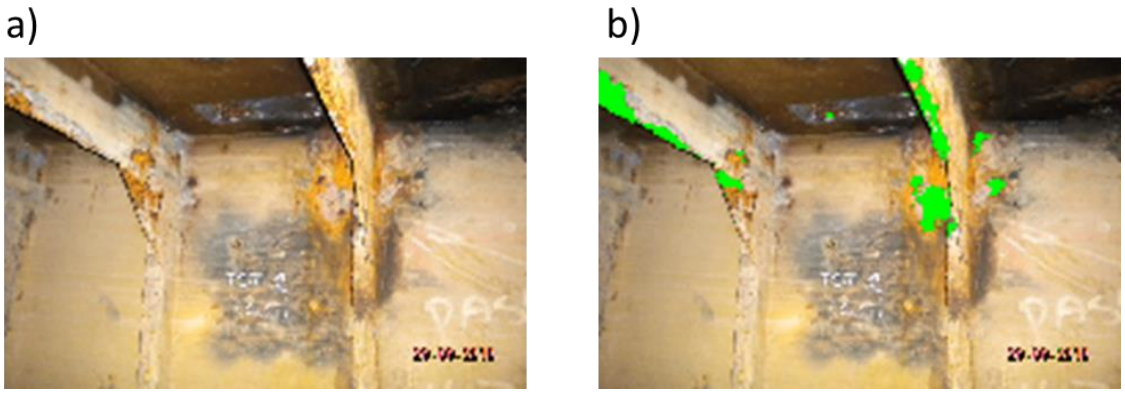

Figure 5.13. Coating assessment images: (a) Input image; (b) Coating breakdown mask

As with the Iris flower classification problem, a SIR approach with 50,000 particles is used to perform the Bayesian inference of the coating condition percentage, θ. An uninformed prior of $\theta \sim U[0,1]$ is chosen and the posterior distributions are determined taking into consideration the confidence measure for each of the pixel classifications. The resulting posteriors are shown in Figure 5.14.

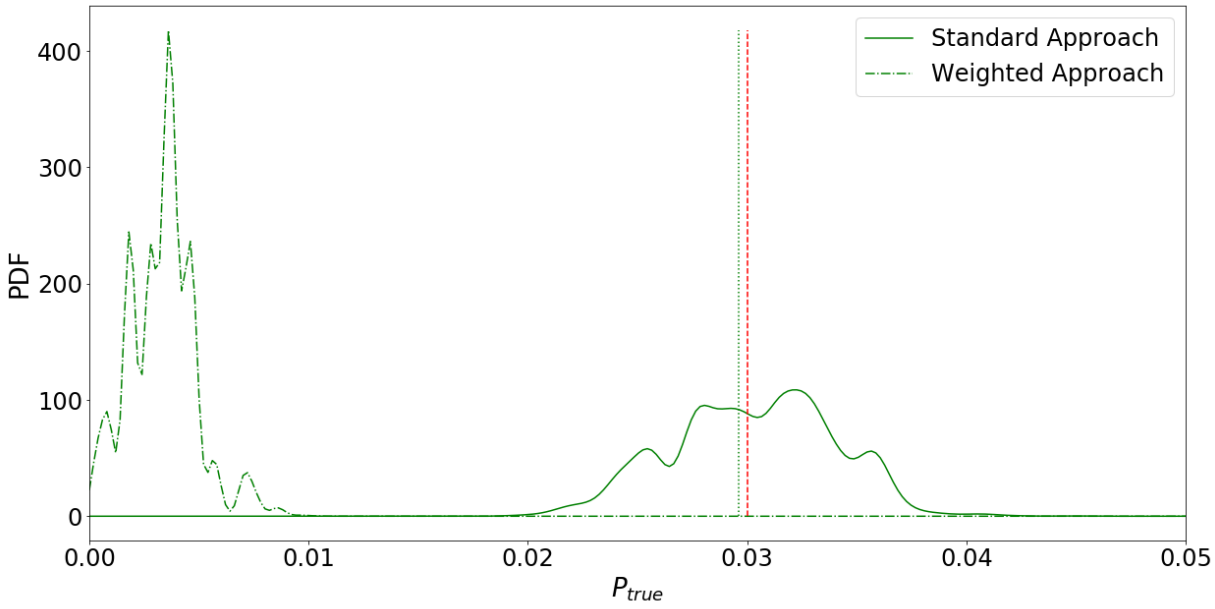

Figure 5.14. Posteriors for coating condition

In Figure 14, the decision threshold between GOOD and FAIR is shown as the red dashed vertical line. It can be seen that using the traditional approach (solid line), there is significant uncertainty about which coating condition grade should be decided. After applying the proposed approach (dashed line), the mass of the posterior shifts further into the GOOD zone. This is likely the result of the low confidence measures for pixels being classified as corroded, so those data points are then weighted lower in the Bayesian inference process. The practical outcome is that with the proposed approach, the vessel compartment would more likely be graded to be in the GOOD condition. As with most visual inspection processes relying on subjective determinations, it is impossible to determine what the "true" condition of this particular vessel compartment is for comparison.

5.5 Application to Digital Twin

Consider the interconnection of the physical reality of interest and the virtual representation in the probabilistic Digital Twin. The updating process of the state variables and model parameters can follow a Bayesian approach to incorporate the uncertainty in the observed data. In this Chapter, that uncertainty arises from the confidence measure associated with the categorical data resulting from the classification models. The methodology given in Section 5.2 can be applied to the updating of a probabilistic Digital Twin for both the state variables and model parameters. This allows the Digital Twin to maximize the value of the available data, even when the observed data may be uncertain.

An example of this type of application is a Digital Twin to represent the condition of a ship cargo or ballast tank with respect corrosion and coatings. As discussed in Section 5.4, these tanks typically have coatings applied their surfaces to

reduce the corrosion effects due to seawater and/or corrosive cargos. However, over time these coatings begin to breakdown and the corrosion process begins on the exposed steel underneath. Once corrosion begins, the thickness diminution due to corrosion can be modeled using a bi-linear model for example, where the corrosion (plate thickness diminution, *d*) increases linearly over time, *t*, with rate, *r*, beginning at time, T_c, which represents the coating life.

$$d(t) = \begin{cases} r(t - T_c) & t > T_c \\ 0 & t \leq T_c \end{cases} \tag{5.15}$$

Then the overall plate thickness, *W*, can be represented by:

$$W(t) = \hat{w} + M - d(t) \tag{5.15}$$

where

$W(t)$ = thickness of the plate a time, t

$\hat{w}$ = design thickness

M = thickness margin

In the Digital Twin, the state variables and model parameters representing the tank structure and corrosion model can be given as a Bayesian network updated by observations of both coating breakdown and measurements of the steel plate thickness, $Z(t)$. Due to the correlations that exist between the multiple levels of a complex ship structural system, the Bayesian network can be given as a hierarchical model as shown in Figure 5.15. These correlations at each system level exist for a number of reasons, some of which are outlined in Table 5.3

Table 5.3 Condition model hierarchy

System Hierarchical Level	**Correlation factors**
Fleet	Vessel type
Vessel	Operational profile, operator diligence
Compartment	Environmental conditions
Frame	Construction/repair grouping
Structural Element	Similar design properties
Single Plate	Lowest level, modelled as a random field

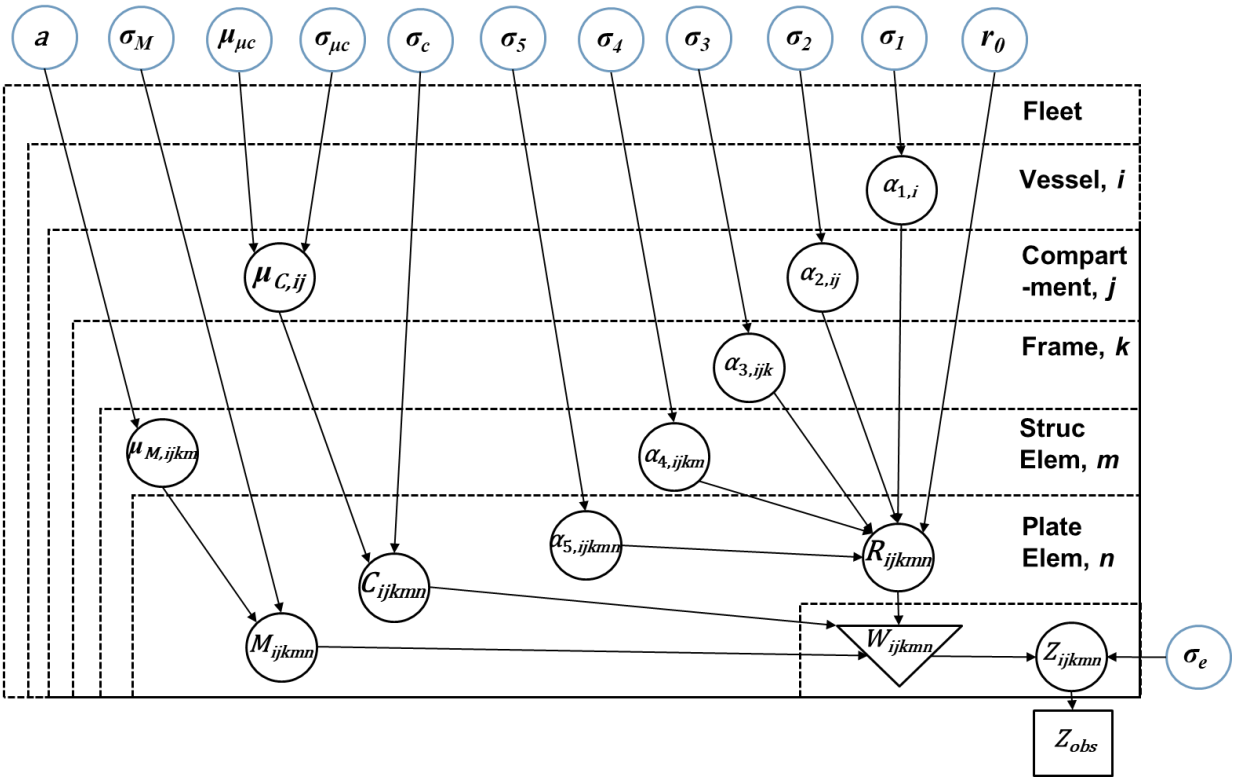

Figure 5.15 Bayesian network for Digital Twin condition model

In the basic form of the Digital Twin updating process, this condition model is updated following a thickness measurement campaign which typically occurs every five years. The challenge is that due to the complexity of the engineering system, there are a large number of unknown parameters to infer, and while the hierarchical model form increases the statistical power, identifiability can be an issue. This is because a number of possible combinations of corrosion rate, coating life, and thickness margin can result in the same measured plate thickness. To address this, we can incorporate additional observations that inform the condition model, such as observations of the coating condition to inform the parameter T_c given in Eq. 5.15

As discussed in Section 5.4, the grades for coating breakdown are typically provided based on expert examination of the structure. However, this manual inspection is subjective and can result in substantial variations from inspector to inspector. An alternative is to obtain these observations from a classification model that is applied to images taken of the structures. The resulting categorical results of the classification models along with their corresponding confidence measures can be used to update the Digital Twin condition model to update the model parameter corresponding to the coating life, T_c.

5.6 Summary

This Chapter presented a methodology for incorporating classification model confidence measures in performing Bayesian analysis using uncertain categorical data from classification models. This is meaningful in the context of the update process for a probabilistic Digital Twin, where the state variables and model parameters of the virtual representation are represented by distributions and can incorporate the uncertainty in the observed data. The general Bayesian methodology is presented through the incorporation of a weighting term applied to the likelihood function for the observed classification result data. This effectively gives more weight in the posterior to the data that is less ambiguous (i.e. further from the classification model decision threshold). It is then demonstrated that this process can then be extended to the case of multiple classifications by first evaluating the posterior for each pairwise class comparison and then evaluating a weighted combination of the resulting posterior distributions based on a Jensen-Shannon divergence measure. This process can be integrated into the Bayesian inference process through well-established sampling techniques, such as Sampling Importance Resampling (SIR).

This approach was first illustrated using the well-known Iris flower dataset and classification. Three different classification models were considered, each with similar overall performance but using a different form of confidence measure. It was seen in the provided example that poor classification model performance in distinguishing between two of the flower classes would lead to bias in the posterior if performing Bayesian inference using the traditional approach, and the proposed approach lessened the impact of this bias.

This approach was then applied to a practical case of coating condition assessment based on the classification of visual inspection data. A neural network model trained to identify coating breakdown was applied in a segmentation approach that individually classified each pixel in an image for coating breakdown. The results of this classification model also included a confidence measure in the form of a relative probability of coating breakdown for each pixel. This data was used in a Bayesian inference process to obtain the posterior distribution for the overall coating breakdown percentage for the observed area. This result could then be used to assign a coating condition grade.

The proposed methodology provides a flexible and general approach for performing Bayesian inference with classification model data while incorporating the individual confidence for each observation. When compared to the traditional method of Bayesian inference, the proposed approach can assist in reducing some potential bias, especially when the classification model is poor, but will also result in posteriors with a larger variance. This can be important in decision-making as it provides the decision maker with a better understanding of the uncertainty in the posterior resulting from the classification model that provided the categorical data.

CHAPTER 6

CONCLUSION

Digital Twin represents an important technological concept of this era and will likely continue to be a tool that is used to support digitalization of many industries well into the future. The increased interest around Digital Twins is led by the many potential and perceived benefits of the Digital Twin concept, including reducing costs [2–4] and risk [5]; improving efficiency [6], improving service offerings [7,8], security [9], reliability [10,11] and resilience [12]; and supporting decision-making [13–15]. However, despite all of this interest and perceived benefits, there is still significant room for development of the concept as well as the many individual technologies that support the implementation of this concept to ensure that these benefits can be realistically realized. This work has sought to provide a generalized concept of a Digital Twin and its implementations that can be expanded upon for each specific use case. It has also sought to start addressing some of the many challenges that exist in successfully implementing a Digital Twin in practice, particularly those challenges associated with uncertain and imperfect data.

6.1 Summary of Accomplishments

The overall goal of this dissertation is to propose a generalized approach for the implementation of Digital Twins and address some of the challenges that arise in this implementation due to imperfect and uncertain data. The various accomplishments of this dissertation can be classified into two categories: (1) Digital Twin implementation; and (2) incorporation of imperfect data.

First, this dissertation proposed a generalized definition and characterization for Digital Twin is proposed based on analysis of a number of existing definitions in the literature. By reviewing 46 existing definitions and assessing the lexicon and key components highlighted in each definition, a concise and generalized definition was provided. Following this definition, a detailed characterization of the key components of the Digital Twin was described, including the distinctions between a Digital Twin and similar concepts and models. Based on this definition and characterization, a framework for Digital Twin implementation was developed, outlining the approach for addressing each of the key components of the Digital Twin outlined in its characterization.

The practical end-to-end development, integration, and automation of this Digital Twin implementation framework was illustrated for the monitoring of fatigue damage accumulation in a vessel's critical structural connection. This implementation included the development of the technical architecture and model updating methodologies, with a specific emphasis on addressing challenges due to the lack of or uncertainty in input data.

The second major accomplishment of this dissertation was the development of methods for addressing the incorporation of imperfect data in the Bayesian inference, which is a key step in a probabilistic Digital Twin. Two types of imperfect data were considered; (1) abstracted data; and (2) uncertain categorical data. A novel methodology was developed to leverage the arc reversal process to incorporate "observations" of abstracted data through a Bayesian network representation to enable the Bayesian inference process. The proposed approach was based on a Bayesian network representation, which can be easily extended beyond the simple inference of distribution parameters of random variables (based on observations of that random variable) to the calibration of model parameters in Digital Twins. An example of the application of this methodology to incorporate abstracted material test data in a probabilistic Digital Twin representing a fatigue crack in a critical connection was discussed. Finally, a methodology was developed to incorporate "observations" in the form of classification model results to enable the Bayesian inference process in the presence of uncertainty in the classification model results. A confidence measure was assigned for each individual classification model result, which was then incorporated in the Bayesian inference procedure. The use of this Bayesian inference process in the update of a probabilistic Digital Twin structural condition model was presented. Pictures of the structural condition graded using a classification machine learning model could be used to update the coating breakdown parameter in the corrosion model within the probabilistic Digital Twin.

6.2 Future Work

6.2.1 Digital Twin Implementation Challenges

There are still a number of challenges associated with developing and incorporating Digital Twins in practical applications in additional to some possible paths forward. Many of the enabling technologies for Digital Twins are in various states of advancement, progressing as a function of both industry need and technology readiness/maturity. Digital Twin solutions, driven by specific desired outcomes, are being pieced together based on industry need, but there are still some significant challenges limiting the Digital Twin technology potential, including consistent terminology, standardization, organizational culture, technology maturity, verification & validation, and automation.

Digital Twins incorporate a variety of technologies from several different fields. The associated development needs and opportunities can be related to several general categories:

- Improved Digital Twin capabilities for automation through the connecting of data models and computational models that existed in previously independent silos, with the aim of increasing the efficiency and speed at which asset information can be kept current and exchanged between these silos.
- Improving model accuracy and fidelity, reducing the model uncertainty, and development of artificial intelligence/machine learning models.

- Quantifying, reducing and communicating the uncertainties that arise in the data and models, such as propagation of measurement noise and errors, modeling errors and approximations, and nuisance parameters in the model. This includes the continued development of methods to incorporate new forms of imperfect and uncertain input data which may arise in future use cases.
- Visualization techniques that present insights in an intuitive and interactive manner and support decisions, including augmented reality/virtual reality capabilities.
- Improvement of Data Infrastructure and Management: Communication infrastructure such as 5G, satellite communication, and improved network capabilities, in order to facilitate larger volume and higher frequency data transfer, local technologies such as wireless sensors, RFID, and IOT to allow greater flexibility in data transfer between data collection components and communication systems, and cloud computing for scalable and cost-efficient data processing and storage.

As highlighted in this research, the ability of the Digital Twin to maximize the use of all available data is important for its overall implementation success. Practical implementation of Digital Twins will encounter many potential forms of uncertain and imperfect input data. In addition to the imperfect forms of input data highlighted in this work, another large area of imperfect data that should be captured in a Digital Twin includes potentially ambiguous input data, such as what might arise from qualitative data sources, such as linguistic data or inspection reports. For example, there may be ambiguity in the interpretation between "good" and "very good" in an inspection report, and there are opportunities to extract further information that would support the Digital Twin updating process by incorporating this data while accounting for its uncertainty.

Another area of interest is with respect to validation of Digital Twin results. In other words, how do we determine when or if the Digital Twin is "good enough." As discussed in this work, the architecture of the Digital Twin is comprised of both data models and computational models, and validation of the Digital Twin would seek to validate these models individually in addition to how they perform overall as an integrated solution which provides additional complexity. This effort is therefore twofold, (i) to validate that the states stored within the data models accurately reflect the states of the physical system of interest, and (ii) to validate that the computational models accurately reflect the processes that simulate the changes to the states of the system (both in the virtual representation and the physical reality). A unique challenge that arises in the consideration of a Digital Twin is that by definition the Digital Twin represents a single instance of a physical system, therefore the set of information available to calibrate the Digital Twin is the same set of information available to validate the Digital Twin. One could consider the use of the calibrated computational models to forecast future states of the physical system. These forecasts could then be compared with the actual measured states at that future point in time, giving an idea of the Digital Twins accuracy. But as the physical system changes over time, the models are continually

being updated and therefore the associated uncertainty will be ever-changing, so any determination of Digital Twin accuracy based on model forecasts would be a lagging metric.

Finally, while Digital Twins are perceived to have many potential benefits, a common challenge in evaluating Digital Twins is practical and quantitative demonstration of their business value. This is often because they align with an existing process that may already provide a majority of the overall business value and the advantage the Digital Twin provides is the digitalization of that process to provide further efficiency or automation, which may be difficult to quantify. Also, another perceived benefit provided by a Digital Twin is as a type of insurance, reducing risks and costs during emergency scenarios which may only occur in rare instances. Finally, as a Digital Twin is intended for use during the entire life of the asset, the accumulated benefits may take time to observe and quantify. Developing appropriate key performance indicators that can quantify this value will aid greatly in further Digital Twin development and adoption.

6.3 Concluding Remarks

The various contributions of this dissertation and the above future work recommendations are directed toward the continued advancement of both the understanding and successful implementation of Digital Twins. As the use of Digital Twins expands to new domains and becomes more prevalent, a clear and concise understanding of a Digital Twins definition and its results will be critical in supporting an effective decision-making process. The importance of incorporating and quantifying uncertainties in the Digital Twin process will only continue to increase as Digital Twins are applied to new and more challenging domains. Therefore, the methodologies applied to Digital Twins will also need to continue to evolve to address these challenges and continue to support meaningful, risk-informed, and effective decision-making.

REFERENCES

[1] Delen D, Demirkan H. Data, information and analytics as services. Decis Support Syst 2013;55:359–63. https://doi.org/10.1016/j.dss.2012.05.044.

[2] Ben Miled Z, French MO. Towards A Reasoning Framework for Digital Clones Using the Digital Thread. 55th AIAA Aerosp. Sci. Meet., Reston, Virginia: American Institute of Aeronautics and Astronautics; 2017. https://doi.org/10.2514/6.2017-0873.

[3] Hu L, Ngoc-Tu N, Tao W, Leu M-C, Liu XF, Shahriar MR, et al. Modeling of Cloud-Based Digital Twins for Smart Manufacturing with MT Connect. Procedia Manuf 2018;26:1193–203. https://doi.org/10.1016/j.promfg.2018.07.155.

[4] Grieves M. Digital Twin : Manufacturing Excellence through Virtual Factory Replication. White Pap 2014.

[5] Millwater H, Ocampo J, Crosby N. Probabilistic methods for risk assessment of airframe digital twin structures. Eng Fract Mech 2019;221:106674. https://doi.org/10.1016/j.engfracmech.2019.106674.

[6] Kusiak A. Smart manufacturing must embrace big data. Nature 2017;544:23–5. https://doi.org/10.1038/544023a.

[7] Martinez V, Neely A, Ouyang A, Burstall C, Bisessar D. Service business model innovation: the digital twin technology. EurOMA Conf., 2018. https://doi.org/10.17863/CAM.35482.

[8] Meierhofer J, West S, Rapaccini M, Barbieri C. The Digital Twin as a Service Enabler: From the Service Ecosystem to the Simulation Model. Lect. Notes Bus. Inf. Process., vol. 377 LNBIP, Springer; 2020, p. 347–59. https://doi.org/10.1007/978-3-030-38724-2_25.

[9] Bitton R, Gluck T, Stan O, Inokuchi M, Ohta Y, Yamada Y, et al. Deriving a cost-effective digital twin of an ICS to facilitate security evaluation. Lect. Notes Comput. Sci. (including Subser. Lect. Notes Artif. Intell. Lect. Notes Bioinformatics), vol. 11098 LNCS, Springer Verlag; 2018, p. 533–54. https://doi.org/10.1007/978-3-319-99073-6_26.

[10] Glaessgen EH, Stargel DS. The digital twin paradigm for future NASA and U.S. Air force vehicles. Collect Tech Pap - AIAA/ASME/ASCE/AHS/ASC Struct Struct Dyn Mater Conf 2012:1–14. https://doi.org/10.2514/6.2012-1818.

[11] Reifsnider K, Majumdar P. Multiphysics Stimulated Simulation Digital Twin Methods for Fleet Management. 54th AIAA/ASME/ASCE/AHS/ASC Struct. Struct. Dyn. Mater. Conf., Reston, Virginia: American Institute of Aeronautics and Astronautics; 2013. https://doi.org/10.2514/6.2013-1578.

[12] Karve PM, Guo Y, Kapusuzoglu B, Mahadevan S, Haile MA. Digital twin approach for damage-tolerant mission planning under uncertainty. Eng Fract Mech 2020;225:106766. https://doi.org/10.1016/j.engfracmech.2019.106766.

[13] Macchi M, Roda I, Negri E, Fumagalli L. Exploring the role of Digital Twin for Asset Lifecycle Management. IFAC-PapersOnLine 2018;51:790–5. https://doi.org/10.1016/j.ifacol.2018.08.415.

[14] Li C, Mahadevan S, Ling Y, Choze S, Wang L. Dynamic Bayesian network for aircraft wing health monitoring digital twin. AIAA J 2017;55:930–41. https://doi.org/10.2514/1.J055201.

[15] Zhou C, Xu J, Miller-Hooks E, Zhou W, Chen CH, Lee LH, et al. Analytics with digital-twinning: A decision support system for maintaining a resilient port. Decis Support Syst 2021:113496. https://doi.org/10.1016/j.dss.2021.113496.

[16] Lee EA, Seshia SA. Introduction to Embedded Systems, A Cyber-Physical Systems Approach. Second Edi. MIT Press; 2017.

[17] Ashton K. The “Internet of Things” thing. RFiD J 2009.

[18] Merriam-Webster.com. “system.” Merriam-Webster 2011. https://www.merriam-webster.com (accessed March 28, 2020).

[19] Mohammadi A, Jahromi MG, Khademi H, Alighanbari A, Hamzavi B, Ghanizadeh M, et al. Understanding Kid’s Digital Twin. Int’l Conf. Inf. Knowl. Eng., 2018, p. 41–6.

[20] Verdouw C, Kruize JW. Digital twins in farm management: illustrations from the FIWARE accelerators SmartAgriFood and Fractals. 7th Asian-Australasian Conf Precis Agric 2017:1–5. https://doi.org/10.5281/zenodo.893662.

[21] Tangirala A. Principles of System Identification: Theory and Practice. CRC Press; 2017.

[22] Kritzinger W, Karner M, Traar G, Henjes J, Sihn W. Digital Twin in manufacturing: A categorical literature review and classification. IFAC-PapersOnLine 2018;51:1016–22. https://doi.org/10.1016/j.ifacol.2018.08.474.

[23] Qi Q, Tao F. Digital Twin and Big Data Towards Smart Manufacturing and Industry 4.0: 360 Degree Comparison. IEEE Access 2018;6:3585–93. https://doi.org/10.1109/ACCESS.2018.2793265.

[24] Wärmefjord K, Söderberg R, Lindkvist L, Lindau B, Carlson JS. Inspection Data to Support a Digital Twin for Geometry Assurance. Vol. 2 Adv. Manuf., American Society of Mechanical Engineers; 2017. https://doi.org/10.1115/IMECE2017-70398.

[25] Guo J, Zhao N, Sun L, Zhang S. Modular based flexible digital twin for factory design. J Ambient Intell Humaniz Comput 2019;10:1189–200. https://doi.org/10.1007/s12652-018-0953-6.

[26] Baruffaldi G, Accorsi R, Manzini R. Warehouse management system customization and information availability in 3pl companies: A decision-support tool. Ind Manag Data Syst 2019;119:251–73. https://doi.org/10.1108/IMDS-01-2018-0033.

[27] Boschert S, Rosen R. Digital Twin—The Simulation Aspect. Mechatron. Futur., Cham: Springer International Publishing; 2016, p. 59–74. https://doi.org/10.1007/978-3-319-32156-1_5.

[28] Guo J, Zhao N, Sun L, Zhang S. Modular based flexible digital twin for factory design. J Ambient Intell Humaniz Comput 2019;10:1189–200. https://doi.org/10.1007/s12652-018-0953-6.

[29] Negri E, Fumagalli L, Macchi M. A Review of the Roles of Digital Twin in CPS-based Production Systems. Procedia Manuf 2017;11:939–48. https://doi.org/10.1016/j.promfg.2017.07.198.

[30] Jones D, Snider C, Nassehi A, Yon J, Hicks B. Characterising the Digital Twin: A systematic literature review. CIRP J Manuf Sci Technol 2020:36–52. https://doi.org/10.1016/j.cirpj.2020.02.002.

[31] Madni A, Madni C, Lucero S. Leveraging Digital Twin Technology in Model-Based Systems Engineering. Systems 2019;7:7. https://doi.org/10.3390/systems7010007.

[32] Digital twins - rise of the digital twin in Industrial IoT and Industry 4.0 n.d. https://www.i-scoop.eu/internet-of-things-guide/industrial-internet-things-iiot-saving-costs-innovation/digital-twins/ (accessed April 1, 2020).

[33] Canedo A. Industrial IoT lifecycle via digital twins. Proc. Elev. IEEE/ACM/IFIP Int. Conf. Hardware/Software Codesign Syst. Synth. - CODES ’16, New York, New York, USA: ACM Press; 2016, p. 1–1. https://doi.org/10.1145/2968456.2974007.

[34] Castanedo F. A review of data fusion techniques. Sci World J 2013;2013:704504. https://doi.org/10.1155/2013/704504.

[35] Yin C, McKay A. Introduction to modeling and simulation techniques. Isc. ITCA 2018 - 8th Int. Symp. Comput. Intell. Ind. Appl. 12th China-Japan Int. Work. Inf. Technol. Control Appl., Fuji Technology Press Ltd.; 2018.

[36] Asher MJ, Croke BFW, Jakeman AJ, Peeters LJM. A review of surrogate models and their application to groundwater modeling. Water Resour Res 2015;51:5957–73. https://doi.org/10.1002/2015WR016967.

[37] Liu Z, Meyendorf N, Mrad N. The role of data fusion in predictive maintenance using digital twin. AIP Conf.

Proc., AIP Publishing; 2018, p. 020023. https://doi.org/10.1063/1.5031520.

[38] Abramovici M, Göbel JC, Savarino P. Reconfiguration of smart products during their use phase based on virtual product twins. CIRP Ann 2017;66:165–8. https://doi.org/10.1016/j.cirp.2017.04.042.

[39] Demkovich N, Yablochnikov E, Abaev G. Multiscale modeling and simulation for industrial cyber-physical systems. 2018 IEEE Ind. Cyber-Physical Syst., IEEE; 2018, p. 291–6. https://doi.org/10.1109/ICPHYS.2018.8387674.

[40] Schleich B, Anwer N, Mathieu L, Wartzack S. Shaping the digital twin for design and production engineering. CIRP Ann 2017;66:141–4. https://doi.org/10.1016/j.cirp.2017.04.040.

[41] Shafto M, Conroy M, Doyle R, Glaessgen E, Kemp C, LeMoigne J, et al. DRAFT Modeling, Simulation, information Technology & Processing Roadmap - Technology Area 11. Natl Aeronaut Sp Adm 2010:27.

[42] Majumdar PK, FaisalHaider M, Reifsnider K. Multi-physics Response of Structural Composites and Framework for Modeling Using Material Geometry. 54th AIAA/ASME/ASCE/AHS/ASC Struct. Struct. Dyn. Mater. Conf., Reston, Virginia: American Institute of Aeronautics and Astronautics; 2013. https://doi.org/10.2514/6.2013-1577.

[43] Grieves M, Vickers J. Digital Twin: Mitigating Unpredictable, Undesirable Emergent Behavior in Complex Systems. Transdiscipl. Perspect. Complex Syst., Cham: Springer International Publishing; 2017, p. 85–113. https://doi.org/10.1007/978-3-319-38756-7_4.

[44] Alam KM, El Saddik A. C2PS: A Digital Twin Architecture Reference Model for the Cloud-Based Cyber-Physical Systems. IEEE Access 2017;5:2050–62. https://doi.org/10.1109/ACCESS.2017.2657006.

[45] Talkhestani BA, Jazdi N, Schloegl W, Weyrich M. Consistency check to synchronize the Digital Twin of manufacturing automation based on anchor points. Procedia CIRP 2018;72:159–64. https://doi.org/10.1016/j.procir.2018.03.166.

[46] Schumann C-A, Baum J, Forkel E, Otto F. Digital Transformation and Industry 4.0 as a Complex and Eclectic Change. 2017 Futur. Technol. Conf., 2017, p. 645–50.

[47] Stackowiak R, Stackowiak R. Azure IoT Solutions Overview. Azur. Internet Things Reveal., Apress; 2019, p. 29–54. https://doi.org/10.1007/978-1-4842-5470-7_2.

[48] Digital Twin Physics-Based Simulation & Analytics n.d. https://www.ansys.com/products/systems/digital-twin (accessed April 22, 2020).

[49] GE Power Digital Solutions. GE Digital Twin: Analytic Engine for the Digital Power Plant. 2016.

[50] Perabo F, Park D, Zadeh MK, Smogeli O, Jamt L. Digital Twin Modelling of Ship Power and Propulsion Systems: Application of the Open Simulation Platform (OSP). IEEE Int. Symp. Ind. Electron., vol. 2020- June, IEEE Inc.; 2020, p. 1265–70. https://doi.org/10.1109/ISIE45063.2020.9152218.

[51] Office USGA. Navy Readiness: Actions Needed to Maintain Viable Surge Sealift and Combat Logistics Fleets (Publication No. GAO-17-503). 2017.

[52] Pick JB, Turetken O, Deokar A V., Sarkar A. Location analytics and decision support: Reflections on recent advancements, a research framework, and the path ahead. Decis Support Syst 2017;99:1–8. https://doi.org/10.1016/j.dss.2017.05.016.

[53] Ayyub BM, Assakkaf IA, Kihl DP, Siev MW. Reliability-Based Design Guidelines for Fatigue of Ship Structures. Nav Eng J 2002;114:113–38. https://doi.org/10.1111/j.1559-3584.2002.tb00127.x.

[54] Mao W, Rychlik I, Storhaug G. Safety Index of Fatigue Failure for Ship Structure Details. J Sh Res 2010;Vol. 54:197–208.

[55] Garbatov Y, Guedes Soares C. Uncertainty assessment of fatigue damage of welded ship structural joints. Eng Struct 2012;44:322–33. https://doi.org/10.1016/j.engstruct.2012.06.004.

[56] Moan T, Song R. Implications of inspection updating on system fatigue reliability of offshore structures. J. Offshore Mech. Arct. Eng., vol. 122, ASME; 2000, p. 173–80. https://doi.org/10.1115/1.1286601.

[57] Souza GFM, Ayyub BM. Probabilistic Fatigue Life Prediction for Ship Structures Using Fracture Mechanics. Nav Eng J 2000;112:375–97. https://doi.org/10.1111/j.1559-3584.2000.tb03344.x.

[58] Spencer J, Wirsching P, Wang X, Mansour A. Development of Reliability Based Classification Rules for Tankers. 2003.

[59] Doshi K, Roy T, Parihar YS. Reliability based inspection planning using fracture mechanics based fatigue evaluations for ship structural details. Mar Struct 2017;54:1–22. https://doi.org/10.1016/j.marstruc.2017.03.003.

[60] Aalberts P, van der Cammen J, Kaminski ML. SS: FPSOs and Floating Production Systems: The Monitas system for the Glas Dowr FPSO, Society of Petroleum Engineers (SPE); 2010. https://doi.org/10.4043/20873-ms.

[61] Zou T, Kaminski ML. Applicability of WaveWatch-III wave model to fatigue assessment of offshore floating structures. Ocean Dyn 2016;66:1099–108. https://doi.org/10.1007/s10236-016-0977-4.

[62] Hageman R, Aalberts P. Feasability of using hindcast data for fatigue assessment of permanently moored offshore unites in West-Africa. Proc. ASME 2020 39th Int. Conf. Ocean. Offshore Arct. Eng. OMAE, 2020.

[63] VanDerHorn E, Mahadevan S. Digital Twin: Generalization, Characterization and Implementation [Under Review]. Decis Support Syst 2020.

[64] Magoga T, Aksu S, Cannon S, Ojeda R, Thomas G. Through-life hybrid fatigue assessment of naval ships. Ships Offshore Struct 2019;14:664–74. https://doi.org/10.1080/17445302.2018.1550900.

[65] Thompson IM. Virtual hull monitoring: Continuous fatigue assessment without additional instrumentation. Trans R Inst Nav Archit Part A Int J Marit Eng 2019;161:A479–80. https://doi.org/10.3940/rina.ijme.2018.a3.479tn.

[66] Nielsen UD, Jensen JJ, Pedersen PT, Ito Y. Onboard monitoring of fatigue damage rates in the hull girder. Mar Struct 2011;24:182–206. https://doi.org/10.1016/j.marstruc.2011.03.003.

[67] Hulkkonen T, Manderbacka T, Sugimoto K. Digital Twin for Monitoring Remaining Fatigue Life of Critical Hull Structures. 18th Conf Comput Appl Inf Technol Marit Ind 2019:415–27.

[68] ABS. Guide for Spectral-Based Fatigue Analysis for Vessels. Houston: American Bureau of Shipping; 2016.

[69] Adland R, Jia H, Lode T, Skontorp J. The value of meteorological data in marine risk assessment. Reliab Eng Syst Saf 2021;209:107480. https://doi.org/10.1016/J.RESS.2021.107480.

[70] Zhang M, Montewka J, Manderbacka T, Kujala P, Hirdaris S. A Big Data Analytics Method for the Evaluation of Ship - Ship Collision Risk reflecting Hydrometeorological Conditions. Reliab Eng Syst Saf 2021;213:107674. https://doi.org/10.1016/J.RESS.2021.107674.

[71] Cai M, Zhang J, Zhang D, Yuan X, Soares CG. Collision risk analysis on ferry ships in Jiangsu Section of the Yangtze River based on AIS data. Reliab Eng Syst Saf 2021;215:107901. https://doi.org/10.1016/J.RESS.2021.107901.

[72] Murray B, Perera LP. An AIS-based deep learning framework for regional ship behavior prediction. Reliab Eng Syst Saf 2021;215:107819. https://doi.org/10.1016/J.RESS.2021.107819.

[73] Eriksen T, Greidanus H, Delaney C. Metrics and provider-based results for completeness and temporal resolution of satellite-based AIS services. Mar Policy 2018;93:80–92. https://doi.org/10.1016/j.marpol.2018.03.028.

[74] Patterson T, Kelso NV. World Oceans, 1:110 million (2012) in EarthWorks. North Am Cartogr Inf Soc 2012. https://earthworks.stanford.edu/catalog/stanford-nb441cf3002 (accessed September 3, 2020).

[75] Liu X, Huang W, Gill EW. Wave height estimation from shipborne x-band nautical radar images. J Sensors 2016;2016. https://doi.org/10.1155/2016/1078053.

[76] Tolman HL. User manual and system documentation of WAVEWATCH III version 3.14. NOAA/NWS/NCEP/MMAB; 2009.

[77] Law-chune S. Product User Manual for Global Ocean Waves Multi Year Product GLOBAL_REANALYSIS_WAV_001_032. EU Copernicus Marine Service; 2019.

[78] Thompson I. Virtual hull monitoring of a naval vessel using hindcast data and reconstructed 2-D wave spectra. Mar Struct 2020;71:102730. https://doi.org/10.1016/j.marstruc.2020.102730.

[79] Fu T, Babanin A, Bentamy A, Campos R, Dong S, Gramstad O, et al. ISSC committee i.1: Environment. 20th Int. Sh. offshore Struct. Congr. vol. 1. Int. Sh. Offshore Struct. Congr., 2018, p. 1–99.

[80] Chawla A, Spindler D, Tolman H, Branch A. WAVEWATCH III® Hindcasts with re-analysis winds. Initial report on model setup. Technical Report 291. 2011.

[81] European Center for Medium-range Weather Forecasts. ERA5: fifth-generation of ECMWF atmospheric reanalyses of the global climate. Copernicus Clim Chang Serv Clim Data Storage 2019. https://cds.climate.copernicus.eu/cdsapp.

[82] Stopa JE, Cheung KF. Intercomparison of wind and wave data from the ECMWF Reanalysis Interim and the NCEP Climate Forecast System Reanalysis. Ocean Model 2014;75:65–83. https://doi.org/10.1016/j.ocemod.2013.12.006.

[83] PyKrige — PyKrige 1.5.1 documentation n.d. https://geostat-framework.readthedocs.io/projects/pykrige/en/stable/ (accessed September 3, 2020).

[84] ABS. Guidance Notes on Selecting Design Wave by Long Term Stochastic Method. American Bureau of Shipping; 2016.

[85] Baltrop NDP, Adams AJ. Dynamics of Fixed Marine Structures. 3rd ed. Netherlands: Elsevier Science; 2013. https://doi.org/10.1016/C2013-0-04571-9.

[86] Sankararaman S, Mahadevan S. Likelihood-based representation of epistemic uncertainty due to sparse point data and/or interval data. Reliab Eng Syst Saf n.d.;96:814–824.

[87] Giffin A. Updating probabilities with data and moments: an econometric example. 3rd Econophysics Colloq. 2007, Ancona, Italy: n.d.

[88] Giffin A. Updating probabilities with data and moments: an ecological example. 7th Int. Conf. Complex Syst. 2007, Boston: n.d.

[89] MIL-HDBK-217F Military Handbook, Reliability prediction of electronic equipment n.d.

[90] MIL-HDBK-344A Military Handbook, Environmental stress screening (ESS) of electronic equipment n.d.

[91] Huber PJ. Robust Estimation of a Location Parameter. Ann Math Stat n.d.;35:73–102.

[92] Stigler SM. Do robust estimators work with real data? Ann Stat n.d.;5:1055–1098.

[93] Stigler SMSN. Percy Daniell, and the history of robust estimation 1885-1920. J Am Stat Assoc n.d.;68:872–879.

[94] Pratt JW. Bayesian interpretation of standard inference statements. J R Stat Soc Ser B n.d.;27:169–203.

[95] Blackwell D, Ramamoorthi V. A Bayes but Not Classically Sufficient Statistic. Ann Stat n.d.;10:1025–1026.

[96] Beaumont MA, Zhang W, Balding DJ. Approximate Bayesian computation in population genetics. Genetics n.d.;162:2025–2035.

[97] Beaumont MA. Approximate Bayesian computation in evolution and ecology. Annu Rev Ecol Evol Syst n.d.;41:379–406.

[98] Csilléry K, Blum MG, Gaggiotti OE, François O. Approximate Bayesian computation (ABC) in practice. Trends

Ecol Evol n.d.;25:410–418.

[99] Vrugt JA, Sadegh M. Toward diagnostic model calibration and evaluation: Approximate Bayesian computation. Water Resour Res n.d.;49:4335–4345.

[100] Fearnhead P, Prangle D. Constructing Summary Statistics for Approximate Bayesian Computation: Semi-automatic ABC. J R Stat Soc Ser B n.d.;24:419–474. https://doi.org/10.1111/j.1467-9868.2011.01010.x.

[101] Blum MGB, Nunes MA, Prangle D, Sisson SA. A comparative review of dimension reduction methods in approximate Bayesian computation. Stat Sci n.d.;28:180–208.

[102] Nunes MA, Balding DJ. On optimal selection of summary statistics for approximate Bayesian computation. Stat Appl Genet Mol Biol n.d.;9.

[103] Guan X. A general probabilistic inference framework for prognostics and health management under uncertainty n.d.

[104] Giffin A, Caticha A. Updating probabilities with data and moments. 27th Int. Work. Bayesian Inference Maximum Entropy Methods Sci. Eng., Saratoga Springs, NY: n.d.

[105] Shore J, Johnson R. Axiomatic derivation of the principle of maximum entropy and the principle of minimum cross-entropy. IEEE Trans Inf Theory n.d.;26:26–37.

[106] Guan X, Giffin A, Jha R, Liu Y. Maximum relative entropy-based probabilistic inference in fatigue crack damage prognostics. Probabilistic Eng Mech n.d.;29:157–166.

[107] Friedman K, A S. Jaynes' maximum entropy prescription and probability theory. J Stat Phys n.d.;4:381–384.

[108] Shimony A. The status of the principle of maximum entropy. Synthese n.d.;63:35–53.

[109] Fraassen BC. A problem for relative information minimizers in probability kinematics. Br J Philos Sci n.d.;32:375–379.

[110] Jensen F V. An introduction to Bayesian networks. Springer-Verlag; 1996.

[111] Pearl J. Probabilistic Reasoning in Intelligent Systems: Networks of Plausible Inference. San Mateo, CA: Morgan Kaufmann Publishers, Inc; n.d.

[112] Shachter RD. An ordered examination of influence diagrams. Networks n.d.;20:535–563.

[113] Shachter RD. Probabilistic inference and influence diagrams. Op Res n.d.;36:589–604.

[114] Cinicioglu EN, Shenoy PP. Arc reversals in hybrid Bayesian networks with deterministic variables. Int J Approx Reason n.d.;50:763–777.

[115] Mood AM, Graybill FA, Boes DC. Introduction to the Theory of Statistics. 3rd ed. McGraw-Hill; n.d.

[116] Kmenta J. Elements of Econometrics. New York: Macmillan; n.d.

[117] Fisher RA. The sampling distribution of some statistics obtained from non-linear equations. Ann Eugen n.d.;9:238–249.

[118] Fisher RA. Moments and product moments of sampling distributions. Proc London Math Soc n.d.;2:199–238.

[119] Hendricks WA, Robey KW. The sampling distribution of the coefficient of variation. Ann Math Stat n.d.;7:129–132.

[120] Dinneen LC, Blakesley BC. Algorithm AS 62: A generator for the sampling distribution of the Mann-Whitney U statistic. J R Stat Soc n.d.;22:269–273.

[121] Miller J. The sampling distribution ofd′. Percept Psychophys n.d.;58:65–72.

[122] Botex ZI, Grotowski JF, Kroese DP. Kernel density estimation via diffusion. Ann Stat n.d.;38:2916–2957.

[123] Agresti A, Finaly B. Statistical Methods for the Social Sciences. 3rd ed. Upper Saddle River, NJ: Prentice Hall; n.d.

[124] Casella GB, R.L. Statistical Inference. 2nd ed. New York: Duxbury Press; n.d.

[125] Sullivan III M. Statistics: Informed Decisions Using Data. 4th ed. Pearson; n.d.

[126] Metropolis N, Rosenbluth AW, Rosenbluth MN, Teller AH, Teller E. Equations of state calculations by fast computing machines. J Chem Phys n.d.;21:1087–1092.

[127] Hastings WK. Monte Carlo sampling methods using Markov chains and their applications. Biometrika n.d.;57:97–109.

[128] Smith AFM, Gelfand AE. Bayesian Statistics without Tears: A Sampling-Resampling Perspective. Am Stat 1992;46:84. https://doi.org/10.2307/2684170.

[129] Ling Y. Uncertainty quantification in time-dependent reliability analysis n.d.

[130] Bates GE. Joint distributions of time intervals for the occurrence of successive accidents in a generalized polya scheme. Ann Math Stat n.d.;26:705–720.

[131] VanDerHorn E, Wang G. A statistical study on the material properties of shipbuilding steels. Sustain Marit Transp Explor Sea Resour n.d.:371–378.

[132] Hess PE, Bruchman DD, Assakkaf I, Ayyub BM. Uncertainties in Material Strength. Geom Load Var ASNE Nav Eng J n.d.;114:139–165.

[133] Gelman A, Hill J. Data Analysis Using Regression and Multilevel/Hierarchical Models. First. Cambridge University Press; n.d.

[134] Haldar A. Probabilistic evaluation of welded structures. J Struct Eng Div ASCE n.d.;108:1943–1955.

[135] Ospina R, Ferrari S. Inflated beta distributions. Stat Pap n.d.;51. https://doi.org/10.1007/s00362-008-0125-4.

[136] Ling Y, Mullins J, Mahadevan S. Selection of model discrepancy prior in Bayesian calibration. J Comput Phys n.d.;276:665–680.

[137] Hasofer AM, Lind NC. Exact and invariant second-moment code format. J Engrg Mech Div n.d.;100:111–121.

[138] Sankararaman S, Mahadevan S. Model parameter estimation with imprecise and unpaired data. Inverse Probl Sci Eng 2012;20:1017–41. https://doi.org/10.1080/17415977.2012.675505.

[139] Fenton N, Neil M. Risk Assessment and Decision Analysis with Bayesian Networks. Second Edition. | Boca Raton, Florida : CRC Press, [2019]: Chapman and Hall/CRC; 2018. https://doi.org/10.1201/b21982.

[140] Murphy AH, Winkler RL. Reliability of Subjective Probability Forecasts of Precipitation and Temperature. Appl Stat 1977;26:41. https://doi.org/10.2307/2346866.

[141] Hughes MD. Practical Reporting of Bayesian Analyses of Clinical Trials: Http://DxDoiOrg/101177/009286159102500308 2016;25:381–93. https://doi.org/10.1177/009286159102500308.

[142] Johnson SR, Tomlinson GA, Hawker GA, Granton JT, Feldman BM. Methods to elicit beliefs for Bayesian priors: a systematic review. J Clin Epidemiol 2010;63:355–69. https://doi.org/10.1016/J.JCLINEPI.2009.06.003.

[143] Zhang X, Mahadevan S, Deng X. Reliability analysis with linguistic data: An evidential network approach. Reliab Eng Syst Saf 2017;162:111–21. https://doi.org/10.1016/J.RESS.2017.01.009.

[144] Tötsch N, Hoffmann D. Classifier uncertainty: evidence, potential impact, and probabilistic treatment. PeerJ Comput Sci 2021;7. https://doi.org/10.7717/PEERJ-CS.398/SUPP-1.

[145] Tanner MA, Wong WH. The calculation of posterior distributions by data augmentation. J Am Stat Assoc 1987;82:528–40. https://doi.org/10.1080/01621459.1987.10478458.

[146] Schafer J. Analysis of incomplete multivariate data. CRC Press; 1997.

[147] Daniels MJ, Kass RE. Nonconjugate Bayesian Estimation of Covariance Matrices and its Use in Hierarchical Models. J Am Stat Assoc 1999;94:1254–63. https://doi.org/10.1080/01621459.1999.10473878.

[148] Geweke JF, Keane MP, Runkle DE. Statistical inference in the multinomial multiperiod probit model. J Econom 1997;80:125–65. https://doi.org/10.1016/S0304-4076(97)00005-5.

[149] Zhang X, Boscardin WJ, Belin TR, Wan X, He Y, Zhang K. A Bayesian method for analyzing combinations of continuous, ordinal, and nominal categorical data with missing values. J Multivar Anal 2015;135:43–58. https://doi.org/10.1016/J.JMVA.2014.11.007.

[150] Absi GN. Multi-Fidelity Information Fusion for Structural Dynamics Model Calibration. Ph.D. Dissertation, Vanderbilt University, Nashville, TN, 2019.

[151] VanDerHorn E, Mahadevan S. Bayesian model updating with summarized statistical and reliability data. Reliab Eng Syst Saf 2018;172:12–24. https://doi.org/10.1016/j.ress.2017.11.023.

[152] Jeffrey R. The Logic of Decision, 2nd ed. Synthese 1983;48:473–92.

[153] Berkson J. Are there Two Regressions? J Am Stat Assoc 1950;45:164–80. https://doi.org/10.1080/01621459.1950.10483349.

[154] Fuller WA. Measurement Error Models. Hoboken, NJ, USA: John Wiley & Sons, Inc.; 1987. https://doi.org/10.1002/9780470316665.

[155] Sankararaman S, Mahadevan S. Integration of model verification, validation, and calibration for uncertainty quantification in engineering systems. Reliab Eng Syst Saf 2015;138:194–209. https://doi.org/10.1016/j.ress.2015.01.023.

[156] Agostinelli C, of LG-P of the 46th SM, 2012 undefined. Weighted likelihood in Bayesian inference. Sis-StatisticaIt n.d.

[157] Zhang R, Mahadevan S. Reliability-based reassessment of corrosion fatigue life. Struct Saf 2001;23:77–91. https://doi.org/10.1016/S0167-4730(01)00002-9.

[158] Ling Y, Mahadevan S. Integration of structural health monitoring and fatigue damage prognosis. Mech Syst Signal Process 2012;28:89–104. https://doi.org/10.1016/j.ymssp.2011.10.001.

[159] Sankararaman S, Mahadevan S. Bayesian methodology for diagnosis uncertainty quantification and health monitoring. Control Heal Monit 2013;19:88–106. https://doi.org/10.1002/stc.476.

[160] Filho TS, Song H, Perello-Nieto M, Santos-Rodriguez R, Kull M, Flach P. Classifier Calibration: How to assess and improve predicted class probabilities: a survey. CoRR 2021;abs/2112.1.

[161] Pisner DA, Schnyer DM. Support vector machine. Mach. Learn. Methods Appl. to Brain Disord., Academic Press; 2020, p. 101–21. https://doi.org/10.1016/B978-0-12-815739-8.00006-7.

[162] Menéndez ML, Pardo JA, Pardo L, Pardo MC. The Jensen-Shannon divergence. J Franklin Inst 1997;334:307–18. https://doi.org/10.1016/S0016-0032(96)00063-4.

[163] Fisher RA. The Use of Multiple Measurements In Taxonomic Problems. Ann Eugen 1936;7:179–88. https://doi.org/10.1111/J.1469-1809.1936.TB02137.X.

[164] Koch GH, Brongers MPH, Thompson NG, Virmani YP, Payer JH. “Corrosion Costs and Preventive Strategies in the United States” n.d.

[165] IACS. IACS Recommendation 87: Guidelines for Coating Maintenance & Repairs for Ballast Tanks and

Combined Cargo/Ballast Tanks on Oil Tankers. 2015.

[166] ABS. ABS Guidance Notes on Maintenance and Repair of Protective Coatings. 2017.

[167] Gu H, Wen F, Wang B, Lee A-K, Xu D. Machine Learning-based image recognition for visual inspections 2019.